The Cenozoic Magmatism of East Africa: Part V – Magma Sources and Processes in the East African Rift

Tyrone O. Rooney

Dept. of Earth and Environmental Sciences, Michigan State University, East Lansing, MI 48823, USA

Abstract

The generation of magmas in the East African Rift System (EARS) is largely the result of either: (A) melting of easily fusible compositions located within the lithospheric mantle due to thermobaric perturbations of the lithosphere, or (B) melting of the convecting upper mantle due to decompression caused by thinning of the plate during extension. Melt generated from amphibole- or phlogopite-bearing metasomes within the lithospheric mantle yields alkaline, silica-undersaturated lavas, while more silica-saturated lavas are primarily a function of melting material within the convecting upper mantle. Sourcing of silica-undersaturated melts within the lithospheric mantle is consistent with the observed tendency for initial melts within any given region to exhibit trace element characteristics consistent with melting of lithospheric metasomes, likely reflecting the initial destabilization and thinning of the lithospheric mantle. With continued lithospheric thinning, the trend towards more silica-saturated compositions coincides with a shift towards compositions interpreted as melting of the convecting upper mantle. Contributions from these two sources may oscillate where extension is pulsed – melts of the convecting upper mantle are favored during periods of plate thinning; melting of either existing or recently formed metasomes may be favored during periods of relative extensional quiescence. The isotopic systematics of East African magmatism reveals significant complexity

Figure 1

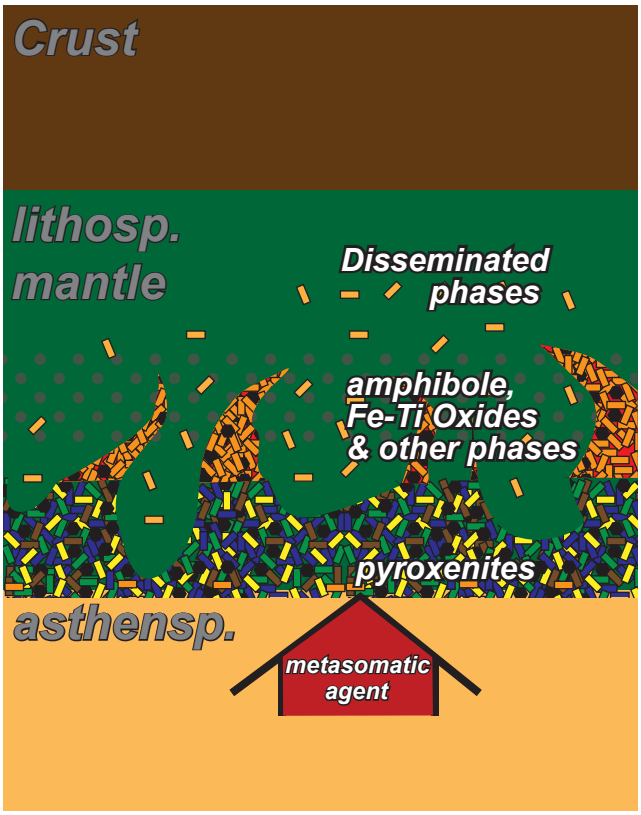
Crust
lithosp.
mantle
Disseminated
phases
amphibole,
Fe-Ti Oxides
& other phases
pyroxenites
asthensp.
metasomatic
agent

Figure 2

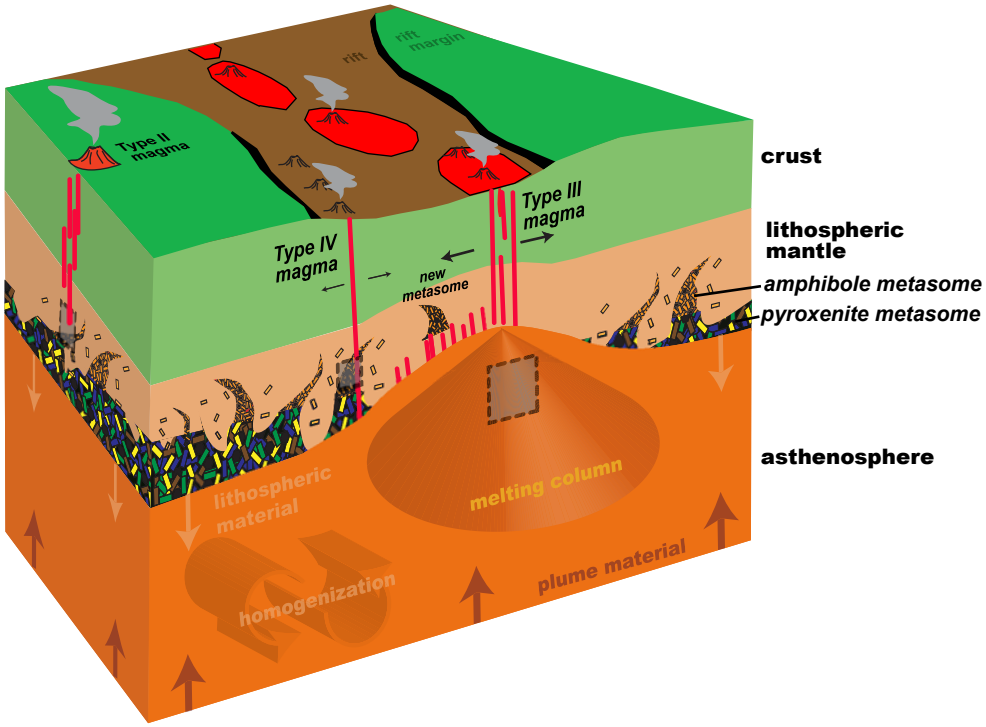
rift
rift margin
Type II magma
Type III magma
Type IV magma
new metasome
crust
lithospheric mantle
amphibole metasome
pyroxenite metasome
asthenosphere
lithospheric material
melting column
homogenization
plume material

Figure 3

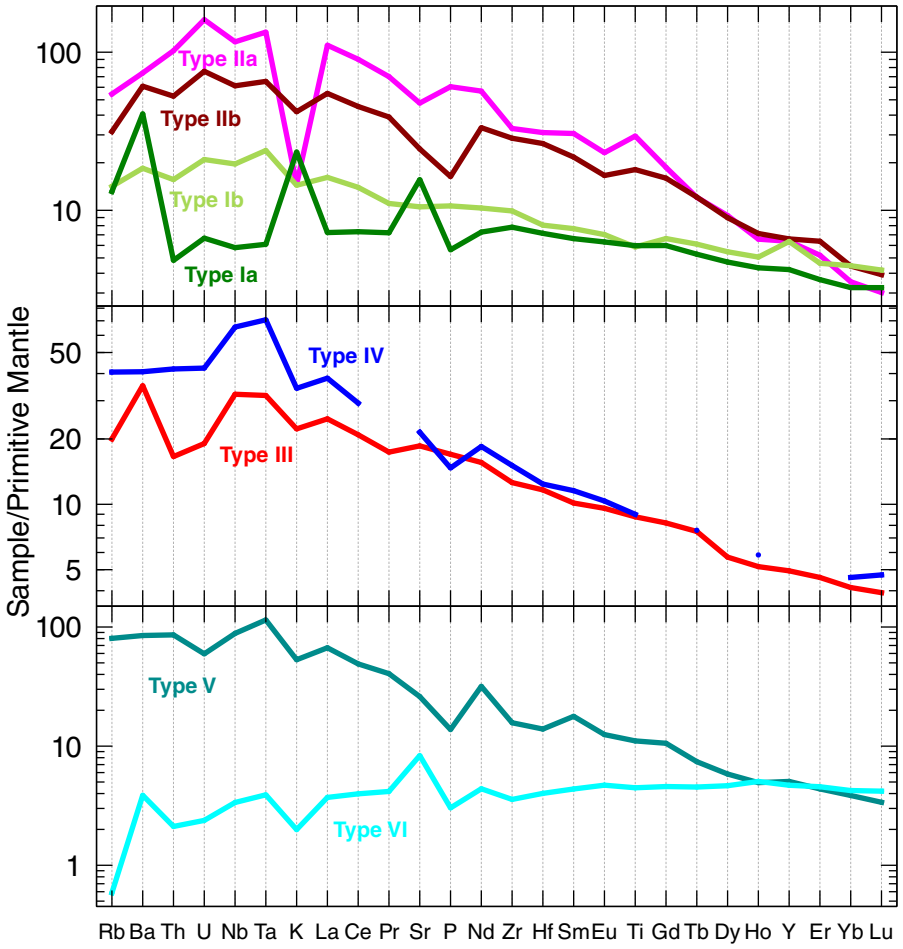
Type IIa
Type IIb
Type Ib
Type Ia
Type IV
Type III
Type V
Type VI
Sample/Primitive Mantle
100
10
50
20
10
5
100
10
1
Rb Ba Th U Nb Ta K La Ce Pr Sr P Nd Zr Hf Sm Eu Ti Gd Tb Dy Ho Y Er Yb Lu

Figure 4

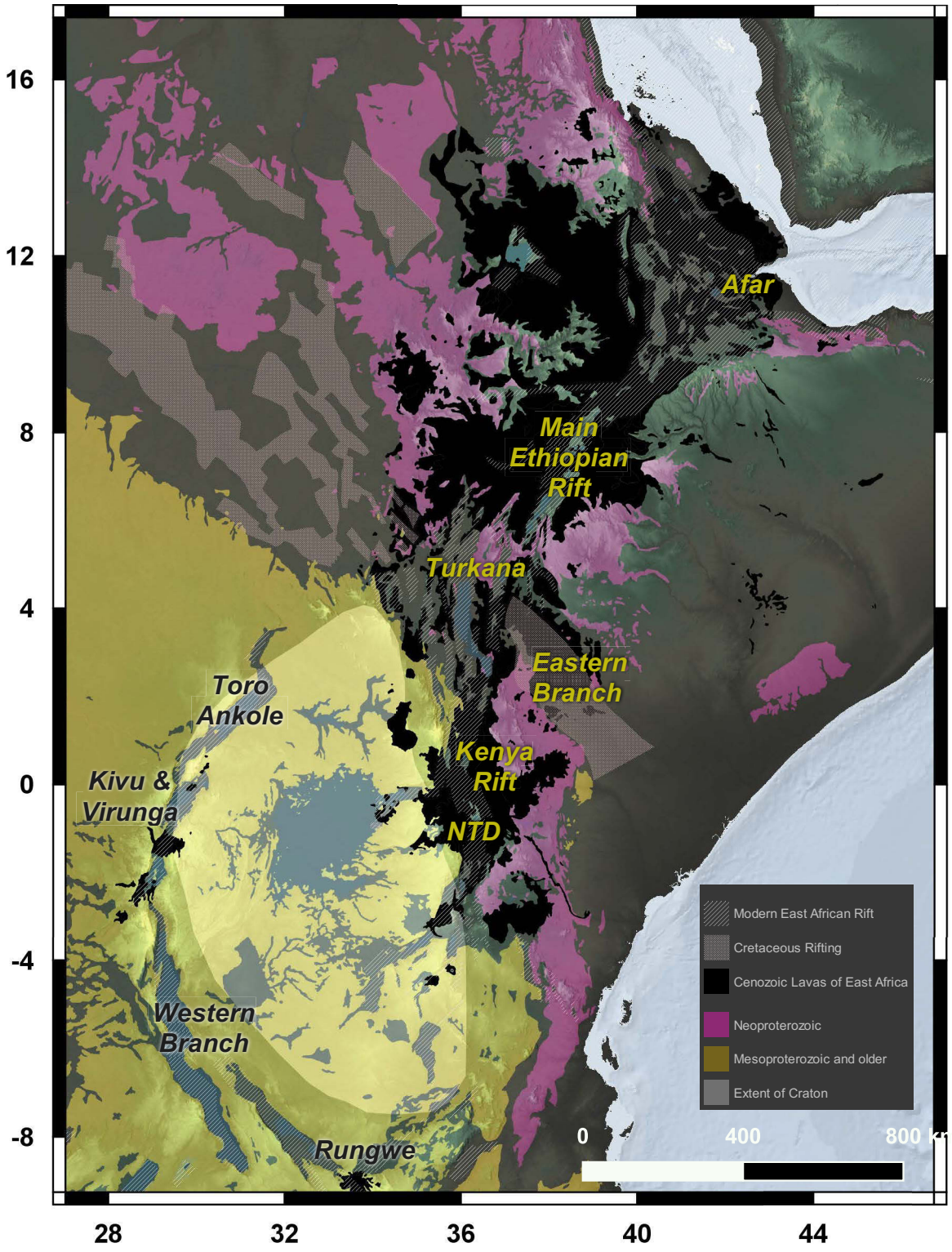
16
12
8
4
0
-4
-8
28
32
36
40
44
Afar
Main Ethiopian Rift
Turkana
Eastern Branch
Kenya Rift
NTD
Toro Ankole
Kivu & Virunga
Western Branch
Rungwe
Modern East African Rift
Cretaceous Rifting
Cenozoic Lavas of East Africa
Neoproterozoic
Mesoproterozoic and older
Extent of Craton
0
400
800 km

Figure 5

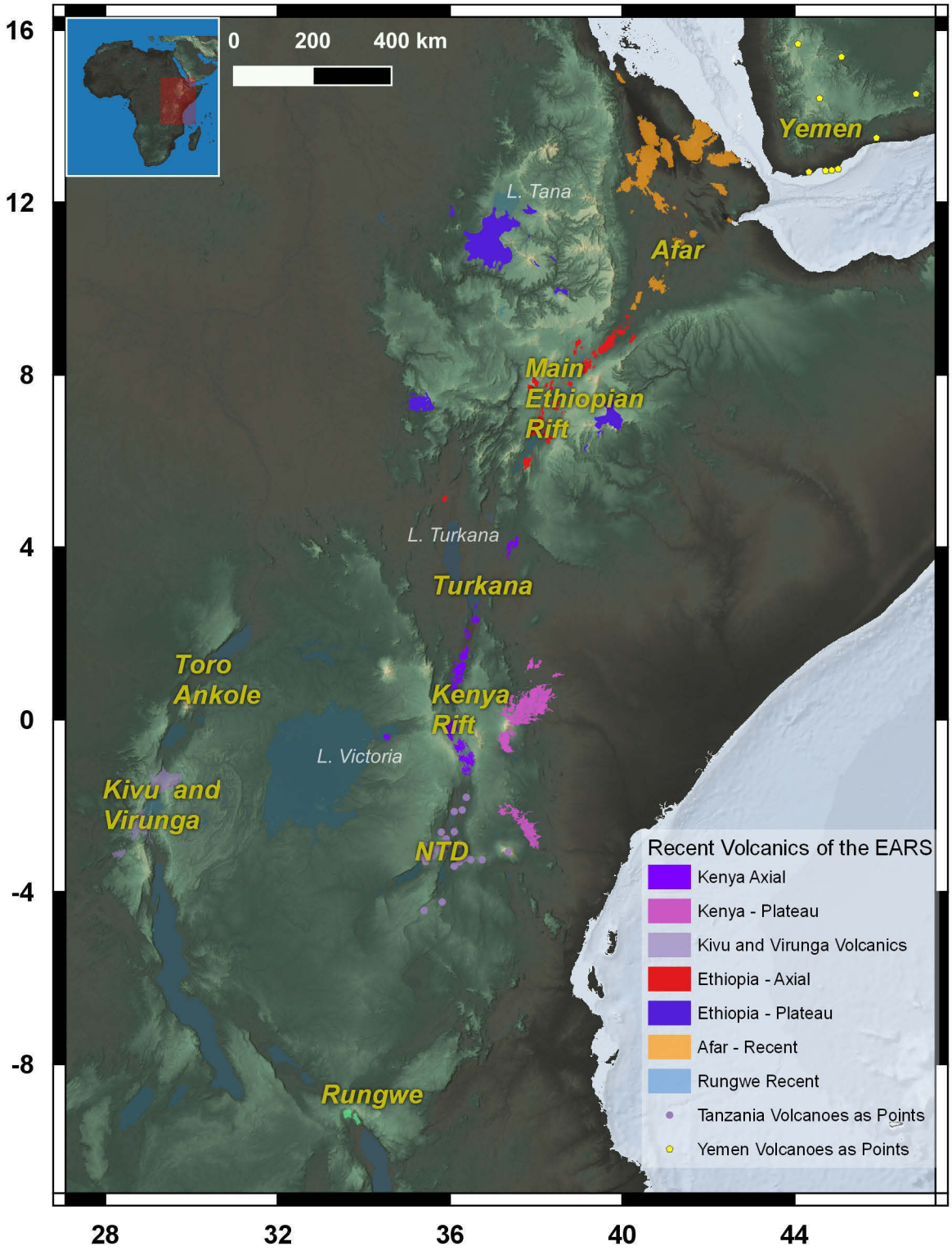
0 200 400 km
Yemen
L. Tana
Afar
Main Ethiopian Rift
L. Turkana
Turkana
Toro Ankole
Kenya Rift
L. Victoria
Kivu and Virunga
NTD
Rungwe
Recent Volcanics of the EARS
Kenya Axial
Kenya - Plateau
Kivu and Virunga Volcanics
Ethiopia - Axial
Ethiopia - Plateau
Afar - Recent
Rungwe Recent
Tanzania Volcanoes as Points
Yemen Volcanoes as Points
16
12
8
4
0
-4
-8
28
32
36
40
44

Figure 6

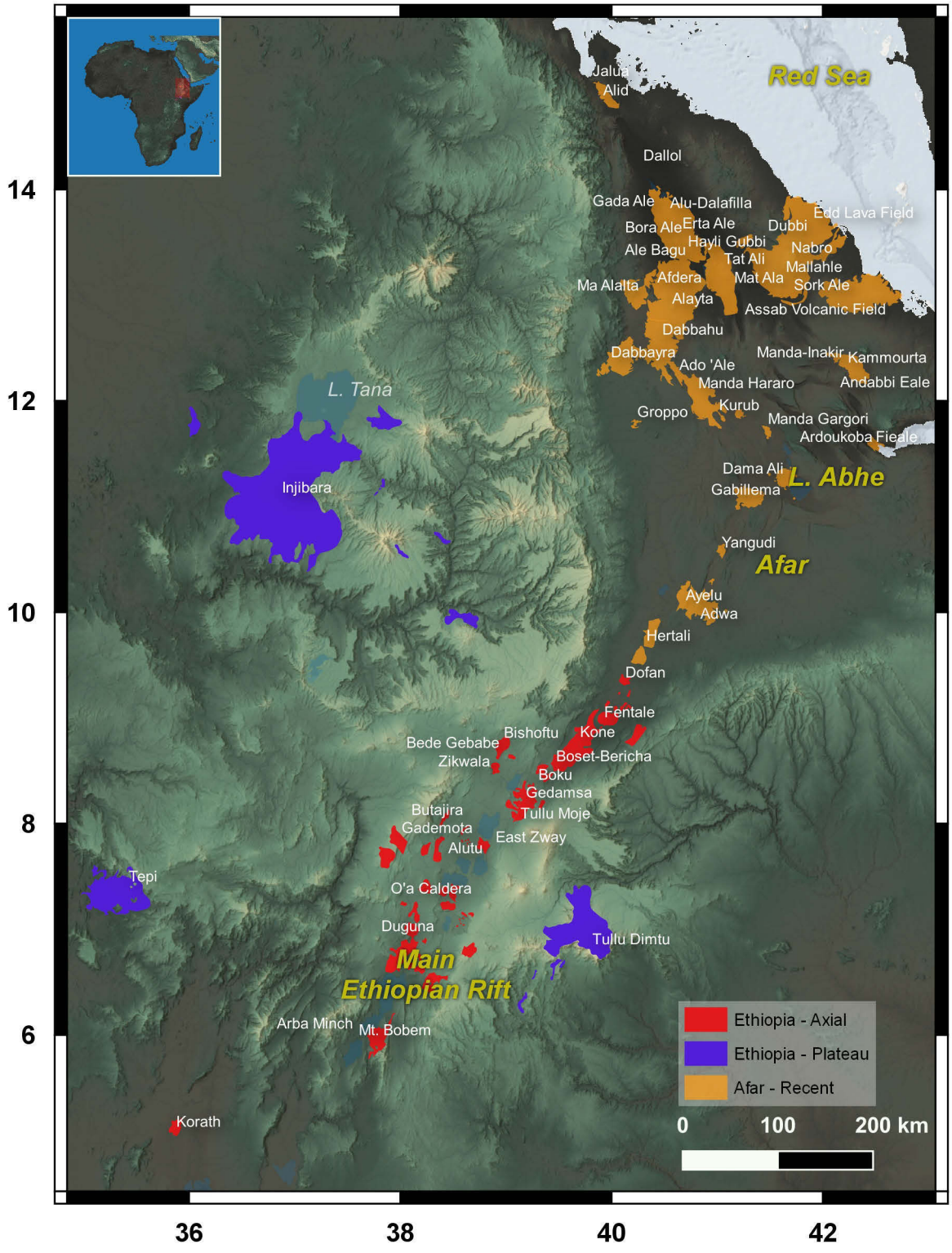
Red Sea
Jalua
Alid
Dallol
Gada Ale
Alu-Dalafilla
Edd Lava Field
Bora Ale
Erta Ale
Dubbi
Hayli Gubbi
Ale Bagu
Tat Ali
Nabro
Mallahle
Ma Alalta
Afdera
Mat Ala
Sork Ale
Alayta
Assab Volcanic Field
Dabbahu
Dabbayra
Manda-Inakir
Kammourta
Ado 'Ale
Manda Hararo
Andabbi Eale
L. Tana
Kurub
Groppo
Manda Gargori
Ardoukoba Fieale
Dama Ali
L. Abhe
Injibara
Gabillema
Yangudi
Afar
Ayelu
Adwa
Hertali
Dofan
Fentale
Bishoftu
Kone
Bede Gebabe
Zikwala
Boset-Bericha
Boku
Gedamsa
Butajira
Tullu Moje
Gademota
East Zway
Alutu
Tepi
O'a Caldera
Duguna
Tullu Dimtu
Main
Ethiopian Rift
Arba Minch
Mt. Bobem
Korath
Ethiopia - Axial
Ethiopia - Plateau
Afar - Recent
0
100
200 km
14
12
10
8
6
36
38
40
42

Figure 7

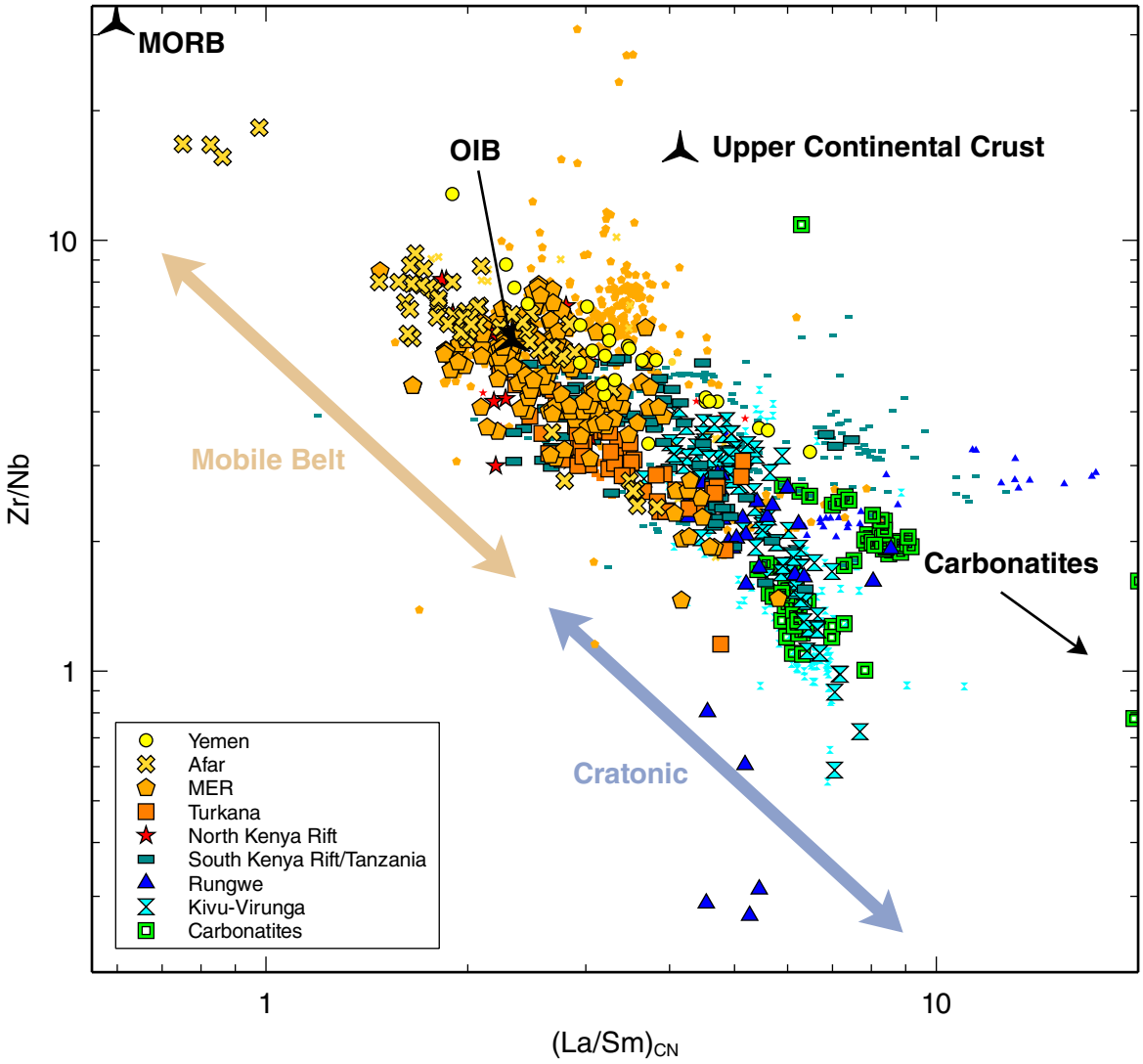
MORB
OIB
Upper Continental Crust
Mobile Belt
Carbonatites
Cratonic
Yemen
Afar
MER
Turkana
North Kenya Rift
South Kenya Rift/Tanzania
Rungwe
Kivu-Virunga
Carbonatites
10
1
1
10
Zr/Nb
(La/Sm)CN

Figure 8

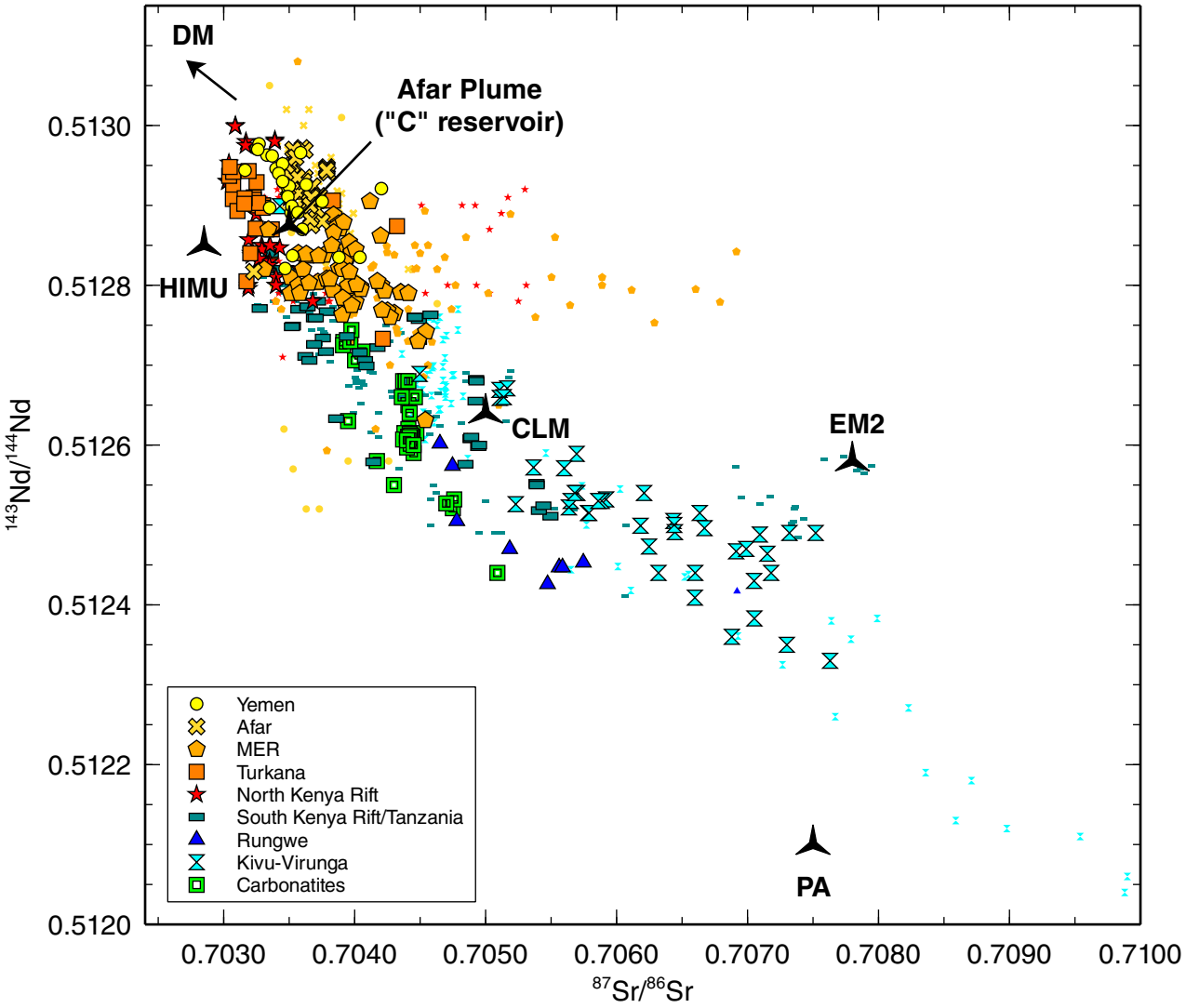
DM
Afar Plume
("C" reservoir)
HIMU
CLM
EM2
PA
Yemen
Afar
MER
Turkana
North Kenya Rift
South Kenya Rift/Tanzania
Rungwe
Kivu-Virunga
Carbonatites
0.5130
0.5128
0.5126
0.5124
0.5122
0.5120
0.7030
0.7040
0.7050
0.7060
0.7070
0.7080
0.7090
0.7100
143Nd/144Nd
87Sr/86Sr

Figure 9

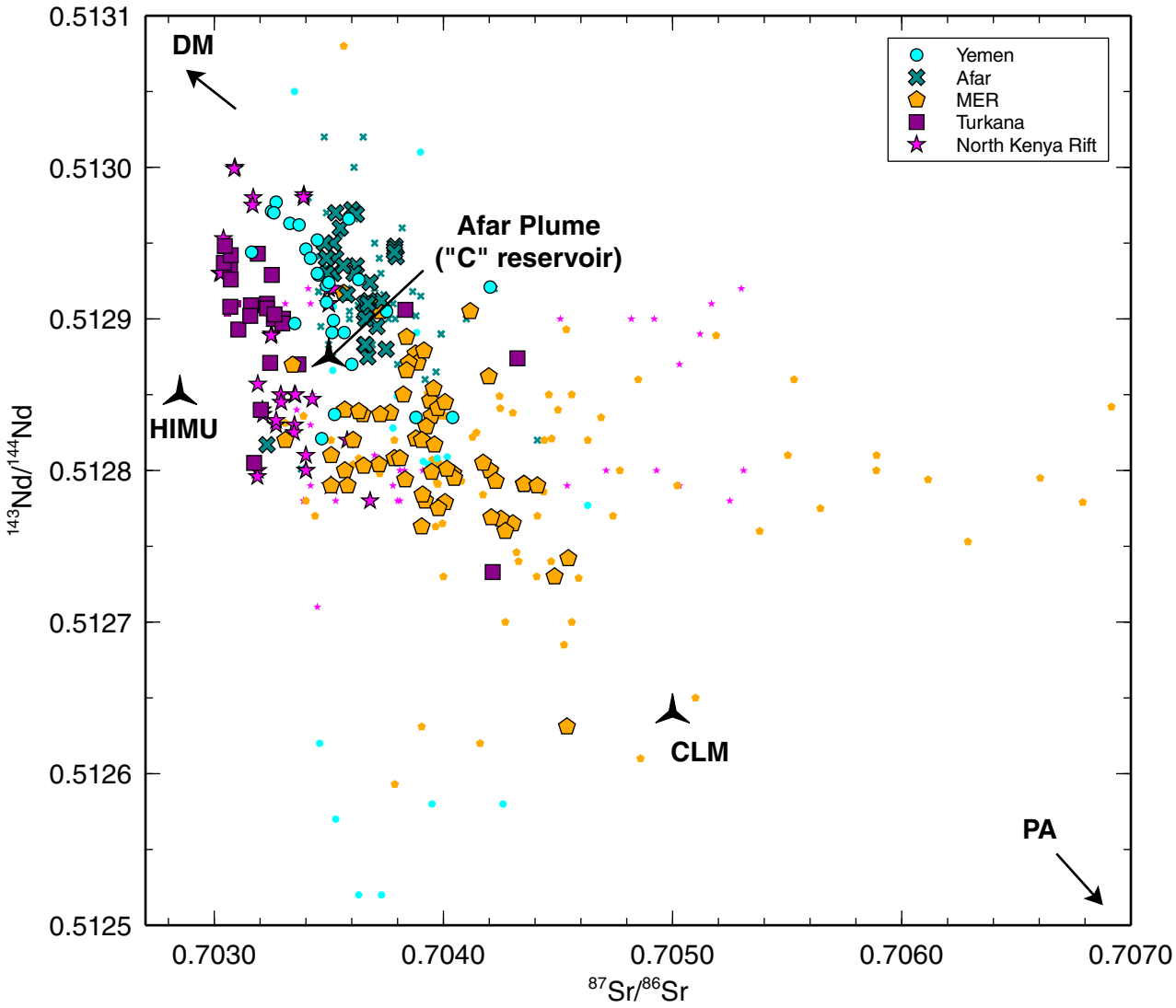
DM
HIMU
Afar Plume
("C" reservoir)
CLM
PA
Yemen
Afar
MER
Turkana
North Kenya Rift
0.5131
0.5130
0.5129
0.5128
0.5127
0.5126
0.5125
0.7030
0.7040
0.7050
0.7060
0.7070
143Nd/144Nd
87Sr/86Sr

Figure 10

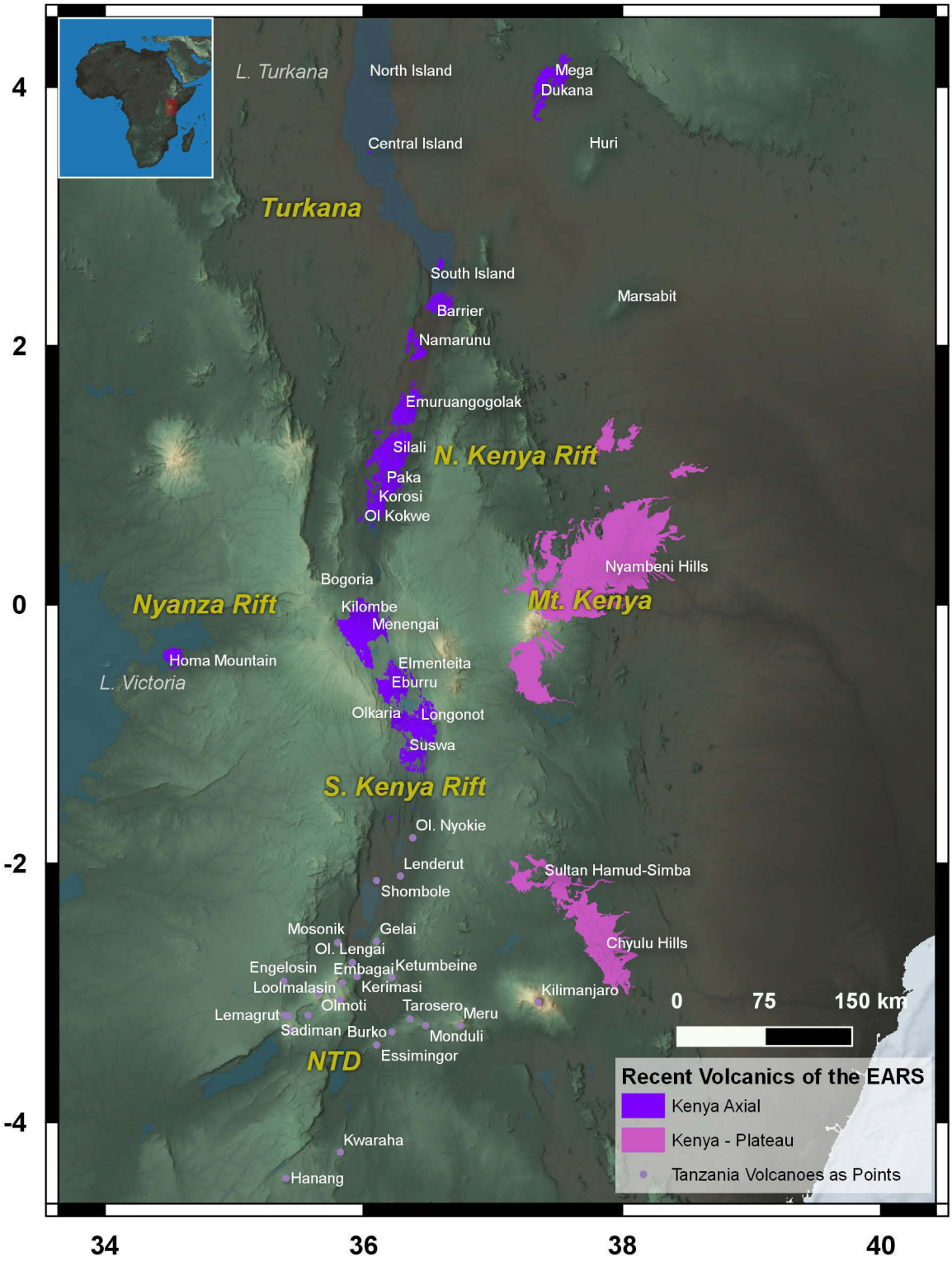
L. Turkana
North Island
Mega
Dukana
Central Island
Huri
Turkana
South Island
Marsabit
Barrier
Namarunu
Emuruangogolak
Silali
N. Kenya Rift
Paka
Korosi
Ol Kokwe
Nyambeni Hills
Bogoria
Nyanza Rift
Kilombe
Mt. Kenya
Menengai
Homa Mountain
Elmenteita
L. Victoria
Eburru
Olkaria
Longonot
Suswa
S. Kenya Rift
Ol. Nyokie
Lenderut
Sultan Hamud-Simba
Shombole
Mosonik
Gelai
Ol. Lengai
Chyulu Hills
Engelosin
Embagai
Ketumbeine
Loolmalasin
Kerimasi
Kilimanjaro
Olmoti
Tarosero
Lemagrut
Meru
Sadiman
Burko
Monduli
NTD
Essimingor
Kwaraha
Hanang
0
75
150 km
Recent Volcanics of the EARS
Kenya Axial
Kenya - Plateau
Tanzania Volcanoes as Points
4
2
0
-2
-4
34
36
38
40

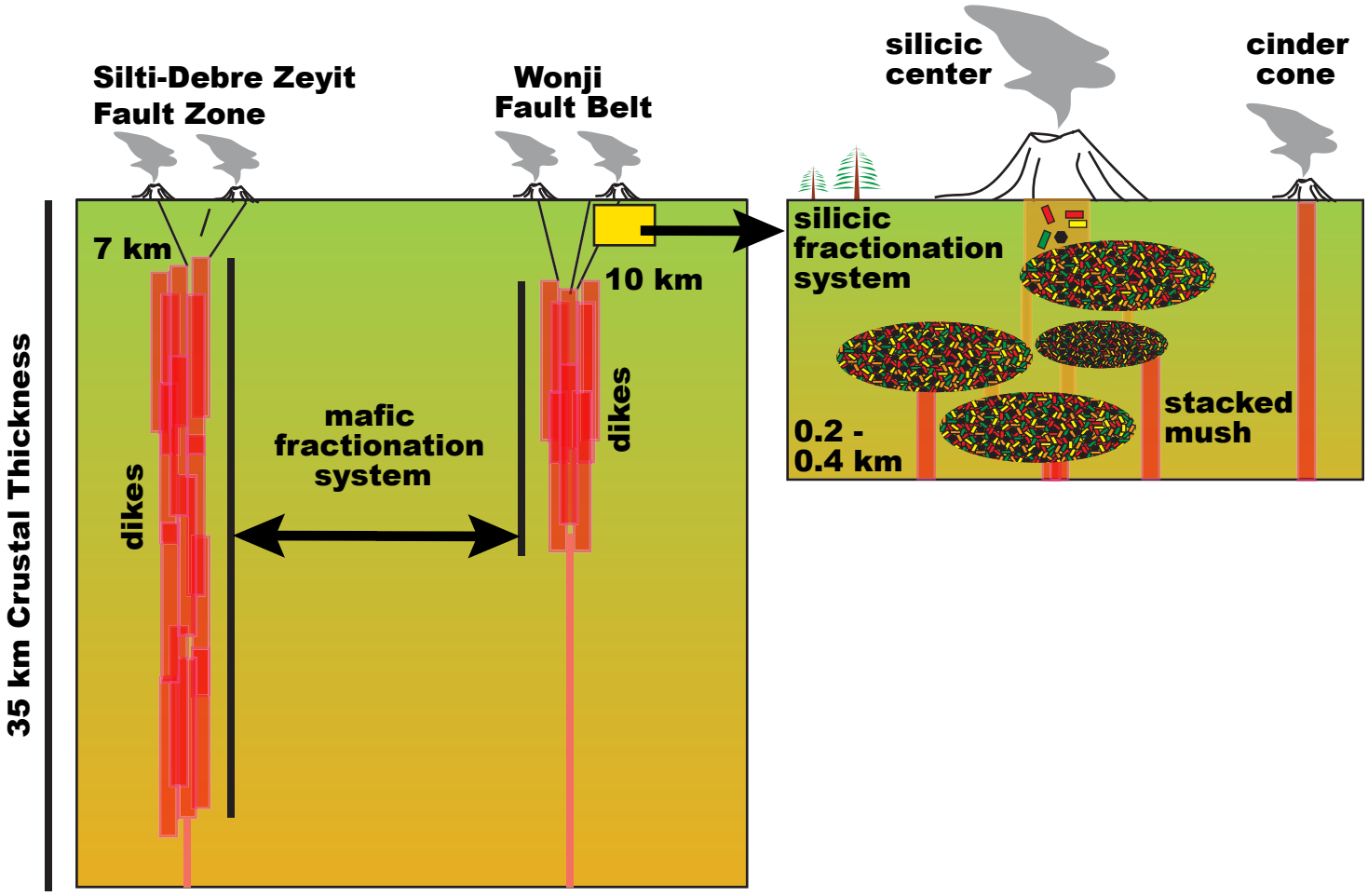
Silti-Debre Zeyit
Fault Zone
Wonji
Fault Belt
silicic
center
cinder
cone
7 km
10 km
dikes
dikes
mafic
fractionation
system
35 km Crustal Thickness
silicic
fractionation
system
stacked
mush
0.2 -
0.4 km

Figure 12

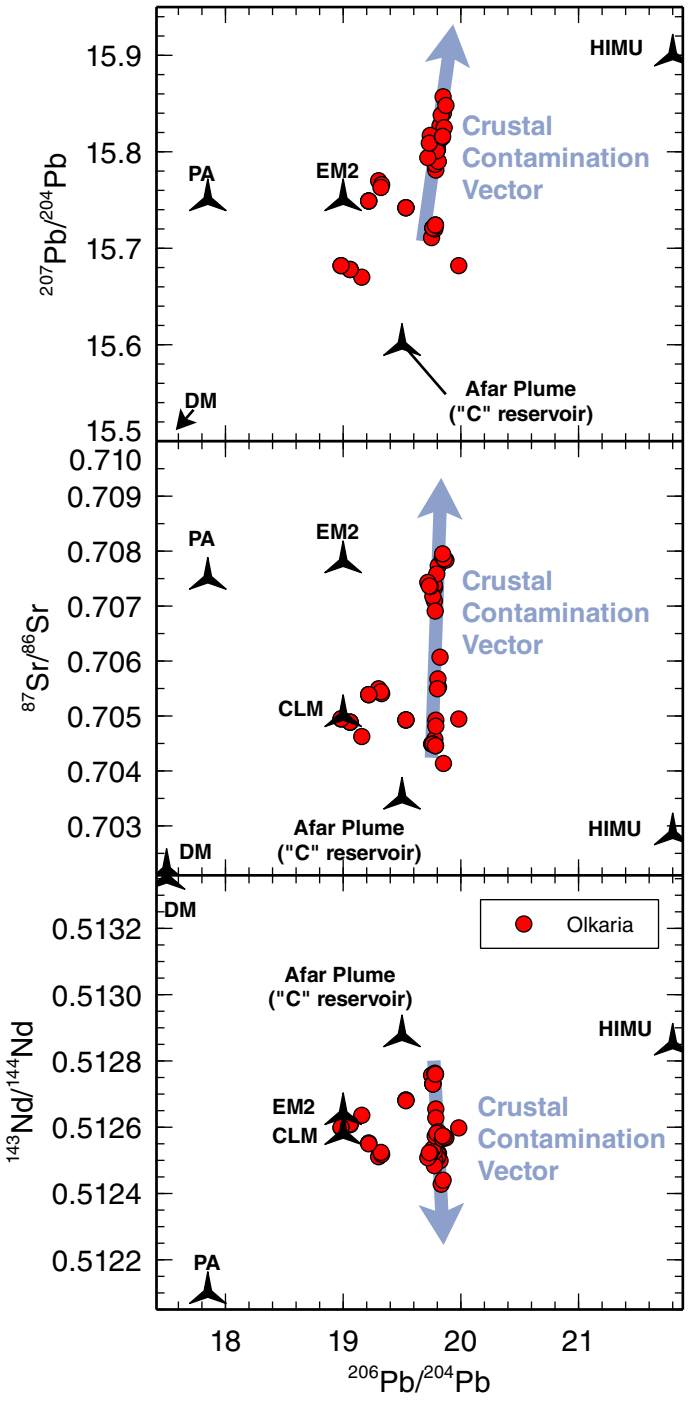
15.9
15.8
15.7
15.6
15.5
$^{207}Pb/^{204}Pb$
HIMU
PA
EM2
Crustal
Contamination
Vector
DM
Afar Plume
("C" reservoir)
0.710
0.709
0.708
0.707
0.706
0.705
0.704
0.703
$^{87}Sr/^{86}Sr$
PA
EM2
Crustal
Contamination
Vector
CLM
Afar Plume
("C" reservoir)
HIMU
DM
DM
Olkaria
0.5132
0.5130
0.5128
0.5126
0.5124
0.5122
$^{143}Nd/^{144}Nd$
Afar Plume
("C" reservoir)
HIMU
EM2
CLM
Crustal
Contamination
Vector
PA
18
19
20
21
$^{206}Pb/^{204}Pb$

Figure 13

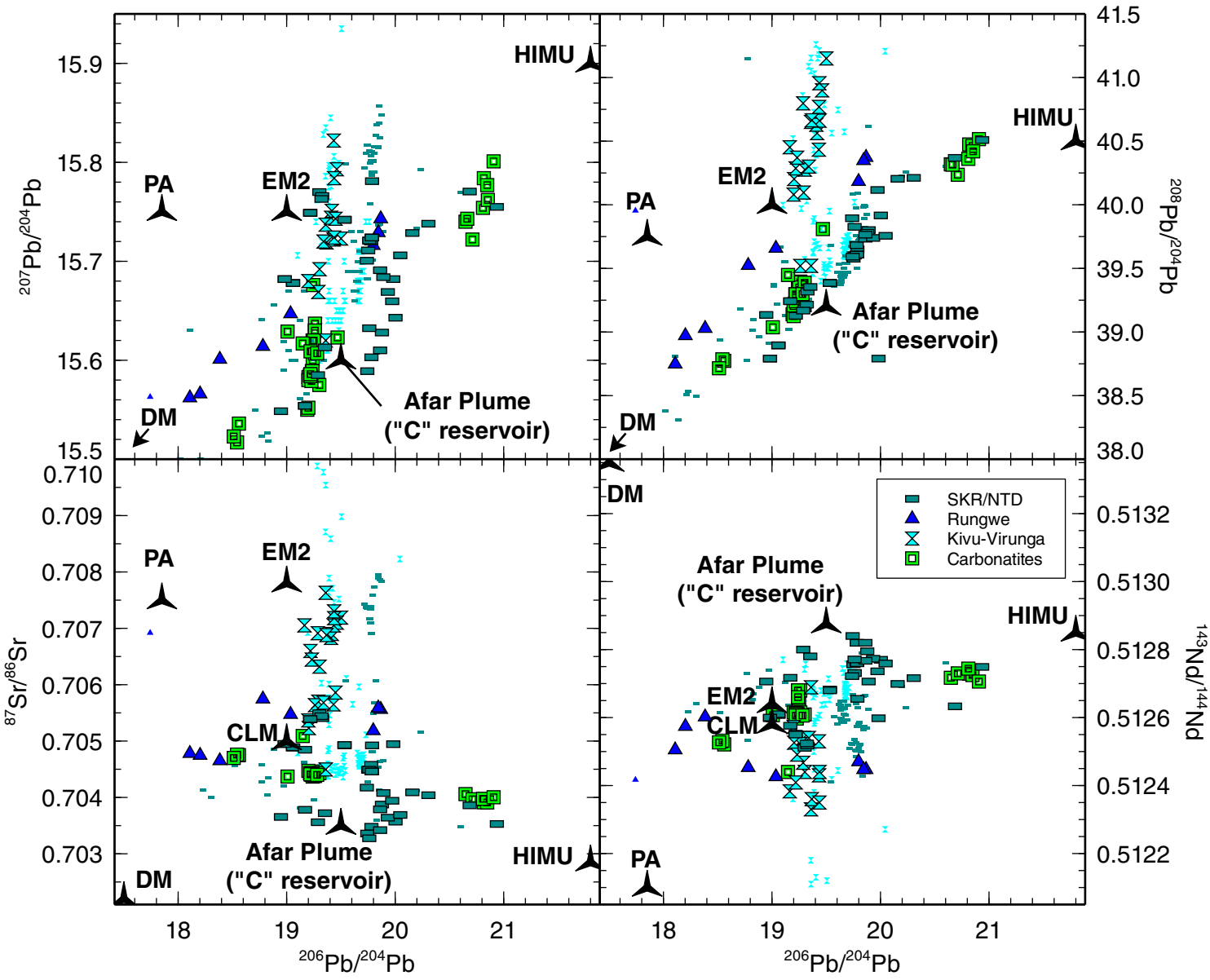
HIMU
PA
EM2
DM
Afar Plume
("C" reservoir)
CLM
SKR/NTD
Rungwe
Kivu-Virunga
Carbonatites
15.9
15.8
15.7
15.6
15.5
41.5
41.0
40.5
40.0
39.5
39.0
38.5
38.0
0.710
0.709
0.708
0.707
0.706
0.705
0.704
0.703
0.5132
0.5130
0.5128
0.5126
0.5124
0.5122
18
19
20
21
$^{207}Pb/^{204}Pb$
$^{208}Pb/^{204}Pb$
$^{87}Sr/^{86}Sr$
$^{143}Nd/^{144}Nd$
$^{206}Pb/^{204}Pb$

Figure 14

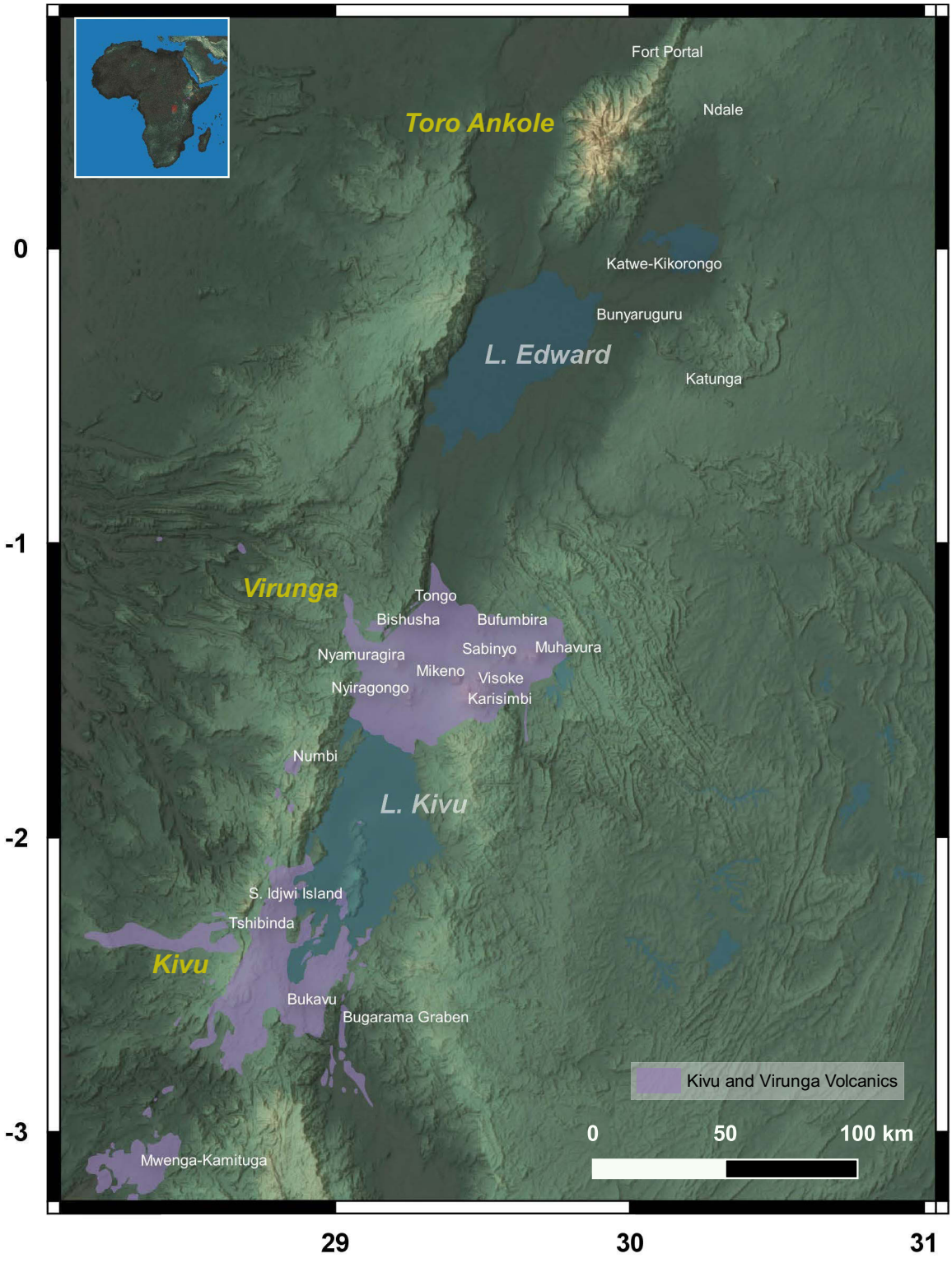
Fort Portal
Ndale
Toro Ankole
0
Katwe-Kikorongo
Bunyaruguru
L. Edward
Katunga
-1
Virunga
Tongo
Bishusha
Bufumbira
Nyamuragira
Sabinyo
Muhavura
Mikeno
Visoke
Nyiragongo
Karisimbi
Numbi
L. Kivu
-2
S. Idjwi Island
Tshibinda
Kivu
Bukavu
Bugarama Graben
Kivu and Virunga Volcanics
0
50
100 km
-3
Mwenga-Kamituga
29
30
31

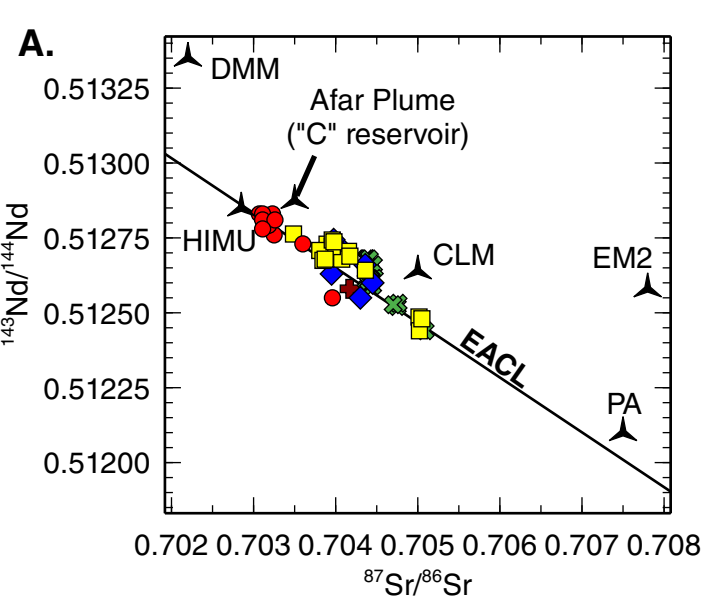
A.
DMM
Afar Plume
("C" reservoir)
HIMU
CLM
EM2
EACL
PA
0.51325
0.51300
0.51275
0.51250
0.51225
0.51200
143Nd/144Nd
0.702 0.703 0.704 0.705 0.706 0.707 0.708
87Sr/86Sr

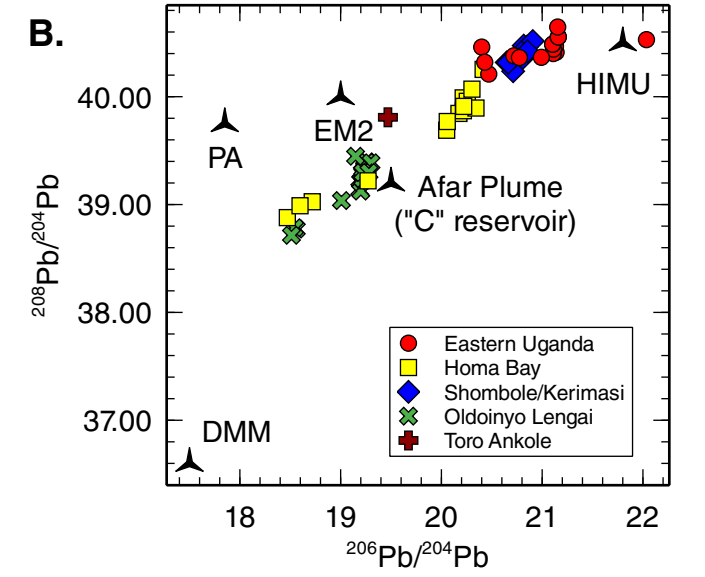
B.
HIMU
EM2
PA
Afar Plume
("C" reservoir)
DMM
40.00
39.00
38.00
37.00
208Pb/204Pb
18 19 20 21 22
206Pb/204Pb
Eastern Uganda
Homa Bay
Shombole/Kerimasi
Oldoinyo Lengai
Toro Ankole

Figure 16

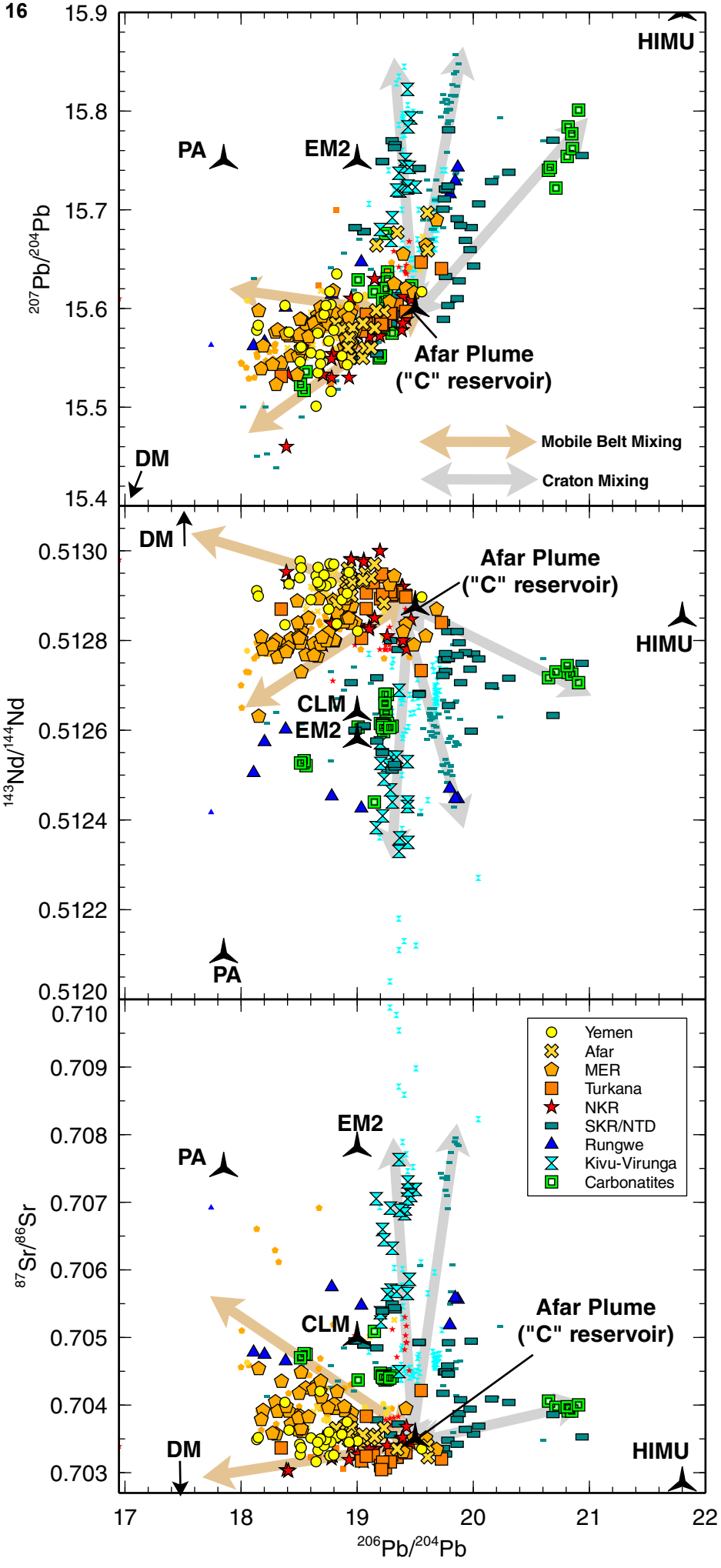
HIMU
PA
EM2
Afar Plume
("C" reservoir)
Mobile Belt Mixing
Craton Mixing
DM
$^{207}Pb/^{204}Pb$
15.9
15.8
15.7
15.6
15.5
15.4
DM
Afar Plume
("C" reservoir)
HIMU
CLM
EM2
PA
$^{143}Nd/^{144}Nd$
0.5130
0.5128
0.5126
0.5124
0.5122
0.5120
Yemen
Afar
MER
Turkana
NKR
SKR/NTD
Rungwe
Kivu-Virunga
Carbonatites
EM2
PA
CLM
Afar Plume
("C" reservoir)
DM
HIMU
$^{87}Sr/^{86}Sr$
0.710
0.709
0.708
0.707
0.706
0.705
0.704
0.703
17
18
19
20
21
22
$^{206}Pb/^{204}Pb$

Figure 17

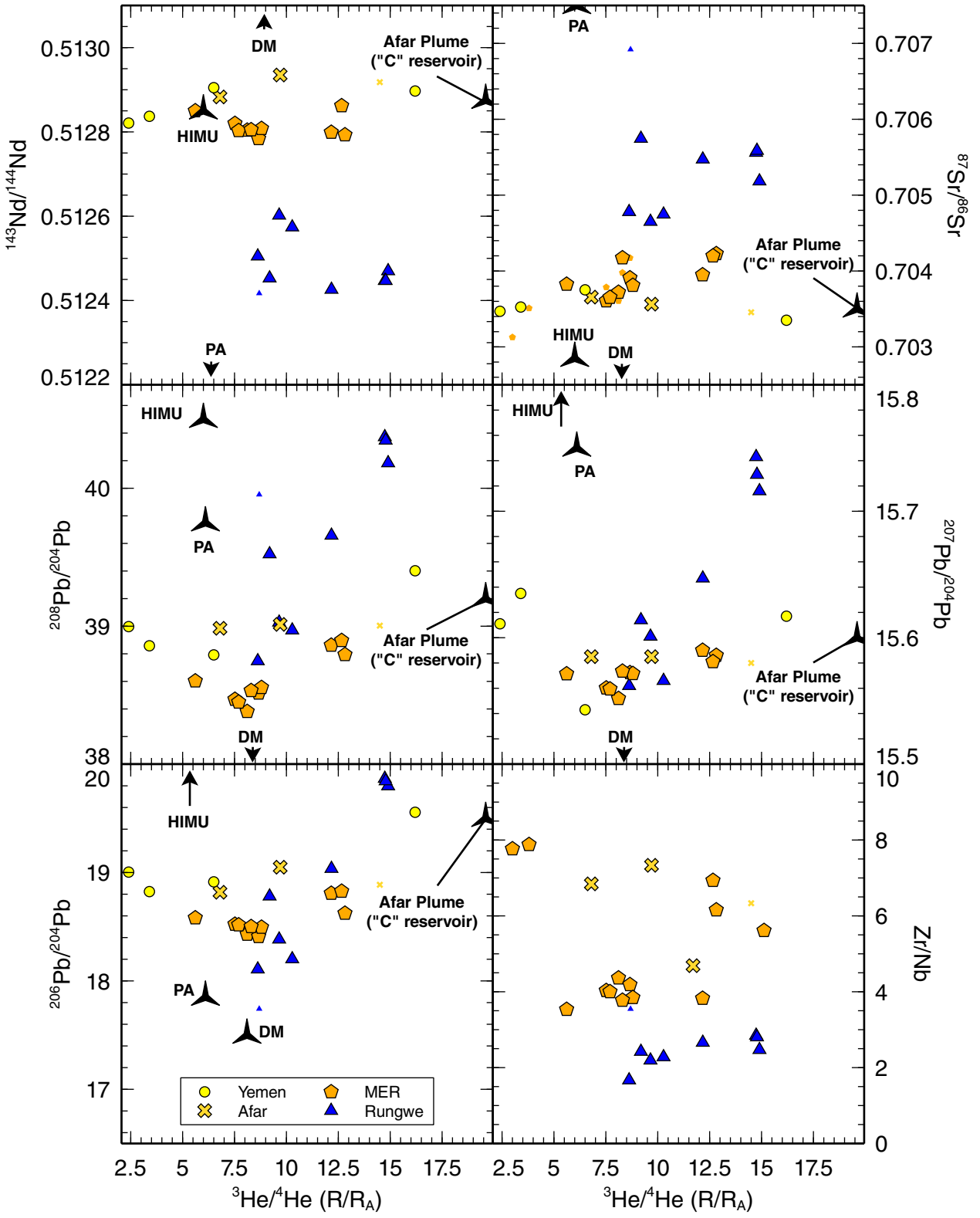
DM
Afar Plume
("C" reservoir)
HIMU
PA
$^{143}Nd/^{144}Nd$
$^{87}Sr/^{86}Sr$
$^{208}Pb/^{204}Pb$
$^{207}Pb/^{204}Pb$
$^{206}Pb/^{204}Pb$
Zr/Nb
$^{3}He/^{4}He$ (R/R_A)
Yemen
Afar
MER
Rungwe

Figure 18

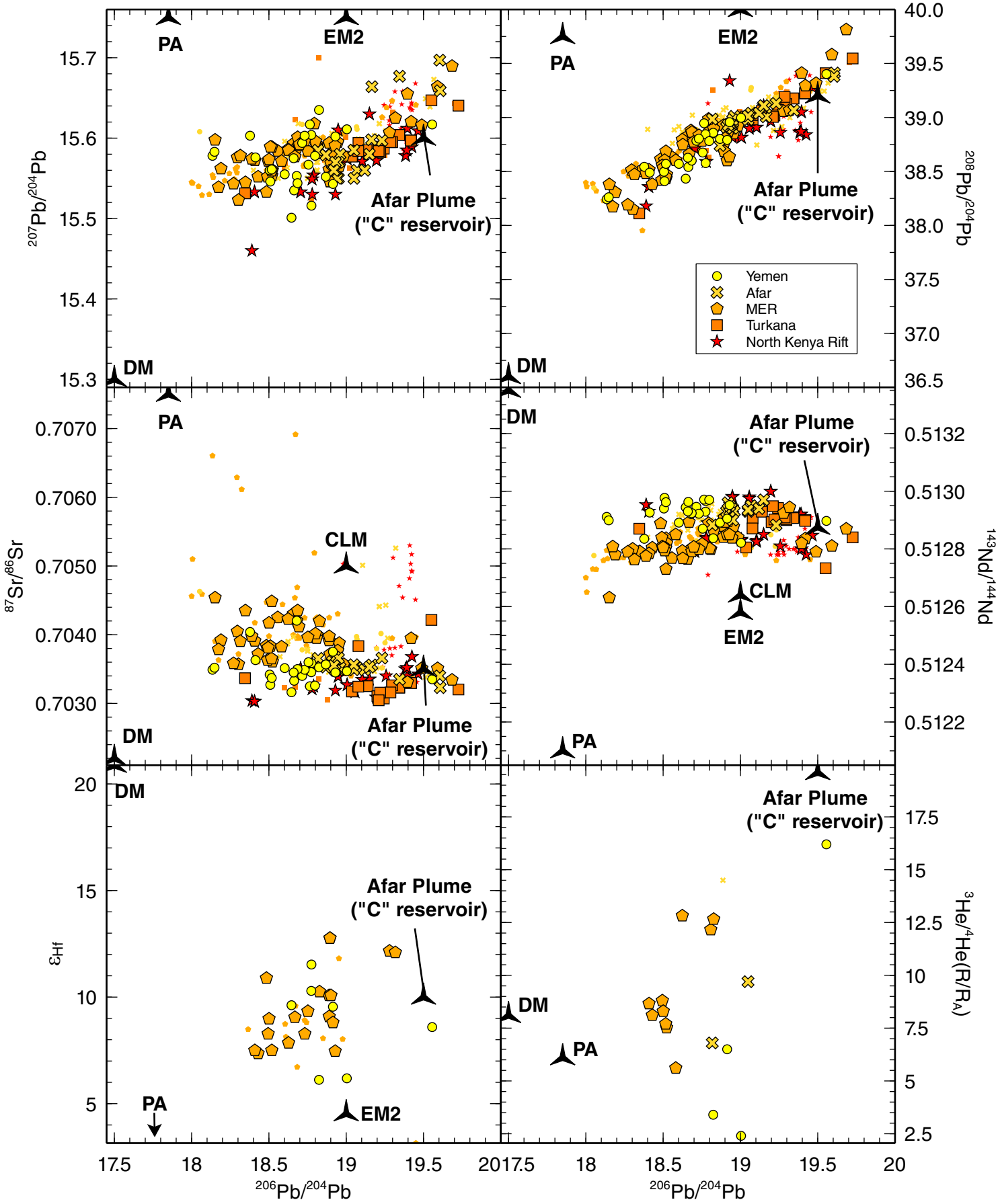
PA
EM2
DM
CLM
Afar Plume
("C" reservoir)
Yemen
Afar
MER
Turkana
North Kenya Rift
$^{207}Pb/^{204}Pb$
$^{208}Pb/^{204}Pb$
$^{87}Sr/^{86}Sr$
$^{143}Nd/^{144}Nd$
ε_{Hf}
$^{3}He/^{4}He(R/R_A)$
$^{206}Pb/^{204}Pb$
$^{206}Pb/^{204}Pb$

Figure 19

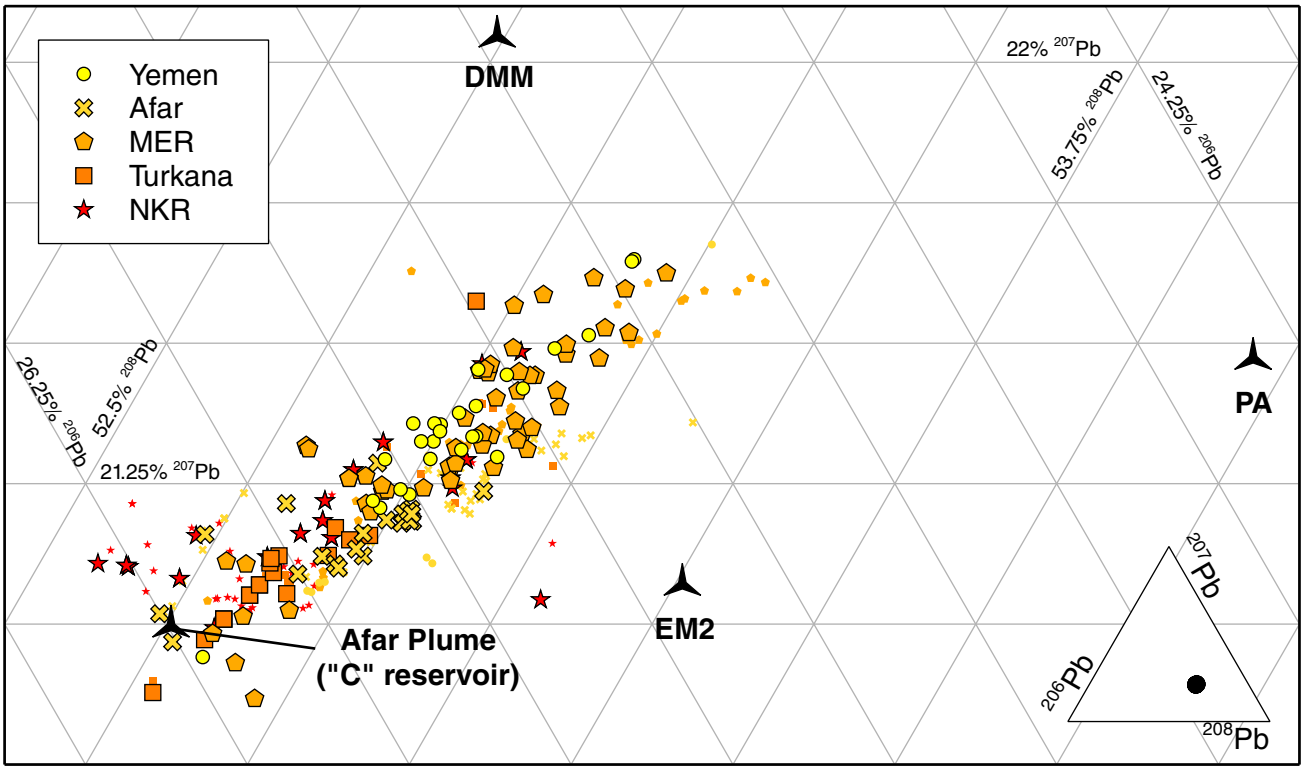
Yemen
Afar
MER
Turkana
NKR
DMM
22% 207Pb
53.75% 208Pb
24.25% 206Pb
PA
26.25% 206Pb
52.5% 208Pb
21.25% 207Pb
EM2
Afar Plume
("C" reservoir)
207Pb
206Pb
208Pb

as to the specific reservoirs that may participate in the melting processes noted above. The lithospheric mantle beneath East Africa has undergone enrichment through the percolation of sub-lithospheric derived melts and fluids over an extended interval, which close to the Tanzania craton, has resulted in a layered lithospheric mantle exhibiting extreme isotopic ratios. Elsewhere, the lithospheric mantle has also undergone enrichment but given the more juvenile age of this lithosphere, less extreme isotopic values have developed. Material rising from the African Large Low Shear Velocity Province (LLSVP) has also metasomatized the lithospheric mantle, and thus lavas exhibiting a trace element signature linked to melting within the lithospheric mantle may exist as any number of reservoirs or mixtures of the same. Material derived from the convecting upper mantle incorporates the Afar Plume endmember, a depleted mantle endmember, and some form of lithospheric endmember. The isotopic characteristics of magma suites from throughout the region form arrays that broadly converge on the composition of the Afar Plume, despite some complexity where the plume material has formed a hybrid plume-lithosphere component. The convergence of these arrays strongly supports a model whereby the prevalent composition of material rising from the African LLSVP beneath the EARS is broadly equivalent to the composition of the Afar Plume.

1. Introduction

The spatial and temporal variability in alkalinity and silica saturation of lavas within the East African Rift System (EARS) is a first order observation in any synthesis of regional magmatism (Baker, 1987; Foley et al., 2012). There is a general trend within the rift for a progression of decreasing alkalinity over time – this is particularly apparent in the Kenya Rift where transitional basalts do not manifest until ca. 7 Ma; the earlier magmatic periods are dominated by alkaline lava series. There is also a spatial variability where, in comparison to activity in Turkana and Ethiopia, the magmatic products of the Kenya Rift, and Western Branch are typically much more

alkaline and less silica-saturated. The cause of this distinct compositional difference appears linked to the presence of the Tanzania craton and it's reworked margin (MacDonald et al., 2001; Foley et al., 2012). MacDonald et al. (2001) argues that on the traverses across the rift, the degree of silica-saturation (and under-saturation) in erupted lavas varies: for regions on the craton 80% of the rocks were nephelinites or basanites, while 20% are mix of alkali basalts and hypersthene-normative basalts; along the reworked margin, 33% were nephelinites or basanites and 67% were alkali basalts and hypersthene-normative basalts; for the mobile belt, these values are reversed and 21% are the more alkaline rocks which 74% are transitional to sub-alkaline. These observations, while not fully representative of the range of rocks found in these regions, suggested that there was a greater alkalinity and degree of silica-undersaturation in lavas associated with the Tanzania craton. However, the specific causes for these observations of lava heterogeneity with proximity to the craton remained uncertain.

In order to further constrain the potential mechanisms associated with the varying alkalinity in the region, temporal observations of the variation of alkalinity at any given location provided some initial clues. These broad-scale observations noted that at any location, the degree of silica-saturation would increase over time. These observations resulted in a model for magma formation which envisaged that the process of rift development would result in the depth of melt generation becoming progressively shallower, and the degree of melting increasing over time. This model was consistent with the necessity of thinning the lithospheric mantle during rift development, however the model was soon realized to be overly simplistic. MacDonald (1994) showed that at individual volcanic centers (e.g. Olorgesailie), the entire spectrum of silica-undersaturated rocks types can be observed to erupt almost synchronously. Further problems with this temporal model were apparent within the Northern Tanzania Divergence, where lavas exhibit an initial temporal shift towards more Si-saturated lavas, followed by a sharp reversal back towards silica-undersaturated compositions (Neukirchen et al., 2010).

Despite these temporal setbacks, MacDonald et al. (2001) used the Ce/Y vs Zr/Nb (as proxies for heavy rare earth elements - HREE) to argue that the transition from nepheline-normative to hypersthene-normative lavas is coincident with a shallowing of the mantle source, consistent with the broad hypotheses of a depth of melting-related control on the degree of silica-saturation in erupted lavas. This depth-related correlation was observed throughout the region, spanning within-rift, and rift-marginal suites (Le Roex et al., 2001; MacDonald et al., 2001; Späth et al., 2001). However, the correlation between the degree of melting and degree of silica-saturation was less clear. MacDonald et al. (2001) suggested that on the basis of their dataset in the Kenya rift, no such correlation was evident. In contrast, authors working in the Northern Tanzania Divergence (NTD) showed some degree of correlation between these observations (Le Roex et al., 2001; Späth et al., 2001; Mana et al., 2015). The origin of this dichotomy has been unclear if interpreted in terms of a simple peridotite melting model, however the melting of more complex lithologies might help resolve this apparent conflict. Mana et al., (2015) suggest that within the North Tanzania Divergence, melting depths range from 140-85 km. Given that lithospheric mantle xenoliths provide evidence that the lithospheric mantle continues to a depth of at least ~145-160km at the nearby Labait/Lashaine cones, it was suggested that melt generation in the NTD occurs solely within the sub-continental lithospheric mantle (Mana et al., 2015). The realization that much of the melt generation within that region occurred within the continental lithospheric mantle, where unusual hydrous phases such as amphibole and phlogopite are stable (e.g., Class and Goldstein, 1997), presented an opportunity to explore the role of mantle metasomes on melt generation and perhaps resolve the long-standing questions about silica-saturation in rift lavas that still remain unanswered. Metasomes are defined herein as non-peridotite lithologies within the lithospheric mantle that are created by the percolation of melts/fluids and can contain a diverse suite of minerals – e.g. amphibole, phlogopite, apatite, carbonate, Fe-Ti oxides, pyroxenes (Fig. 1).

In this contribution, I collate the combined insights on the origin of magmatism in East Africa presented in parts I to IV of this synthesis series to explore the geochemical characteristics of rift magmatism from origin to eruption. The results of this synthesis demonstrate that rift lavas preserve evidence of complex lithosphere-asthenosphere interaction. Melt generation occurs dominantly within two regions – enriched metasomes located in the lithospheric mantle, and within the convecting upper mantle (Fig. 2). This assertion might seemingly frame the concept of rift magmatism as a simple story revolving around two sources, however the details are labyrinthine. When considering a metasome within the lithospheric mantle one must consider its modal mineralogy and antiquity; the lithospheric mantle has been accumulating such metasomes since its formation, resulting in myriad generations and compositions of easily fusible domains that may yield melt during a thermobaric disturbance. These metasomes may span much of the isotopic space defined by the upper mantle. When considering potential melt sources located in the convecting upper mantle, one must consider the relative role of the depleted MORB mantle, thermochemically distinct material rising into the upper mantle from the African Large Low Shear Velocity Province (LLSVP), and the potential contamination of the upper mantle by lithospheric material mixed into it. Melt from each of these domains may also mix and hybridize to form erupted lava compositions.

The natural complexity that accompanies such processes yield vectors in compositional and isotopic space that reveal the mechanisms of magma formation and the sources of rift lavas. The isotopic data arrays converge on the composition defined for the Afar Plume, which is broadly equivalent to the “C” mantle reservoir of Hanan & Graham (1996). While I term this component the Afar Plume in this paper, the convergence of such arrays suggests that this component contributes to magmatism throughout the EARS – an observation consistent with existing geochemical and geophysical evidence for the widespread presence of anomalous

material within the East African upper mantle (Rooney et al., 2012c). Thus, this common isotopic signature may reflect a significant component of material rising from the African LLSVP.

While the Afar Plume signature appears ubiquitous, in many cases its contribution to rift magmatism is indirect. Where there is lack of clear correlation between isotopic fingerprints and trace element characteristics, it is proposed that the interaction of melts derived from the Afar Plume with the lithospheric mantle yields mantle metasomes with the isotopic fingerprint of the Afar Plume. Melts of these plume-related metasomes then interact with other potentially much older metasomes at shallower levels within the lithosphere to generate hybrid isotopic arrays. The composition of the older metasomes contributing to this rift magmatism vary significantly as a function of proximity to the Tanzania craton: older metasomes with more extreme isotopic compositions are evident in proximity to the craton; less extreme isotopic enrichment is evident within the Pan-African mobile belt domains. The insights presented herein will undoubtedly evolve over time as continued investigation reveals new mechanisms and reservoirs and thus this contribution should be seen as a waypoint – a window into what the accumulated knowledge has deduced thus far.

2. Background

The EARS preserves within it the largest range in magma types on the planet. From the early studies of the ultrapotassic rocks of the western branch of the EARS (Holmes, 1937) to the voluminous Stratoid basalts of Afar, the diversity in lavas requires a multitude of magmatic processes. The existing divisions, which are based upon alkalinity and silica-saturation, are helpful as observational tools, but are of limited utility is assessing the mode of origin of rift lavas. For this reason I have divided primitive lavas within the EARS into Types I – VI on the basis of primitive mantle normalized patterns of incompatible trace elements collected on bulk

rock samples (Fig. 3). Samples selected as exemplars are basalts (excepting Type IIa, which is a nephelinite) that range from 6.7- 8.7 wt. % MgO (exception is Type V, which has 14.9 wt. % MgO). These patterns fingerprint the source material which melted to form the derivative lava and are thus more effective probes as to the origin of these magmas. Fuller descriptions of each lava type and the necessity for its creation are found in volumes I through IV of the synthesis series but are summarized here for completeness.

2.1 Type I – An Incompatible Trace Element Depleted Family of Magmas

This magma type is defined primarily from flood basalts erupted during the Eocene and Oligocene. Group Ia is defined by the distinctive trace element patterns evident in Low Titanium (LT) Oligocene Flood Basalts from the NW Ethiopian Plateau. The extreme depletions in most elements (relative to other magma series) is notable. This group is generally restricted to the Oligocene and does not participate in rift magmatism. Group Ib is typified by magmas from the Eocene flood basalt event. In particular, the Amaro flood basalts show a similarly depleted signature to the LT flood basalts that typify Type Ia. However, this group does not show the LILE spikes that are ubiquitous in Type Ia lavas (Fig. 3). In aggregate Type I lavas are not observed in the EARS post Oligocene. The origin of these lavas is associated with a mantle plume, however the precise mode of origin remains uncertain (though some work is currently under way exploring this issue - e.g., Krans et al., 2018).

2.2 Type II – The OIB family of Magmas

Type II magmas have been previously divided into an A and B variety. Group IIa magmas are typically MgO rich and have moderate SiO_2 and CaO values. In contrast, Group IIb magmas typically have much lower SiO_2 content and much higher CaO and indicative of derivation for a carbonated source. The source of these lavas remains controversial, with potential origin within the sub-lithosphere through eclogite melting (Natali et al., 2016), convective destabilization

(drip) (Furman et al., 2016), or within the lithospheric mantle through destabilization of ancient or recent metasomatism (Beccaluva et al., 2009; Rooney et al., 2014b, 2017). The OIB family of magmas have particular significance when considering the rifting events in East Africa. As has been outlined in Parts II, III, and IV, these magma types are typically encountered during the initial stages of lithospheric destabilization (Fig. 2). In particular, within the southern Kenya Rift, these magmas types are typically the first erupted, subsequently transition to mixed source melts, and then eventually to melts derived from the convecting upper mantle. The extant data strongly points to a lithospheric origin for these magmas (Fig. 2). It should be noted that the isotopic characteristics of these magmas varies widely. The reason for this relates to the potential origins of the metasomes that destabilize and melt to form Type II lavas. Simply put, the trace element signature observed (Fig. 3) is controlled by the mineralogy of the metasome, and the composition of the melt that initially formed it. However, the isotopic composition of these magmas may vary based upon the antiquity of the metasome. There is clear evidence for the Afar plume interacting with the lithospheric mantle and forming recent metasomes that have subsequently destabilized (Menzies and Murthy, 1980; Baker et al., 1997; Nelson et al., 2019). These metasomes, which are relatively young, are dominated by the isotopic signature of the Afar Plume. In contrast, ancient metasomes have evolved insitu and can exhibit isotopic signatures that are distinct from the Afar Plume (Rooney et al., 2014b). A key issue in any study that encounters this family of magmas is resolving these potential signatures.

2.3 Type III – The Moderate Family of Magmas (The Ambient Upper Mantle)

This group of magmas is typified by a distinctive Ba peak, a U-Th trough, and a Nb-Ta peak (Fig. 3). The slope of the REE are controlled by the depth and degree of melting. This family of magmas is ubiquitous within the EARS. Clues as it its origin come from temporal constraints as to when this signature first appears within a given suite of rift lavas. Type III magmas are found

throughout the well-developed rifts in Afar, MER, and Northern Kenya Rift, where lithospheric mantle reservoirs currently have limited contribution to erupted lavas (Fig. 2). In contrast, within the craton-influenced southern Kenya Rift, the initial dominance of Type II magmas gives way (through an intermediate phase – see Type IV) to the appearance of Type III. These observations are consistent with its hypothesized origin within the sub-lithospheric mantle as a mixture of plume, depleted mantle, and African lithosphere (Rooney et al., 2012a; Rooney, 2017). The occurrence of this magma type regionally, supports a somewhat consistent composition within the East African Upper mantle (Fig. 2).

2.4 Type IV – An intermediate composition

This magma type was not recognized in the initial synthesis of older lavas within the EARS (Rooney, 2017). Its type locality is in the modern magmatism occurring in parts of the Turkana Depression and the ca. 6 Ma magmatism in the Kenya Rift. It is typified by a pattern that is a simple mix of Type II and Type III magma (Fig. 3). The primitive mantle normalized plot displays the broad curved characteristics of Type II magmas in the more incompatible trace elements with a pronounced negative K anomaly, but also has a Nb-Ta peak and a break in slope for U-Th (Fig. 3). This pattern is clearly the result of the influence of a Type III magma on a Type II magma and suggests that Type IV magmas are hybrids. This assertion is consistent with observations from the southern Kenya Rift where this lava type is found temporally between the early Type II rift magmas, and the modern Type III magmas (Fig. 2). Caution is advised when considering the isotopic composition of these lava types as they may exhibit a wide range of compositions that relate to the original composition of the metasome that created the Type II magma, and the precise ratio of endmembers within the Type III magma (Fig. 2). Recognition of this group is, however, important as the miscategorization of this magma as a Type III may result in erroneous interpretations as to the magnitude of plume contribution to rift magmatism in

a given region. Equally, the miscategorization of such lavas as Type II could be used as justification for an origin of all Type II lavas in a region from sub-lithospheric reservoirs.

2.5 Type V – Potassic Metasomes

This magma pattern is typified by one of the major magmatic trends within the Virunga Volcanic Province within the western branch of the EARS. In particular, the composition of lavas from Nyamuragira, Karisimbi, Sabinyo, Muhavura, old Bisoke, and Gahinga define Type V lavas. These lavas have a relatively flat pattern in the most incompatible elements within the primitive mantle normalized figure, with small negative anomalies in U and K, and a mild depletion in Zr-Hf (Fig. 3). The origin of these lavas has been described by Furman & Graham (1999) as melts derived from a phlogopite-bearing lithospheric mantle metasome.

2.6 Type VI – Depleted Source

Type VI lavas are defined on the basis of two rare occurrences and are characterized by extreme depletion in the most incompatible trace elements (Fig. 3), have unradiogenic Pb isotopes, and radiogenic $^{143}Nd/^{144}Nd$. These lava types are found only within the Afar Depression, and even then only in lavas that are <5 Ma. It might be tempting to connect such lavas with melts of the depleted MORB mantle, however there are unusual peaks in LILE (Fig. 3), and $^{87}Sr/^{86}Sr$ in these samples is more radiogenic than would be consistent with a modern MORB source. The current model for the genesis of such lavas is through melting of a depleted component ‘intrinsic’ to the Afar plume (Barrat et al., 2003; Daoud et al., 2010). However, further examination of these lavas is necessary to constrain the origin of this rare component.

2.7 Conditions of Melting

The existing data clearly show that both lithospheric and sub-lithospheric reservoirs are contributing to magmatism along the EARS. When magmatic flux within the rift is examined (on

the basis of total melt generation, not erupted volumes), the resulting values are 0.03 km^3/yr and require upwelling rates of 40-140mm/yr, consistent with a mantle plume contributing to melt in the region (Latin et al., 1993). Other intensive parameters such as mantle potential temperature also argue for elevated temperature in the regional upper mantle. The clearest constraints on magma generation processes have derived from mafic lavas in the Turkana Depression, the MER, and Afar. In a general sense, decompression melting of the upper mantle during rifting will generate magmas, however the lack of a strong sense of lithospheric thinning throughout most of the rift requires that either composition or elevated temperatures be a factor in melt generation. Composition may play a role in melt generation where metasomatic enrichment of the lithospheric mantle may yield unstable metasomes (Rogers et al., 1998; Rooney et al., 2017). However, the signature of such exotic metasomatic lithologies is not present in all EARS lavas. Existing studies of basaltic magmatism in Afar have suggested mantle potential temperatures (T_P) that exceed ambient conditions by about 100K (Ferguson et al., 2013; Armitage et al., 2015). These results are consistent with broader results from the EARS that found the mantle beneath the entire rift is commonly elevated by 100K, and in places up to 140K (Rooney et al., 2012c). This observation of a rift-wide enhanced T_P is consistent with isotopic constraints that suggest the presence of deep mantle material within the upper mantle extending from Rungwe to Afar (Halldórsson et al., 2014). It is thus apparent that a primary factor in melt generation in the EARS is the presence of warm, deep mantle material carried into the upper mantle (Furman et al., 2006a; Rooney et al., 2012a).

Within actively extending immature rift environments, the depth at which magma is generated is frequently close to the lithosphere-asthenosphere boundary (or within the lithospheric mantle – see discussion later). This results in only the upper most portion of the convecting mantle being decompressed sufficiently to generate melt. While a potentially useful blunt tool at assessing lithospheric thickness variations (Rooney, 2010), the depth at which

asthenospheric-derived magmas are generated is complicated by the impact of enhanced T_P. Where the mantle exhibits increased T_P, the consequent earlier commencement of melting at deeper levels within the melting column will result in an apparent 'deeper' signature in the resultant magmas. Such a result is evident for lavas in Afar; here axial magmas exhibit a trace element signature consistent with deeper melting, while off-axis magmas are seemingly derived from shallower levels in the mantle (counter to the lithospheric thickness conceptual model) (Ferguson et al., 2013). This inconsistency is easily resolved when considering that axial magmas contain a greater component of the Afar plume, and this thermally anomalous plume material began melting at deeper levels, resulting in the observed trace element signature in the erupted lavas (Ferguson et al., 2013). Thus, the depth of melt generation in the asthenosphere beneath East Africa appears to be fundamentally controlled by both the degree of lithospheric thinning, and the temperature of the ambient mantle. In a broad sense, melting conditions within the Afar and the Ethiopian rift appear to be in the range of 55 -100 km depth (Rooney et al., 2005; Furman et al., 2006a; Ferguson et al., 2013), and potentially deeper along the rift margin (Chiasera et al., 2018).

Uranium series isotopes provide an insight into the melting and melt transport processes in the region. Fundamentally, the fractionation of Th from U during melting or melt transport creates relatively short-lived disequilibrium that is evident in terms of $^{230}Th/^{232}Th$ vs. $^{238}U/^{232}Th$. This isotopic perturbation will eventually return to equilibrium as the rocks age. Most young mantle-derived rocks plot above the equiline (i.e. a line representing a slope of unity – 1:1: Dickin (2018)) , consistent with the role played by residual garnet in fractionating Th from U during mantle melting (e.g., Macdougall, 1995). A corollary to this is that older rocks, where decay has occurred, have returned to equilibrium and plot on the equiline. Young Kenya Rift lavas exhibit disequilibrium (i.e. above the equilin), consistent with most MORB and OIB type lavas (Rogers et al., 2006). Lavas from the Kenya Rift exhibit significant fractionation in ^{238}U and

^{230}Th that cannot be accounted for through partitioning associated with garnet. An alternative mechanism for creating disequilibrium between these isotopes is through a dynamic melting process. This dynamic process continuously removes melt as the mantle upwells, and disequilibrium is a function of the upwelling rate and mantle porosity (lower upwelling rates results in greater disequilibrium). A dynamic melting regime (or equilibrium melt transport) was suggested by Rogers et al. (2006), who indicate that the lowest mantle upwelling rate created maximum disequilibrium. To allow such upwelling to occur, this melting model requires an origin for magmatism within the asthenosphere. However, this asthenospheric origin must be reconciled with the clear evidence from other isotopic systems and trace element behavior for a contribution from the sub-continental lithospheric mantle (SCLM).

Rogers et al. (2006) noted that the behavior of ^{230}Th/^{232}Th and ^{238}U/^{232}Th was inconsistent with asthenospheric sources and instead deviated towards SCLM derived lavas. Moreover, the observed elevated Zr/Hf (and low Zr) characteristics of Kenya rift lavas is not common in most mantle reservoirs and likely required metasomatism in the source of such lavas (Rogers et al., 2006). Thus, a SCLM source with asthenosphere-like melting behaviors may be needed. Rogers et al. (2006) suggested that these observations were consistent with thermo-mechanical erosion of the SCLM during rifting. This model envisages material from the SCLM being incorporated into the upper mantle and melting. Such a model is also proposed for the mantle beneath the MER and may thus be an important mechanism acting to thin the SCLM (Rooney et al., 2012a).

It is important to note that these melting models are based upon source compositions that are defined on the presumption of a peridotite lithology, however lavas erupting in East Africa do not all derive from melting of peridotites (e.g., Rosenthal et al., 2009; Rooney et al., 2017). If Kenya Rift lavas were derived directly from the SCLM (which can contain non-

peridotite lithologies such as pyroxenites and amphibolites), could the U series isotopes be explained? The observed lack of a correlation between $^{230}Th/^{238}U$ and the degree of HREE depletion (where residual garnet controlled this relationship), might point towards HREE depleted amphibole in the melting source, but melting of such a lithology would not significantly fractionate ^{230}Th from ^{238}U as there is little difference in the behavior of these elements (e.g., Latourrette et al., 1995). It should be noted that amphibole has a particularly low partition coefficient for U and Th (e.g., Latourrette et al., 1995).Thus, other minor phases within the metasome that may have higher partition coefficients could control the behavior and potential fractionation of these elements during melting. While a dynamic melting model is consistent with the available data, further work is needed on the impact of other phases within mantle metasomes in terms of Th and U fractionation during melting of a mantle metasome.

2.8 Craton vs Mobile Belt

This synthesis of East African magmatism has been arranged in terms of magmas erupted in proximity to the Tanzania craton, and those that erupted through the Pan-African mobile belt (Fig. 4). The rationale for this division is the profound impact the lithosphere imparts upon the composition of the erupted products. This is not a new concept and has been discussed by prior authors (e.g., MacDonald et al., 2001; Foley et al., 2012). I have focused upon lavas erupted during the Quaternary throughout this contribution when considering variation with the province and examine the spatial variation from Yemen to Rungwe (Fig. 5). For Quaternary samples that lie outside of the primary axis of the East African Rift (e.g., on one of the plateaus), they have been assigned to the nearest region adjacent to the plateau (e.g., Quaternary lavas from the Bale Mountains/Tullu Dimtu on the Eastern Ethiopian Plateau are assigned to the Main Ethiopian Rift; Fig. 6). Throughout this contribution, I show lavas that are above 5 wt. % MgO as large symbols, and lavas less than 5 wt. % MgO or where the MgO content is not known as

smaller symbols. Approximate potential source reservoirs are also shown, though it should be noted that these reservoirs may occupy a larger space than the average value plotted.

The most pronounced trace element difference between the two regions (cratonic and mobile-belt) is the degree of enrichment of the most incompatible trace elements. Most lavas form an array with some notable outliers. In Afar, some particularly depleted samples plot in a space closer to depleted mantle, in contrast some samples from Rungwe fall off the array towards low Zr-Nb resulting from the influence of apatite in their source (Fig. 7). Carbonatites extend to much more enriched values, however these bulk rock data are likely not reflective of liquid composition given the potential for the accumulation of trace element enriched crystal phases and post-eruption alteration (e.g., Weidendorfer et al., 2017). The carbonatite data are included here given the influence carbonatites have historically had on magmatic models in East Africa. On first inspection there is a pronounced separation in the warm and cold colors (Fig. 7). Cool colors have been assigned to cratonic-related samples and these should typically show more enrichment in incompatible trace elements than the warm colored samples that are assigned to the mobile belt. The least incompatible trace element enriched samples are derived from Afar, while the most enriched (excluding carbonatites) are from the Virunga-Kivu region. More evolved samples (i.e., lower MgO) are typically displaced to higher values of Zr-Nb at the same La/Sm for mobile-belt samples (Fig. 7). In contrast, evolved samples from the craton are deflected towards lower Zr-Nb and higher $(La/Sm)_{CN}$.

Even more profound differences between the cratonic and mobile-belt magmas are evident in isotopic space. Variation in $^{87}Sr/^{86}Sr$ and $^{143}Nd/^{144}Nd$ show a sharp division between the magmas erupted in the two regions (Fig. 8). Lavas erupted in the cratonic regions of the rift exhibit evidence of interaction with old lithospheric reservoirs – manifesting as very radiogenic $^{87}Sr/^{86}Sr$ and unradiogenic $^{143}Nd/^{144}Nd$ (Fig. 8). Contamination with lithospheric materials of

more evolved samples in the mobile-belt regions results in elevated $^{87}Sr/^{86}Sr$ without any sympathetic change in $^{143}Nd/^{144}Nd$, while contamination of lavas in the cratonic region seems to result in changes to both the isotope ratios (Fig. 8). Differences within regions are also evident. When considering mafic samples from mobile-belt regions alone (i.e. MgO > 5 wt. %), two parallel trends are observed wherein Yemen and Afar form an array at elevated $^{87}Sr/^{86}Sr$ for a given value of $^{143}Nd/^{144}Nd$, in comparison to Turkana and the North Kenya Rift that have less radiogenic $^{87}Sr/^{86}Sr$ (Fig. 9). Such variations begin to reveal the influence of distinct isotopic lithospheric and sub-lithospheric reservoirs contributing to rift magmatism.

3. Alkalinity, Silica-Saturation and Magma Series in the East African Rift

The data presented in the prior section make a compelling case that both lithospheric and sub-lithospheric reservoirs were involved in melt generation within the EARS. Resolving these contributions is more complex. Lavas erupted in the East African Rift are all potentially subject to interaction with the continental lithosphere. The nature of this interaction can range from magmas being generated wholly within the lithosphere, mixing between sub-lithosphere derived and lithosphere-derived melts, or by magma evolution (and contamination) at lithospheric depths. Thus, prior to any discussion about potential convecting upper mantle reservoirs, it is critical that the geochemical fingerprint of the lithosphere on rift lavas is fully constrained. In a broad sense there are two domains wherein rift lavas may gain a lithospheric signature: (A) within the continental crust; (B) within the lithospheric mantle. Below I initially focus on the more evolved rocks within the East African Rift (i.e. those on the high SiO_2 side of the Daly Gap; Peccerillo et al. 2007). These evolved rocks have had the maximum residence time within the lithosphere, and thus are most likely to display evidence of lithospheric processes.

3.1 Magma Evolution within the Continental Crust

3.1.1 Fractional Crystallization

Fractional crystallization is currently regarded as the most prevalent process facilitating magmatic evolution within Afar, the MER, and the northern and central Kenya Rift. Exploring the earlier literature, the reader will encounter a period where there was some debate over the relative role for crustal anatexis over fractionation (e.g., Davies and Macdonald, 1987; MacDonald et al., 1987). In the intervening years, a consensus has developed wherein fractional crystallization became the dominant guiding principle driving models of magma evolution within the region (e.g., Peccerillo et al., 2003; MacDonald and Scaillet, 2006)

Examination of the major elements and the degree of silica undersaturation provides some potential constraints on where fractionation may occur. While deep fractionation of Ca-pyroxene at pressures of about 0.8 GPa may result in enhanced silica-undersaturation (e.g., George and Rogers, 2002), fractionation of assemblages at lower pressures tends to have the opposite effect (MacDonald, 1994). Mildly alkaline modern rocks from the rift (e.g., Ol Tepsi in the southern portion of the rift, and young volcanic centers elsewhere: Paka, Silali, Emuruangogolak, Barrier and the flanks) (Fig. 10) plot close to the critical plane of silica-undersaturation suggesting fractionation at pressure equivalent to the base of the crust (MacDonald, 1994; MacDonald et al., 2001). Similar observations have been made in the Afar, the MER, and Kenya Rift, where evolved compositions are typically associated with composite central volcanoes (e.g., Weaver et al., 1972; Weaver, 1977; Field et al., 2013; Siegburg et al., 2018). The depth at which fractionation occurs can be quite variable and has a strong control on the fractionation assemblage. In less well-developed rift sectors, fractionation of mafic lavas occurs initially at depth, and then through a series of shallower systems prior to eruption (Rooney et al., 2005). Where the magma plumbing system is better developed, some fractionation may still occur at depth but the majority of magmas ascend to shallower crustal

depths before fractionating (Rooney et al., 2007, 2011). The silicic lavas of the Ethiopian Rift and Afar are typically derived from much shallower magma chambers that have been fed by the evolving mafic system (Fig. 11). Given the presence of calderas, and Interferometric Synthetic Aperture Radar (INSAR)-detected inflation and deflation responses around edifices, there is a very shallow component to these silicic systems (Biggs et al., 2011).

The crystal assemblage fractionating from silica-undersaturated magmas includes olivine, pyroxenes, feldspars and feldspathoids, titanite, and apatite. The phases found within the more alkaline suites varied significantly on the basis of the alkalinity and magma type, (e.g., Kabeto et al., 2001a; Clément et al., 2003). Alkali basalts typically contain olivine, clinopyroxene, and plagioclase; with increasing differentiation apatite and Fe-Ti oxides appear. More evolved compositions can contain fayalite, clinopyroxene, amphiboles, aenigmatite, alkali feldspar and feldspathoids.

Studies that have examined oxygen fugacity in rift lavas have consistently reported values around the QFM buffer (Weaver, 1977; Scaillet and MacDonald, 2003). The evolution from basalt to trachyte is a function of olivine, clinopyroxene, plagioclase, and Fe-Ti oxide fractionation (Weaver, 1977). For trachytes, variation is a result of alkali feldspar fractionation and to a lesser extent, clinopyroxene, fayalite, and Fe-Ti oxides (Weaver, 1977). In peralkaline rhyolites there are additional roles for biotite, amphibole, aenigmatite, and zircon (MacDonald et al., 1987). The OH-bearing phases in peralkaline rhyolites may actually contain significant volumes of F, and this may alter the stabilities of these phases such that amphibole persists to low pressures (Scaillet and MacDonald, 2001). Where the oxidation state deviates from these typical values, unusual phases are evident locally. Baudouin et al. (2016) found that nephelinites in Hanang (at the very southern edge of the NTD; Fig. 10), also contained phenocrysts of garnet and pyrrhotite. The presence of these phases was explained by a more

oxidized magma in Hanang, in contrast to the slightly more reduced nephelinites further north in the NTD, which can have wollastonite (Baudouin et al., 2016). It should be noted that melilites can also evolve through differentiation into low-Mg nephelinitic magmas (Baudouin et al., 2016)

Cyclicity is observed where multiple periods of a basalt-to-trachyte transition may be observed at a single edifice such as Emuruangogolak (Weaver, 1977) (Fig. 10), which highlights continuing connectivity between mantle-derived basalts and crustal magma differentiation systems. Equally, such cyclicity may also be evident in a much wider spatial sense: Evolved magma centers may define distinct magmatic cycles throughout an entire province such as the central MER (and not just a single edifice) (Hutchison et al., 2016). In such instances, magmatic flare-ups are associated with an initial widespread pulse of basalt volcanism, which subsequently differentiates and erupts as more evolved compositions (Hutchison et al., 2016). These cyclicity observations are strong evidence of a continued linkage between mantle-derived magmas and the crustally-hosted magma chambers of the more evolved central volcanoes.

3.1.2 Crustal Assimilation

It was argued that, based on the preservation of silica undersaturation and the inference that rocks did not have a significant residence time in the crust, minimal crustal assimilation has occurred in many suites along the Kenya Rift (MacDonald, 1994). The lack of a recognizable signature of crustal interaction was supported by the high concentrations of incompatible trace elements. For example, it was argued that high concentrations of Sr in a rift lava would minimize potential crustal contamination of the $^{87}Sr/^{86}Sr$ isotopic system (Rogers et al., 2000). Despite this ambiguity in assessing the role of crustal assimilation more broadly, there is consensus that there is strong evidence for the involvement of the crust in lavas from many evolved edifices such as in Naivasha (Olkaria) (Davies and Macdonald, 1987; MacDonald et al., 1987). These rocks, which exhibit shallow fractionation characteristics and evidence of basalt-crust interaction

(MacDonald, 1994), are thought to have undergone intra-crustal differentiation at depths from 20 to 5 km. It is suggested that crustal interaction produced the unusual silica-saturated compositions at this edifice, typified by the presence of hypersthene- and quartz-normative lavas. Crustal melts also explained the isotopic characteristics of radiogenic $^{207}Pb/^{204}Pb$, $^{87}Sr/^{86}Sr$, and unradiogenic $^{143}Nd/^{144}Nd$ (Davies and Macdonald, 1987) (Fig. 12).

In a general sense, the high concentration of incompatible trace elements, extreme variability in the isotopic composition of parental magmas, and the similarity in isotopic ratios between the crustal rocks and lavas within the mobile belt make it difficult to assess possible crustal influence in many parts of the EAR without a sufficient volume of data in order to detect contamination vectors. While evidence of crustal assimilation is evident in some rocks in this region (Kabeto et al., 2001a; Clément et al., 2003; Mollel et al., 2009; Mana et al., 2012), complexities exist in terms of assessing a common assimilant for the whole region. In particular, the variability in the isotopic composition of parental magmas (Fig. 8;13) and wide range of trace element concentrations in lavas in the region (Fig. 3; 7) make it difficult to establish unique mixing trajectories. Thus, a focus on the relationship between the degree of magma evolution and isotopic variability in individual volcanoes is necessary. The data available at Olkaria is unusually abundant, allowing for the resolution of distinct vectors (Fig. 12). This permits identification of the component being assimilated and determining the potential source reservoirs. In cratonic regions, such as along the NTD, the isotopically more exotic crustal rocks may leave a sufficiently distinct fingerprint that could be detected upon close examination. I thus focus on the NTD as an important case study in the influence of crustal components and their influence on erupted rocks. In the NTD, the large central volcanoes (Fig. 10), which erupt evolved compositions, require extended crustal residence time for magmas, and are thus potential targets in examining the influence of crustal assimilation.

Within the NTD (Fig. 10), the radically different concentrations of Pb, Sr, and Nd between various magmas makes the radiogenic isotopes for these elements variably sensitive to contamination. When one considers individual volcanoes in the NTD we see the following: (1) For Monduli there is an endmember that plots at unradiogenic values of $^{206}Pb/^{204}Pb$, $^{207}Pb/^{204}Pb$, and $^{143}Nd/^{144}Nd$, and radiogenic values of $^{87}Sr/^{86}Sr$. This endmember is clearest in the trachyte samples from the volcano that contains lower concentrations of Pb (~7ppm). (2) For Ketumbeine volcano, the Pb concentration is particularly low (~4ppm), and this endmember is evident again in some of the more evolved samples. Indeed, excepting one sample from Monduli (MD93-7: Paslick et al., 1995), the rocks that exhibit this unradiogenic Pb signature are evolved in composition, having MgO of less than 4%. (3) For samples from Essimingor, Mana et al. (2012) demonstrated that evolved samples are displaced towards less radiogenic values of $^{206}Pb/^{204}Pb$, experiencing open system processes. However, the degree of this contamination is less significant than Monduli and Ketumbeine, given the higher Pb concentration in Essimingor lavas (e.g., ~20 ppm). (4) Mollel et al. (2008) shows that for Ngorongoro, $^{87}Sr/^{86}Sr$ and $^{143}Nd/^{144}Nd$ correlate with differentiation and show some degree of assimilation. For these rocks, where $^{143}Nd/^{144}Nd$ drops to 0.5122, the $^{206}Pb/^{204}Pb$ ratios are ~18, though the elevated Pb concentration in these rocks may prevent a less radiogenic Pb isotope signature being imparted on these lavas. Notably, the less evolved samples from Ngorongoro typically have $^{206}Pb/^{204}Pb$ ~ 19.5. (5) For Kilimanjaro, a recent survey of the mountain (Nonnotte et al., 2011) found that most of the lavas are relatively evolved (MgO < 5 wt. %), however the more primitive, dominantly parasitic cone-derived samples, clustered at $^{87}Sr/^{86}Sr$ of 0.7035 and $^{143}Nd/^{144}Nd$ of 0.51275 – typically uncontaminated values. In contrast, the more evolved samples exhibited an array of compositions that extend away from this value towards a component (or components) with radiogenic $^{87}Sr/^{86}Sr$ and unradiogenic $^{143}Nd/^{144}Nd$. It would appear that the Shira and Mawenzi stages of Kilimanjaro are the most impacted by this process. It is possible that the

radiogenic $^{87}Sr/^{86}Sr$ signature and unradiogenic $^{143}Nd/^{144}Nd$ and $^{206}Pb/^{204}Pb$ signature is that of the cratonic mantle. On the basis on this model, the initial melts (Shira) are derived from an ancient metasome, while later events tapped a more primitive source. However, it is notable that as SiO_2 increases, the isotopic signature of the samples becomes progressively more impacted by the radiogenic $^{87}Sr/^{86}Sr$ endmember.

While not precluding the existence of parallel reservoirs located within the SCLM, the progressive change in isotopic compositions during melt evolution in the NTD suggests that there exists a reservoir in the continental crust characterized by radiogenic $^{87}Sr/^{86}Sr$, and unradiogenic $^{143}Nd/^{144}Nd$ and $^{206}Pb/^{204}Pb$. The variable fingerprint of this contamination within the NTD lavas seems linked to the concentration of Sr, Nd, and Pb in the evolving magma. Such a phenomenon has been noted further north within the rift where Plateau-Type phonolites exhibit significant $^{87}Sr/^{86}Sr$ contamination due to the low Sr concentration imposed upon the lavas resulting from plagioclase fractionation (Kabeto et al., 2001a). In contrast, the Nd concentration in such lavas is relatively high and is thus not prone to contamination in terms of $^{143}Nd/^{144}Nd$ (Kabeto et al., 2001a). When comparing lavas from Monduli and Ketumbeine, the contaminated lavas from both volcanoes have similar Nd concentrations, but the lavas from Monduli have a more contaminated $^{143}Nd/^{144}Nd$, even though the $^{206}Pb/^{204}Pb$ from both is almost identical. Thus, while Monduli lavas appear to be more significantly contaminated in terms of $^{143}Nd/^{144}Nd$, the elevated Pb concentrations at Monduli in comparison to Ketumbeine, have reduced the impact of assimilation on $^{206}Pb/^{204}Pb$. The consequence of this is to make the $^{143}Nd/^{144}Nd$ less radiogenic at Monduli for a given Pb isotope ratio. The potential source of contamination within the continental crust is unlikely to be the Pan-African domains exposed at the surface near the NTD (e.g., Usambara, Umba, and Pare Mountains) as their isotopic characteristics are insufficiently exotic (in particular for $^{143}Nd/^{144}Nd$) to allow for effective mixing arrays (Möller et al., 1998). In contrast, reworked rocks from the craton (Uluguru Mountains)

exhibit values that could result in a plausible contamination of the NTD rocks (Möller et al., 1998). While these rocks are more distant from the erupted lavas, it has already been noted that the surface rocks in the NTD are a thin Proterozoic thrust sheet lying over the cratonic basement (Dawson, 2008; Foley et al., 2012), thus it is entirely plausible that the composition of the Archean rocks in the region are an appropriate endmember as a crustal contaminant for an open system evolution. It should be noted that observations of crustal assimilation cannot explain all the isotopic properties of rocks erupted in the region (i.e., a complex lithospheric mantle reservoir is still required), however caution should be exercised in terms of interpreting changes in the isotopic composition of more evolved rocks in the region as solely mantle processes. Such warnings have particular resonance when considering the isotopic properties of carbonatites – rocks derived from evolved lavas that have potentially experienced open-system evolution in the crust (see discussion on carbonatites later). While the concentration of incompatible trace elements in carbonatites may render them somewhat inert to crustal assimilation, the same cannot be said for the lavas from which are derived through immiscibility.

3.1.3 Magma Mixing

While fractional crystallization exerts significant control over the diversity of magmatic products within the East African Rift, magma mixing is an often overlooked process that may contribute to the observed compositional diversity within the rift. It can sometimes be challenging to detect the influence of such mixing, but clues are typically evident in terms of xenocrystic materials, resorbed crystals, and magma evolution trends that are inconsistent with fractionation. Xenocrysts are a helpful indicator as to the potential for a mixed magmas, but such phases may also have been assimilated from cumulates or basement rocks (e.g., Pinzuti et al., 2013). Within the southern Ethiopian rift, basaltic magmas exhibiting evidence of mixing with a more evolved liquid contain quartz and amphibole xenocrysts (Rooney, 2010). Further north in the Ethiopian

rift, some volcanic cones contain norite xenoliths, likely derived from the interaction with the trachytic magmas of the nearby shield volcano (Yerer). Similar to xenocrysts, crystals from one liquid (such as feldspars) that are mixed into a second may be significantly out of equilibrium with a new hybrid magma, resulting is resorption (Rooney, 2010). The xenocrystic phases found within these lava suites correlated with evidence of magma mixing in the behavior of elements (e.g., linear arrays instead of exponential relationships in some elements) (Rooney, 2010; Rooney et al., 2014a). Magma mixing relationships are even more pronounced when considering alkaline compositions (discussed below), where isotopic disequilibrium between crystals and melt is commonplace (Simonetti and Bell, 1993, 1994; Muravyeva et al., 2014).

The discovery of isotopic disequilibrium between lavas and their accompanying crystals is becoming more common in the study of highly alkaline rocks of East Africa (Davies and Lloyd, 1989; Simonetti and Bell, 1993; Muravyeva et al., 2014). Initially noticed in the pyroxenite xenoliths and accompanying megacrysts of the Recent Toro Ankole eruptions (Davies & Lloyd 1989), this phenomenon has also been observed in the Miocene alkaline volcanism of eastern Uganda (Simonetti and Bell, 1993), and Recent lavas from northern Tanzania (Paslick et al., 1996). Davies & Lloyd (1989) found that pyroxenite nodules and macrocrystic pyroxenes within the Katwe-Kikorongo field of Toro Ankole (Fig. 14) exhibited similar $^{87}Sr/^{86}Sr$-$^{143}Nd/^{144}Nd$ values to their host lavas, but differed significantly in terms of their Pb isotope ratios. Similar results are reported by Muravyeva et al. (2014) who further noted that the characteristics of the clinopyroxene erupted in the Bunyaruguru field of Toro Ankole not only exhibit Pb and Sr isotope disequilibrium but also were likely derived from another magma. Paslick et al. (1996) suggest that the crystals carried by the alkali basalts and nephelinites from N. Tanzania are partially xenocrystic, and exhibit a different isotopic signature than the host lavas. This evidence was used to suggest that earlier phases of basaltic activity were captured in the crust, and became contaminated; crystals from these earlier events were then scavenged by later magmas

(Paslick et al., 1996). Simonetti & Bell (1993, 1994) also show that there is isotopic disequilibrium and complex zoning in clinopyroxene crystals at Napak volcano, and suggest an origin by either the continued mixing of two magmas or continual assimilation of a lower crustal granulite.

Outside of any single locality, a unified model of crustal assimilation explaining the almost universal feature of clinopyroxene crystals having less radiogenic Pb isotopes than their co-existing host lavas is difficult to reconcile (e.g., Paslick et al., 1996). Disaggregation of cumulates stored in the lithosphere may resolve the issue (Davies and Lloyd, 1989; Paslick et al., 1996), but then one must ask, what is the origin of those cumulates? Paslick et al. (1996) suggest that a prior batch of magma became contaminated with crustal materials and formed such cumulates. However, pyroxenites from Toro Ankole do not exhibit ε_{Nd} perturbations that would be anticipated for such a model. The answer may lie in the observations by Rosenthal et al. (2009) that the Toro Ankole melts exhibited evidence of a derivation from isotopically distinct metasomes within the lithospheric mantle. The isotopes within these metasomes have evolved independently such that $^{87}Sr/^{86}Sr$ of the whole rock data were dominated by relatively recently formed carbonate-bearing metasomes, while $^{143}Nd/^{144}Nd$ and $^{176}Hf/^{177}Hf$ were dominated by an older MARID-type metasome (Rosenthal et al., 2009). The less radiogenic Pb values present within the clinopyroxene may reflect an origin in a melt derived preferentially from MARID-type metasomes where U/Pb is likely lower than the more carbonate rich metasomes. This supports a model of magma mixing for the origin of these crystals (Simonetti and Bell, 1993), but does not necessarily require derivation of these two melts from different parts of the lithosphere or even asthenosphere (Muravyeva et al., 2014).

3.1.4 Mush Model of Magma Evolution

Fractional crystallization is considered the dominant mechanism in most modern central volcanoes, but it has been difficult to link the evolved and primitive lavas (McDonald et al., 1987) (Fig. 11). Indeed, the observed perturbation in isotopic ratios with increasing magma evolution supports a role for crustal contamination in the more evolved magmas regionally (Davies and Macdonald, 1987; Deniel et al., 1994; Hutchison et al., 2018). However, an origin for evolved lavas solely through crustal melting is now discounted (MacDonald et al., 2008). In particular, low Ba and Sr rhyolites are difficult to generate through anatexis of either the Precambrian granites (Marshall et al., 2009) or underplated basalts (Peccerillo et al., 2003). Much of the complexity observed at Olkaria (where an abundant dataset exists), has been linked the processes of magma mixing and mingling. At Olkaria, as in Emuruangogolak, trachytic rocks are produced via fractional crystallization from basalts. However, for more evolved compositions, the complexity of mixing and mingling between melts of an array of compositions makes it difficult to define any single liquid line of descent (MacDonald et al., 2008; Marshall et al., 2009). On the basis of analyses of the inclusions within Olkaria, models have been developed that posit the formation of the more evolved rock types in the region through processes such as mixing and mingling of various magma compositions, and a magma mush model (to allow for the extraction and eruption of crystal poor evolved magmas: MacDonald et al., 2008; Marshall et al., 2009) (Fig. 11). Phase constraints have suggested that the magma mush zone needed to form peralkaline rhyolites at Olkaria is shallow – i.e. 50 MPa and relatively cool at < 700°C (Scaillet and MacDonald, 2001). Additional processes at Olkaria include partial melting of syenites and the separation of alkaline fluids enriched in trace elements (MacDonald et al., 2008). The extreme differentiation needed to account for trace element enrichment in the peralkaline rhyolites requires a high magma flux in order to heat the residual melt (Marshall et al., 2009). These detailed observations at Olkaria might hint at parallel processes in the other

central volcanoes within the rift, and possibly similar magma differentiation systems that are largely controlled by multi-level magma mush zones (Fig. 11), within which complex mixing and mingling between magma types occurs. Further complexity is evident wherein lateral magma transfer between volcanic centers (i.e. Olkaria to Longonot) may also occur (Rogers et al., 2004). On the basis of the eruptive products, the shallow-level magma chambers that host the peralkaline magmas prior to explosive eruptions have been shown to be ubiquitously strongly zoned (MacDonald and Scaillet, 2006). This observations has critical implications for the correlation of tephra in the region – the same eruption may yield a wide array of compositions in terms of major and trace elements, and isotopes (MacDonald and Scaillet, 2006; Rooney et al., 2012b). On the basis of the behavior of Olkaria, these peralkaline systems are considered relatively small (2-10 km^3), with short magma storage times (ca. 22 ka) when compared to systems like Long Valley (Heuman & Davies 2002). To maintain crystallization at near liquidus conditions for small systems such as this, a significant heat engine is required, and is thought to be the continual flux of new basaltic magma (e.g., Heumann and Davies, 2002; Marshall et al., 2009) (Fig. 11).

3.1.5 Phonolites – the Evolution of a Model

Phonolites represent an important rock type in the Kenya Rift, and exceed in volume by several orders of magnitude the total volume of phonolites found elsewhere (Lippard, 1973). Initial work on the phonolite lavas in the region (Lippard, 1973) initially divided the rocks into three groupings:

Gwasi Type (or G-Type) Phonolites. These are rare lavas that are typically associated with nephelinite and melilite lavas.

Plateau Type (or P-Type). These lavas are restricted to the flood phonolite phase and occur as extensive lava sheets.

Kenya Type (or trachyphonolites). These lavas are associated with central volcanoes.

From a geochemical perspective, it has been difficult to separate the Kenya and Plateau types as both have a similar range in trace element concentrations (Lippard, 1973). Minor differences are evident when considering the greater compositional range in major elements for the Kenya phonolites and also a slightly lower Zr/Nb (Lippard, 1973). Ca-plagioclase is stable in these phonolites and it results in a depletion in Sr and Ba. In contrast, G-Type phonolites are distinctive in having high in Ba and Sr compared to P-Type phonolites. G-Type phonolites lack Ca-plagioclase but are characteristically sphene-bearing (Lippard, 1973).

The origin of phonolites, and in particular the vast volumes of flood phonolites erupted during the Flood Phonolite phase, has remained somewhat controversial with two endmember models – crustal anatexis and fractional crystallization. Regardless of which model is evaluated, both require significant quantities of basaltic magmatism intruded into the lower crust in Kenya beginning ca. 18 Ma (Goles, 1976). The fractional crystallization model has seen more support and has shown that Kenya-Type and Gwasi-Type are likely derived from AFC processes. In particular, the wide array of compositions that typically accompany Kenya-Type phonolite occurrences at composite volcanoes supported fractionation models over partial melting models (Clément et al., 2003). Major and trace element variation within these suites of Kenya-Type phonolites are consistent with significant volumes of feldspar fractionation (e.g., Nash et al., 1969; Griffiths and Gibson, 1980; Price et al., 1985). Even in regions that are dominated by Plateau-Type phonolites, but where a suite of broadly contemporaneous rocks are examined (e.g., Samburu Hills), AFC models are preferred, though the anatexis model was not convincingly disproven (Kabeto et al., 2001a, 2001b).

The anatexis model gained support due to the large volumes of fairly homogenous phonolites erupted during the Flood Phonolite phase (in particular during the period from 14-11 Ma). In general, only very minor basaltic flows accompanied these phonolite eruptions. These observations, and the problem of the necessity of large volumes of basaltic magma in order to facilitate a fractional crystallization model (Goles, 1976) resulted in in a trio of anatexis papers by Hay in 1995 (Hay and Wendlandt, 1995; Hay et al., 1995b, 1995a). In these papers, the predominant model for the formation of phonolites is a two-step process whereby the lower crust is initially intruded by alkali basaltic magma. Subsequent rift evolution resulted in a raising of isotherms and melt production from this intruded lower crust. This model was supported with melting experiments that suggest the phonolites are multiply saturated in augite, feldspar, phlogopite, apatite, and oxides – an assemblage consistent with a residuum of melting of an alkali basalt under lower crustal pressure and temperature conditions. An important point from this work is the need for a significant water content in the phonolites (6 wt. %). Further work by Kazuba and Wendtland (2000) demonstrated that partial melting experiments of a hydrated (3-5 wt. % H_2O) alkali basalt in the presence of a significant quantity of CO_2 (2.2 – 12.8 wt. %) could generate compositions approaching Plateau-Type phonolites. While some water could derive from the breakdown of amphibole and phlogopite in the parental basalts, it remains unclear if these phases would have been initially stable in an environment where continued pervasive intrusion would result in a significantly elevated thermal regime. Moreover, this model also requires significant fluxing with CO_2 in order to yield the appropriate melt compositions (Kaszuba and Wendlandt, 2000). A second critical problem impacting the anatexis model is the low Sr concentrations within the Plateau-Type phonolites. Kabeto et al. (2001b) noted that even with a very high bulk distribution coefficient for Sr, it would not be possible to generate the low Sr Plateau-Type phonolites from the Samburu Hills through anatexis of underplated basalts alone. A two-step process was proposed whereby partial melting of the basalt was followed by

45-80% fractionation of the resulting melt (Kabeto et al., 2001b). With this degree of fractional crystallization, the two-step model may conflict with the same kinetic arguments used to support the anatexis model (e.g. Hay et al., 1995).

With the application of MELTS models (Ghiorso and Sack, 1995) to the evolution of rift magmas, new potential constraints on the liquid lines of descent and intensive parameters of crystallization became possible. These models suggested that fractional crystallization was the dominant process, but revealed depth of fractionation differences (e.g. deeper at Suswa, more shallow at Olkaria: White et al., 2012). Moreover, new insights into the potential complexity of magmatic plumbing systems of felsic volcanoes has provided additional mechanisms by which magma evolution could proceed. For example, magma recharge and assimilation of cumulates (specifically anorthite) from prior magmatic events was hypothesized to play an important role in the evolution of the most differentiated products at Suswa volcano from a trachyte to phonolite (White et al., 2012). These observations and models thus revealed an additional mechanism by which magmas from the alkaline magma series may exist at edifices erupting dominantly transitional compositions, all derived from a common basaltic parental magma type (Fig. 11). Continuing work on constraining the evolution of felsic systems in the rift through detailed work on crystals hosted within these lavas may eventually constrain the pathways by which felsic magmas evolve within the rift.

The co-occurrence of central volcanoes and voluminous phonolites in the southern EARS is likely linked to unusually alkaline magmatism and the evolution of these magmas within the continental crust. It has been hypothesized that that the generation of more evolved compositions is linked to the presence of central volcanic edifices. Dawson (2008) notes that the NTD has the unusual feature of having abundant central volcanoes erupting relatively evolved lavas. This is in contrast to areas like the Chyulu Hills, where magmatism is more diffuse and

significantly more mafic. Dawson (2008) speculates that the presence of such central edifices promotes fractional crystallization, driving more mafic compositions entering the magma plumbing system towards trachytes. To deduce the composition of magma entering into the magmatic plumbing system of these large edifices, Mattsson et al. (2013) examined a range of the monogenetic cones/maars scattered in between the central volcanoes. They found that there were two distinctive magma types evident within these cones – melilititic and nephelinitic. They surmised that the melilititic magmas ascended rapidly due to their high volatile content (and were small degree melts), whereas the nephelinitic magmas were generated by slightly higher degrees of melting and underwent olivine fractionation within the crust. It is therefore probable that these magma types, caught by the magma plumbing system beneath the central volcanoes, are the input magma types within this portion of the rift.

With increasing support for a dominantly fractional crystallization model at central volcanoes for at least the modern phonolites within the rift, insights into the origin of other exotic rock types may be revealed. Specifically, observations from phonolites erupted at Suswa volcano (within the Central Rift Peralkaline province) and the Baringo-Bogoria basin (in the north central province) of an immiscible carbonate liquid has implications for the origin of carbonatites in the region (Macdonald et al., 1993; Clément et al., 2003). These studies have shown that a carbonate liquid appears to coexist with the phonolites, supporting an origin by differentiation for such lavas.

3.2.5 Carbonatites – Unmixing of Alkaline Magmas

Carbonatite lavas are a feature of the EARS south of Lake Turkana, but are notably absent in more northerly parts of the rift (with the exception of rare globules of carbonate liquid in some phonolites: Macdonald et al., 1993; Clément et al., 2003). While carbonatites are known from

the Proterozoic and Mesozoic in this region, we focus on the Cenozoic carbonatites that are associated with rifting events in East Africa (e.g., Van Straaten, 1989). These rocks are distributed around the Tanzania craton, and are focused primarily in the Eastern Branch of the rift along the North Tanzania Divergence and in Eastern Uganda, though the complete record of carbonatites in region may be limited by poor preservation (e.g., Guzmics et al., 2019). While only a volumetrically small component of magmatism within the rift, a significant volume of literature has been devoted to the study of carbonatite magmas given: (1) the relatively unusual geochemical and petrographic characteristics of these lavas; and (2) the occurrence of the only active carbonatite volcano in the world (Oldoinyo Lengai) within the North Tanzania Divergence. Our understanding of carbonatite volcanism in the region has been largely the result of investigations at a relatively few well-studied volcanic centers (Oldoinyo Lengai, Kerimasi, Shombole, Napak, and Mt. Elgon). Carbonatite occurrences in the region take the form of tuffs, breccias, plugs, and dikes, in addition to the modern flows at Oldoinyo Lengai (Dawson, 2008). The carbonatites are usually small volume components of larger nephelinitic volcanic centers (Dawson, 2008). Compositionally, the carbonatites in the region are not typically divided into the IUGS classification of calcite-carbonatite, ferrocarbonatite, and dolomite-carbonatites (Le Maitre, 2002). However, natrocarbonatites are distinguished by the presence of Na-Ca-K carbonate minerals, including gregoryite and nyerereite (Le Maitre, 2002).

The origin of carbonatite magmas erupted at the surface has historically been a controversial one. Such controversy results from the potential to derive such magma compositions directly from a carbonated mantle (Eggler and Bell, 1989), and evidence of ubiquitous carbonatite metasomatism in continental lithospheric mantle xenolith suites (Rudnick et al., 1993; Yaxley et al., 1998). It has thus been argued that carbonatites erupted in East Africa may be primary melts derived from a carbonated mantle (e.g., Harmer and Gittins, 1998; Bizimis et al., 2003). The typical restriction of carbonatite lavas to the southern portion of the

EARS, a region where a diverse array of metasomatically influenced lavas are known to erupt, makes intuitive sense. Within this paradigm, the derivation of an unusual magma, such as carbonatite, is attributed to an unusual source – namely exotic volatile-enriched metasomatic compositions in the sub-continental lithospheric mantle of the Tanzania Craton. Based on this model, initial carbonatitic melts are derived from an ascending mantle plume. The interaction of these melts with the lithospheric mantle produced carbonate metasomes that were shortly thereafter destabilized to form the carbonatite melts observed at the surface (Bizimis et al., 2003).

Mattsson et al. (2013) finds metasomes in mantle xenoliths from the NTD containing amphibole, phlogopite, olivine, clinopyroxene, and carbonate. There remains some question as to if this carbonate, observed within the metasomes, contributes to the formation of carbonatites in the region. Investigation of the volatile components at Oldoinyo Lengai have shown that the mantle source of the magmas was not particularly enriched in carbon in comparison to typical mantle reservoirs on the basis of similarities in ratio of $CO_2/^3He$ to the MORB source (Fischer et al., 2009). This observation is consistent with experimental constraints suggesting that the volatiles in carbonatites could be derived from a “mildly depleted peridotite source” without the necessity for events that decouple the volatile and refractory elements (Eggler and Bell, 1989; de Moor et al., 2013). It is thus apparent that the derivation of carbonatites directly from an unusually carbon-enriched mantle source is unnecessary, though not precluded as uncertainties persist about the absolute concentration of CO_2 in the source of rocks in the region. It should be noted, however, that the composition of the carbonatites erupted in East Africa is typically inconsistent with a melt that could be derived directly from the mantle (i.e. one having high Mg + Fe: Ca, and enriched in alkalis: Eggler and Bell, 1989). Furthermore, such carbonated magma compositions are unstable within the mantle and would react with peridotite before being extracted from the mantle (e.g., Eggler and Bell, 1989).

The current consensus, which is based upon parallel evidence from experimental constraints, petrographic observations, and geochemical data, focuses upon an origin for carbonatites through liquid immiscibility (e.g., Brooker and Kjarsgaard, 2011). In this model, carbonated nephelinite or melilitite magmas undergo differentiation under crustal conditions, which induces immiscibility between a silicate and carbonate liquid (Bell and Simonetti, 2010). The most compelling evidence of carbonate-silicate liquid immiscibility derives from the Chaos Crags flow of Oldoinyo Lengai. This flow, derived from a 1993 eruptive event, contained silicates in the form of spheroids hosted within a natrocarbonatite lava (Dawson et al., 1994, 1996; Church and Jones, 1995; Bell and Simonetti, 1996). Initial work considered this texture the result of late stage mixing of two lavas (Dawson et al., 1994, 1996), however the identical isotopic values and textures between the components has been interpreted as evidence of immiscibility of two conjugate liquids (Church and Jones, 1995; Bell and Simonetti, 1996). Parallel results have come from the examination of calciocarbonatites from the nearby Kerimasi volcano. Here, silicate and carbonate melts (in addition to a C-O-H-S fluid phase) are trapped within magnetite and apatite crystals contained within the carbonatite magma (Guzmics et al., 2011). Within increasing calcite fractionation, the residual carbonate lava became progressively more enriched in alkalis, as is evident in a commensurate core to rim increase in alkalis within the trapped melts (Guzmics et al., 2011). Modelling and experimental studies suggest that continued calcite and apatite fractionation might drive the residual liquid towards the natrocarbonatite compositions seen at Oldoinyo Lengai (Weidendorfer et al., 2017).

Despite the existence of models that suggest common processes in the generation of carbonatite lavas, difficulties arise when considering trace element enrichment between carbonatite lavas in the region. These differences have been used to argue that carbonatite magmas at Kerimasi and Oldoinyo Lengai have different parental silicate magmas. The calciocarbonatites of Kerimasi are a cumulate (calcite + apatite) derived a carbonate melt that

was earlier exsolved from a melilite-nephelinite magma that undergoes fractionation of apatite and perovskite, thus depleting the remaining liquid in trace elements compatible in these phases (Guzmics et al., 2015). In contrast, Oldoinyo Lengai is thought to have a nephelinite source, which resulted in both a differential in partitioning of elements during the immiscibility process and subsequent fractionational crystallization, resulting in more enrichment in incompatible trace elements at Oldoinyo Lengai (Guzmics et al., 2015). Furthermore, immiscibility processes within carbonated silica-undersaturated lavas are complex and can involve silicate, carbonate, fluid, and sulfide phases in differing proportions with heterogeneous impacts on element partitioning (Guzmics et al., 2012, 2019; Sharygin et al., 2012). Indeed, as carbonate melt evolution proceeds, immiscibility may also occur between different carbonate liquids and a halide phase (Potter et al., 2017). The recognition of such complexity, in addition to the problem of the dissolution of some of the more water-soluble components argues for an increased focus on melt-inclusion studies to refine the evolution of carbonatite magmas.

Given that it is difficult to ascribe the existence of carbonatites to volatile-enrichment in the lithospheric mantle (Fischer et al., 2009; de Moor et al., 2013), it has been recognized that the alkali contents of rift magmas are the dominant controlling influence on carbonatite formation (Brooker and Kjarsgaard, 2011). There is broad recognition that the presence of a sufficient concentration of alkalis (~7-10 wt. %) is a fundamental pre-requisite in order to facilitate carbonate-silicate immiscibility in systems that are undersaturated in CO_2 (Mitchell, 2009; Brooker and Kjarsgaard, 2011; Guzmics et al., 2012). Thus, the alkali content of the lavas is a controlling factor on carbonatite genesis. Alkali-rich silicate magmas such as nephelinites/melilites and more-evolved phonolites, are the magma compositions most likely to intersect the solvus at crustal depths (Brooker and Kjarsgaard, 2011). Given the origin of carbonatite lavas through immiscibility processes at crustal levels, the parental mafic magmas

are now widely considered either to be nephelinites or melilites. Thus, comprehending the origin of carbonatites requires a focus on the origin of the silicate magmas in this region.

Within the portion of the EARS that is south of Lake Turkana, rift lavas are, on average, more alkaline than those further to the north. This observation is consistent with the presence of carbonatites in the southern EARS, but it raises a parallel question - could metasomes in the Tanzania craton contribute to the alkalinity of rift lavas in the southern EARS? Metasomes within the sub-continental lithospheric mantle of the Tanzania craton undoubtedly contribute to the genesis of ultra-potassic lavas in the western branch of the EARS (Rosenthal et al., 2009; Foley et al., 2012). Phlogopite-rich source compositions, present in the deep cratonic mantle, do not appear to have a parallel in the more northern portions of the EARS. While this is evidence of some degree of heterogeneity in the alkali continent of the rift imposed by exotic metasomatic compositions, the sodic character of rocks within the eastern branch (and coincident with most carbonatite occurrences) are not consistent with a derivation from such a source. Nephelinite and melilitite magmas, in which sodium is the dominant alkali element, are hypothesized to be derived from the melting of amphibole-rich metasomes. However, the presence of amphibole-bearing metasomes is not uniquely constrained to the southern portion of the EAR (Rooney et al., 2014a, 2017). If amphibole-bearing metasomes are available in the lithospheric mantle throughout the rift, the conditions of melt generation may play a controlling role in the alkali content of rift lavas. In particular, near-solidus small degree melts of amphibole-bearing metasomes are dominantly influenced by amphibole, and may thus trend towards generating more alkali-rich melt compositions (e.g., Eggler and Bell, 1989). Consequently, the degree of melting in the mantle may be instrumental in determining the alkali content of rift lavas and by extension, the occurrence of carbonatite lavas. Presuming an identical source composition, the degree of melt generation varies as a function of pressure, temperature, and the rate of change of these intensive parameters. For melt generation from the same amphibole-bearing

metasomatic source, the thicker lithosphere associated with the Tanzania craton, in addition to less rift-related extension in the southern EAR may explain the geographic heterogeneity in magma compositions. While such a model is consistent with the available data, the influence of mantle plumes on the temperature regime of the mantle lithosphere, and the relative role of lithospheric mantle versus the convecting mantle may complicate this simplistic approach.

3.2 Derivation of Magma from the Sub-Continental Lithospheric Mantle – Major and Trace Element Constraints.

The composition of melts erupting in the Kenya Rift and NTD are inconsistent with derivation from a volatile free peridotite (e.g., Foley et al., 2012). The ubiquitous presence of a negative trough in K on primitive mantle normalized diagrams has been used as evidence for the presence of a K-bearing phase in the source of magmas in the region (Class et al., 1994; Le Roex et al., 2001; MacDonald et al., 2001; Späth et al., 2001). These phases (in particular – amphibole, and to a lesser extent – phlogopite), can generate melt when the lithospheric mantle is thermobarically destabilized, for example, during rifting or plume-lithosphere interaction (Rooney et al., 2017). The existence of such phases may explain the generation of magmatism despite relatively low β-factors (stretching factors) calculated for most parts of the EARS (Rogers et al., 2000). Mantle melting models have shown that a peridotite containing residual amphibole could replicate the patterns observed in magma erupted in the region (Späth et al., 2001). Small degree melting of an amphibole-bearing peridotite resolved important aspects of the composition of magmas in the region – specifically, the high alkalinity evident in these melts was imparted by the amphibole, while the silica-undersaturation was related to the partitioning of volatiles (i.e. CO_2) into the small degree melt (Eggler and Bell, 1989). This model was also

consistent with the observation that hypersthene-normative basalts (higher degree of melting) had a less pronounced K trough in comparison to nepheline-normative basalts (MacDonald et al., 2001; Späth et al., 2001).

Closer to the Tanzania craton, the increasingly potassic nature of the erupted lavas has been indicative of the presence of phlogopite within the lithospheric mantle source of such lavas (MacDonald et al., 2001), consistent with xenoliths recovered in this region. The influence of phlogopite-influenced mantle is even more pronounced within the western branch of the EARS, where potassic and ultra-potassic lavas commonly erupt within the Virunga Volcanic Province and Katwe-Kikorongo field at Toro Ankole (Uganda) (Rogers et al., 1992, 1998; Furman and Graham, 1999; Rosenthal et al., 2009). For kamafugites erupted within the Toro Ankole province, the geochemical characteristics of the erupted lavas provide some constraints as to the melting process. In particular, the existence of negative K and P anomalies within the primitive mantle normalized trace element patterns is suggestive of residual phases within the mantle source that formed the lavas (see Part III of this synthesis series for a fuller description of the characteristics of these lavas). Rosenthal et al. (2009) reasoned that such occurrences may be explained by residual phlogopite and apatite occurring within a metasomatic vein. To ensure that these phases remained residual within the source, the source could not have been a peridotite with disseminated phases, as these phases would have melted preferentially (leaving no K- or P-bearing phases in the residuum) (Rosenthal et al., 2009).

With the recognition that amphibole (+ phlogopite, closer to the craton and in the western branch) influenced the composition of the erupted magmas, the depth of melt generation was constrained to be within the stability field of these phases. Amphibole (paragasite) is constrained to approximately the upper 90 km of the lithospheric mantle (Green et al., 2010), while phlogopite can persist to 200 km within the lithospheric mantle (Sato et al., 1997). Rosenthal et al. (2009), using existing experimental data (Green, 1973; Foley et al.,

1999), suggested that lavas that were potassic (Na_2O/K_2O <1) were derived from either a phlogopite + amphibole bearing metasome at depths of less than 90km, or a phlogopite bearing metasome at depths of more than 100 km. Similarly, for more sodic-rich alkaline rocks (Na_2O/K_2O>1), the origin of the lavas was thought to be from an amphibole-bearing metasome at depths of less than 90 km (Rosenthal et al., 2009). These broad depth of melting constraints have been supplemented with other phases within the potential metasomatized peridotite source – namely the garnet-spinel transition.

The destabilization of metasomes within the lithospheric mantle is now widely considered as a viable mechanism by which alkaline, silica-undersaturated melts are generated. However, the mechanisms of melt generation warrant further attention. Current melting models are constructed on the basis of observations from amphibole- and phlogopite-bearing xenoliths wherein amphibole/phlogopite forms a small-percentage, disseminated phase (Späth et al., 2001). Consequently, non-modal melting equations assumed contributions to the melt from all phases in the peridotite. For example, the melting equation used in Spath et al. (2001) suggests a non-modal melt of 5% olivine, 10% orthopyroxene, 33% clinopyroxene, 50% amphibole, and 2% spinel from a spinel lherzolite parent. The assumption that such starting materials dominate metasome-derived melts might not hold. Within mantle xenoliths from the region, veins of amphibole, phlogopite and carbonate are evident crosscutting peridotite (Mattsson et al., 2013), consistent with the concept of amphibole-rich channels associated with chromatographic metasomatism (Stein et al., 1997) (Fig. 1). Melting of such lithologies results in distinctly different behavior, with amphibole contributing entirely to the melt (Pilet et al., 2008). This amphibole-generated melt could then interact with the lherzolite of the lithospheric mantle and dissolve orthopyroxene (Pilet et al., 2008). An important result from these experiments, was that the trace element content of the melt resulting from such metasomes is essentially parallel, though displaced to more enriched values in comparison to the amphibolite that melted (Pilet et

al., 2008). Thus, the trace element pattern of the resulting melt is entirely controlled by the trace element composition of the original amphiboles (or other phases in the metasome), while the enrichment is a function of the degree of melting and dissolution of orthopyroxene in the surrounding peridotite (Pilet et al., 2008).

Support of this model for the origin of magmas in East Africa is provided by the experimental work of Sack et al. (1987). In this study, a tentative constraint on the origin of primitive K-basanite magmas from Karisimbi was 1360 ± 50°C at 18 ± 3 kb depth – shallower than the garnet-spinel transition in peridotite mantle materials. Rogers et al. (1992) noted that this garnet-free source presented difficulties for the interpretation of fractionated REE profiles that would typically be used to indicate the presence of garnet in the source of such magmas. Rogers et al., (1992) reasoned that the primitive K-basanites inherited their trace element characteristics from a prior metasomatic enrichment event. On the basis of the major and trace element composition of the K-basanites, Rogers et al. (1992) suggested a peridotite source with accessory phlogopite, amphibole, ilmenite, and rutile. This compositional model is consistent with metasomatic veins noted above (excluding the peridotite matrix; Fig. 1). Further advances in our understanding of the composition of the mantle lithologies that melt to produce lavas in parts of the EARS come from the northern portion of the western branch at Toro Ankole. Here, potassic lavas, which have significantly fractionated HREE values that range from $(Tb/Yb)_{CN}$ = 3 to 5, have low Al_2O_3 (6-8 wt. %), and are not considered to have significant garnet in their source, but instead are considered dominated by a source comprising phlogopite-rich MARID type metasomes and carbonate metasomes (± peridotite) (Rosenthal et al., 2009).

It is important to note that such metasomes can be created from a wide array of initial magma types, and that accessory phases that form by progressive fractionation of the metasomatic agent may have a profound influence (e.g., rutile) over the metasome trace

element composition (Pilet et al., 2010). Indeed the fractionation of Hf from Lu by such a phase will result in less radiogenic Hf isotope values in magmas derived from such metasomes if sufficient time elapses (Tappe et al., 2008; Rooney et al., 2014b). Thus, as with many cumulates, the metasome itself (and the derivative melt) does not directly reflect the composition of the metasomatic agent which may have formed it. Such insights are important as the nature of the metasomatic agent which impacted the regional lithospheric mantle remains unclear (Paslick et al., 1995). Attempts at discounting a subduction origin for metasomatic enrichment have relied upon a mischaracterization of the metasomatic agent as “mainly created by subduction fluids” and that such fluids do not carry high field strength elements (HFSE) (Castillo et al., 2014). However, as noted in Rooney et al. (2014b) the subduction-related metasomtic agent may be “ancient fluids or magmas derived from a subducting slab during the Pan-African orogenic event” and thus HFSE transport is possible. Indeed high-Nb basalts and arc-related lamprophyres are features of subduction environments, testifying to the operation of this process in the sub-arc mantle (Reagan and Gill, 1989; Kepezhinskas et al., 1996). Moreover, there is a now widespread understanding in modern subduction studies that HFSE are even potentially mobilized in subduction fluids (e.g., Woodhead, 2001). For these reasons we refer to a ‘metasomatic agent’ in Fig. 1 in order to capture the variety of compositions that may have interacted with the lithospheric mantle.

These combined observations have profound implications for the interpretation of REE behavior in metasome-derived or indeed metasome-influenced melts. Consider the creation of an amphibole-rich metasome within the spinel-lherzolite stability field. In such a conceptual model, melts/fluids derived from the garnet-lherzolite stability field (chromatographic reactions) infiltrate into the shallower lithospheric mantle wherein they cross the amphibole stability field. The amphiboles that form from such melts/fluids would exhibit a depletion in HREE, despite being located in a garnet-free zone of the lithospheric mantle. Subsequent melting of the

metasome would yield a magma that had a depletion in the HREE, and which may erroneously be interpreted as melt derived from the melting of a garnet-bearing peridotite. While the initial percolating melt that created the metasome (i.e. metasomatic agent: Fig. 1) might have been derived from a lithology containing residual garnet, that melting event could be as old as the lithosphere itself (Rogers et al., 1992, 1998; Rooney et al., 2014b), and thus have no bearing on the event that destabilized the metasome to form the erupted lava. With such a two-step process, there are a wide array of possible outcomes and complexities in the formation and destabilization of such metasomes (e.g., incongruent melting reactions). However, it is becoming increasingly clear that caution should be exercised in interpreting HREE depletions in rocks where there is evidence for an origin that involves a melt derived from a metasome. If one considers that HREE depletion relates solely to the depth of melt generation, it can be difficult to interpret such depth of melting constraints within a geological framework: (A) Shallowing and deepening trends that may occur over time within the same edifice; (B) Synchronous eruption of seemingly shallowly and deeply derived lavas; (C) Contemporaneous isotopically-defined asthenosphere- and lithosphere-derived lavas having the opposite sense of depth of origin. I contend, that some of the complexities within respect to the apparently differing depths of melt generation in the Kenya Rift and western branch of the EARS may instead reflect the influence of metasomes and not, as is currently assumed, be strictly depth of melting phenomenon. It is thus apparent that additional work is required in order to more completely constrain the potential contribution from these distinct processes.

3.3 Derivation of Magma from the Sub-Continental Lithospheric Mantle – Existing Models of Lithospheric Reservoirs

Observations of the spatial variation in isotopic signatures in rift lavas reveal the potential reservoirs participating in melt production. Major and trace element variation has identified three distinctive domains within the eastern branch of the EARS (Fig. 4;7), which have been named on the basis of the proximity to the Tanzania craton: (1) the craton, (2) the reworked craton margin, and (3) the mobile belt. The most notable spatial observation is that lavas erupted within the portion of the rift that traverses the craton and reworked craton margin exhibit distinctive isotopic characteristics consistent with the melting of a reservoir that has had a long-term isolation from the convecting upper mantle (e.g., Rogers et al., 1998, 2000). Lavas erupted within the craton boundary have high Sr concentration combined with elevated $^{87}Sr/^{86}Sr$ (0.707) that would be difficult to impart solely through crustal assimilation (Rogers et al., 2000). Similarly, lavas derived from the craton and reworked craton margin exhibit unradiogenic $^{143}Nd/^{144}Nd$ (0.5124), suggestive of a source distinct from that of typical upper mantle reservoirs (Rogers et al., 1998). While it is tempting to consider this $^{143}Nd/^{144}Nd$ signature as Archean (consistent with the age of the craton), this is inconsistent with the degree of radiogenic ingrowth, and instead requires an enrichment event in the lower SCLM over the past 1 to 0.5 Ga (Rogers et al., 2000). In contrast to the craton-impacted lavas, lavas that have erupted through the mobile belt extend to isotopic values that highlight the influence of more DMM-like reservoirs: $^{143}Nd/^{144}Nd$ 0.5130; $^{87}Sr/^{86}Sr$ 0.7030. While $^{206}Pb/^{204}Pb$ and $^{208}Pb/^{204}Pb$ isotopes overlap fully among the three regions, there are marginal differences in lavas erupted along the craton and reactivated craton margin where slightly more elevated $^{207}Pb/^{204}Pb$ is prevalent (Rogers et al., 2000). These data highlight that, to a first order, the Tanzania craton impacts the isotopic composition of lavas erupted in the region, consistent with existing major and trace element constraints (MacDonald et al., 2001; Foley et al., 2012).

3.3.1 Insights from Carbonatite Magmatism

The unusual characteristics of carbonatite lavas have attracted significant geologic attention and a wealth of isotopic data, despite being only a relatively minor component of magmatism within the rift. Given the recognition that carbonatite lavas are derived from parental magmas that are broadly the same composition as silicate magmatism in the region, discussions as to the reservoirs sampled by carbonatites must parallel probes into the source of magmatism in the region more broadly. While some authors have considered that carbonatites are relatively unaffected by contamination processes in the lithosphere, and are thus effective probes of the mantle source of regional magmatism (Bell and Tilton, 2001), evidence from crystal separates does suggest complex open system processes in these lavas (Simonetti and Bell, 1993, 1994).

Radiogenic isotope constraints have been used to recognize that carbonatites in East Africa broadly form what has been interpreted as a mixing array – termed the East Africa Carbonatite Line (EACL) (Bell and Blenkinsop, 1987) (Fig. 15). The origin/location of the isotopic endmembers contributing to carbonatites remains controversial, with researchers considering that the signature derives from a mantle plume (Bell and Tilton, 2001; Bizimis et al., 2003; Bell and Simonetti, 2010), the continental mantle lithosphere (Paslick et al., 1995; Kalt et al., 1997), or both (Bell and Simonetti, 1996). Importantly, this hypothesized mixing array has been presented as evidence for the existence of distinctive geochemical reservoirs – namely EM1 and HIMU composition (Simonetti and Bell, 1995; Bell and Tilton, 2001). While the Pb isotope signature evident in the lavas of East Africa does extend to very radiogenic values that lie near the HIMU reservoir, the elevated $^{208}Pb/^{204}Pb$ and $^{87}Sr/^{86}Sr$ requires an origin within a HIMU-like or high-μ reservoir (Paslick et al., 1995) rather than the mantle endmember termed HIMU. The participation of these geochemical reservoirs in melt production within the rift requires long-term isolation from the DMM either through residence in the deep mantle or within the SCLM.

The origin of the EM1 signature noted above is widely considered derived from the SCLM (e.g., Muravyeva et al., 2014), though there is a suggestion that EM1 within the rift carbonatites reflects a plume component stored in the deep mantle (Bell and Tilton, 2001). The origin of the HIMU-like signature remains one of the more contentious geochemical questions in East Africa today, with four broad views as to its origin of this isotopic signature:

(1) The HIMU-like signature evolved within the lithospheric mantle following metasomatism during the Pan-African event ca. 600-700 Ma (Rooney et al., 2014b). In this model subduction-related fluids/magmas induced chromatographic metasomatism within the SCLM and formed amphibole-rich channels/veins (e.g., Stein et al., 1997). The HIMU-like isotopic signature evolved due to the high-μ values within the metasome. This model is supported by depleted mantle melt extraction ages, which yield model ages of ca. 600-700 Ma. When age corrected, the HIMU-like Pb signatures fall upon mixing arrays preserved in the Pan-African subduction-related rocks within the mobile belt, suggesting that the HIMU-like Pb isotopic signature is a function of the subduction and insitu evolution (Rooney et al., 2014b).

(2) A related model suggests that the HIMU-like signature evolved insitu within the SCLM following a metasomatic event initiated by a plume or OIB magma (Paslick et al., 1995; Kalt et al., 1997). This model is commonly invoked for rocks in the southern EARS.

(3) A third model suggests that the HIMU-like signature is the result of recent metasomatism of the SCLM by a HIMU-like plume (e.g., Bell and Simonetti, 1996; Le Roex et al., 2001; Späth et al., 2001). In this model, the isotopic signatures are not the result of long-term insitu radiogenic growth but are instead caused by recent plume-lithosphere interaction towards the base of the SCLM (e.g., MacDonald et al., 2001). This model is supported by the lack of correlation between parent and daughter isotopes and

the concentrations of these elements (Le Roex et al., 2001). However, this observation can also be the result of magma mixing, and source hybridization (e.g., Rogers et al., 2006).

(4) The final model suggests that the HIMU-like signature in lavas is the result of the melting of a HIMU-like component within a mantle plume, and that the SCLM is not required (Furman et al., 2004; Nelson et al., 2012; Muravyeva et al., 2014). In this model, melts of a plume result in lavas with a HIMU-like signature. This model is supported by the presence of HIMU-like picritic lavas erupted in Turkana – a region that experienced Mesozoic rifting, likely destroying any Pan-African metasomes.

3.2.2 A Common Lithospheric Component (CLM)

Another lithospheric component has been identified on the basis of the convergence of isotopic arrays for silicate magmas in the western branch of the EARS. Magmas erupted within the western branch exhibit significant isotopic complexity that reflects derivation from an old lithospheric mantle with multiple metasomatic overprints. Furman and Graham (1999) note the presence of a common lithospheric mantle component on the basis of $^{87}Sr/^{86}Sr$ and $^{143}Nd/^{144}Nd$ (and unpublished Pb isotopes) (Fig. 8;13;15). This common lithospheric mantle (CLM) component is defined on the basis of radiating arrays emanating from a value of $^{87}Sr/^{86}Sr$ = 0.7050, $^{143}Nd/^{144}Nd$ = 0.51264, and $^{206}Pb/^{204}Pb$ = 19.0. Furman and Graham (1999) also point out that some degree of heterogeneity must occur within this CLM component due to slight differences in the convergence depending on specific volcanic fields. This reservoir is interpreted to contain helium isotope values equivalent to the upper mantle on the basis of the helium isotope values for rocks erupted in the western branch (where this CLM signature is most pronounced) (Pik et al., 2006). Furman and Graham (1999) suggest that the CLM

signature is derived from the impact of “widespread metasomatic events between 500 and 1000 Ma” on the continental lithospheric mantle. A widespread metasomatic event is consistent with evidence of recent enrichment evident in xenoliths and lavas along the western branch and in northern Tanzania (Davies and Lloyd, 1989; Paslick et al., 1995). Vollmer and Norry (1983) also note that this event was likely superimposed upon older existing mantle lithosphere given the heterogeneity in $^{143}Nd/^{144}Nd$ values. Indeed, older domains are sampled by lavas in Toro Ankole, where 1.8 Ga mantle lithosphere is evident at shallower levels in the lithospheric mantle (Davies and Lloyd, 1989; Rogers et al., 1998). The evidence points to a layered lithosphere: the deepest levels in the lithosphere exhibit the youngest metasomatic imprint, likely located somewhere around the lithosphere-asthenosphere boundary. With continued rifting, older domains at shallower levels become involved in the melt generation process. This model may explain the more radiogenic $^{87}Sr/^{86}Sr$ values in the more established Virunga volcanic province in comparison to the relatively unradiogenic $^{87}Sr/^{86}Sr$ values evident in the juvenile Toro Ankole Province.

The ubiquity of this signature in rocks from the western branch has resulted in the proposal that the CLM component (or a close analog) is actually the common plume signature evident throughout the EARS (Castillo et al., 2014). In this model, a new plume composition (termed ‘V’) was proposed wherein it had a composition similar to the CLM component, but with elevated $^{3}He/^{4}He$ (Castillo et al., 2014). On the basis of this model, the hypothesized plume component was reasoned by Castillo et al. (2014) to be most developed and best expressed within the nephelinites erupting at Nyiragongo. Significantly, however, existing Pb isotope data show that these rocks are derived from a source that exhibits a ca. 500 Ma age (Vollmer and Norry, 1983; Vollmer et al., 1985; Rogers et al., 1998), complicating the attribution to a recent mantle plume. Castillo et al. (2014) suggests that this component is evident throughout East Africa, however, in terms of isotopic Pb-Sr plots, the EARS data series fails to converge on the hypothesized “V”

plume component; the data are better accommodated by the “C” isotopic endmember (Rooney et al., 2012a). It should be noted that the signature of radiogenic Pb isotopes evident at Nyiragongo ($^{206}Pb/^{204}Pb$ ranges from 19.30 to 19.83, *n = 58*) (Chakrabarti et al., 2009) is disconnected from evidence of plume-like $^{3}He/^{4}He$ isotopes (7.1 to 8.5 R/R_A, *n = 7*) (Pik et al., 2006). Further difficulties with this component are apparent when samples from Rungwe that that should have greatest hypothesized contribution from ‘V’ (i.e. those displaying the highest $^{3}He/^{4}He > 14$ and most radiogenic $^{206}Pb/^{204}Pb > 19.8$) plot at the lithospheric end of the mixing array proposed by Castillo et al. (2014). These same samples also exhibit very radiogenic $^{207}Pb/^{204}Pb$ values (15.716-15.743), indicating that the Pb (in addition to the $^{87}Sr/^{86}Sr$ and $^{143}Nd/^{144}Nd$) budget of these lavas is not controlled by contributions from the hypothesized ‘V’ component ($^{207}Pb/^{204}Pb$ ~15.65), and instead suggest that lithospheric mantle associated with the Tanzania Craton may be influencing the isotopic compositions in these samples. In short, this ‘V’ signature is not correlated with evidence of a deep mantle origin, and instead is further support for the existence of a lithospheric-sourced CLM component.

The slightly elevated helium isotope ratios present at Nyiragongo (7.1-8.5 R/R_A) were argued to preclude derivation of these lavas from the lithospheric mantle, which has helium isotope ratios approaching 6.1 R/R_A (Chakrabarti et al., 2009). However, the assertion of a plume origin for lavas from the Virunga field is problematic as the sodic character of the lavas cannot be imparted by phases stable in the asthenosphere (e.g., phlogopite), and instead requires amphibole, which is stable only under lithospheric temperature and pressure conditions (Rosenthal et al., 2009). The slightly elevated $^{3}He/^{4}He$ evident in the CLM component may derive from its location at the base of the lithospheric mantle, with consequent volatile fluxing from the convecting mantle below it. Indeed the noted disconnect between Pb and He isotopes evident in Rungwe requires mass contributions from plume and lithospheric reservoirs, suggesting that mixing between melts derived from the underlying plume (or material fluxing

from it) and the overlying lithospheric mantle are a common feature of the western branch of the EARS. In summary, the ubiquitous component characterized by elevated Pb isotopes in this region is likely located in the lithospheric mantle, consistent with the initial work of Furman and Graham (1999).

4. Reservoirs in the Convecting Upper Mantle

The formation of metasomes, and the generation of magma where such metasomes may be absent, requires a role for melt generation within the convecting upper mantle. Establishing which reservoirs contributed to melt generation can be effectively probed through isotopic fingerprinting.

4.1 The Depleted Mantle Component

Central to magma production in standard models of rifting is the decompression melting of the depleted upper mantle. While the EARS is clearly influenced by a mantle thermo-chemical anomaly, the depleted upper mantle is a ubiquitous component of most studies that seek to constrain the contribution of various reservoirs to melt production. The composition of the depleted mantle component is exemplified by sub-marine lavas from the East Sheba Ridge along the Gulf of Aden (Schilling et al., 1992). East of 48^{o}E, lavas along the East Sheba ridge exhibit significantly less isotopic variation and are isotopically more depleted-mantle like than those closer to the Asal rift and Afar triple junction (Rooney et al., 2012a). The depleted upper mantle composition used in isotopic mixing models was calculated by Schilling et al. (1992) to encompass the data from the region in terms of ternary mixing. It should be noted that no lavas erupted in the region exhibit this component as their sole composition and evidence of mixing between a depleted mantle source and lithospheric mantle source is required by pseudo-binary arrays in Pb-Pb mixing space (Rooney et al., 2012a). These data reflect an event whereby the

upper mantle beneath the EARS and Gulf of Aden has become variably contaminated with lithospheric material, generating a series of hybrid depleted mantle-lithosphere reservoirs (Rooney et al., 2012a) (Fig. 2). Such contamination of the depleted upper mantle has been previously noted along the Mid-Atlantic ridge (e.g., Carlson et al., 1996; Andres et al., 2004; Blichert-Toft et al., 2005) and Indian ridge (e.g., Hanan et al., 2004; Graham et al., 2006), supporting a model whereby lithospheric detachment during rifting may contaminate the reservoir that contributes to magma generation as a rift evolves to an oceanic spreading center (Rooney et al., 2012a).

Aside from the depleted upper mantle component noted above, studies have noted the presence of other depleted components, but the origin of these components have remained enigmatic. Pik et al. (1999) note a depleted component that manifests in the Oligocene flood basalts that feed the LT-type (low titanium), but the origin of this component may be within the plume itself (Pik et al., 1999; Kieffer et al., 2004), or plume-metasomatized lithospheric mantle (Beccaluva et al., 2009; Natali et al., 2016). It should be noted that this component does not appear again in the basalts of East Africa subsequent to this Oligocene phase of flood basalt activity and is thus not relevant to the more recent rocks within the rift. There is, however, another depleted component that has been identified in Quaternary rocks from Afar that appears distinct from the depleted mantle discussed earlier. A group of LREE-depleted basalts has been identified in Manda Hararo (Ethiopia) and in Hayyabley volcano (Djibouti) (Barrat et al., 2003; Daoud et al., 2010). These authors posit that this depleted component is likely an ‘intrinsic part of the plume’. It should be noted that this component is distinct from that considered to contribute the LT basalts during the Oligocene. These magmas are limited in volume and aerial extent suggesting a relatively minor component.

While initial isotopic work in East Africa identified the DMM as a source of magmatism, it equally noted that an isotopically distinct component with radiogenic Sr, Pb, and unradiogenic Nd was required in order to explain the isotopic properties of erupted basalts. While the continental crust is undoubtedly a factor in some magmas (e.g., Hart et al., 1989; Deniel et al., 1994), it was not possible to explain the entirety of the dataset through crustal assimilation. Such observations required a reservoir that had maintained isotopic disequilibrium with the DMM over a long period in order to facilitate radiogenic ingrowth. These early studies highlighted a role either for 'plums' of isotopically distinct material convecting within the asthenosphere (e.g., Hart et al., 1989), or contributions from the continental lithospheric mantle (e.g., Betton and Civetta, 1984). To a first order, these reservoirs continue to be the primary focus of studies today, though significantly more constraints have been placed upon these possible sources.

4.2 The Plume in Afar & Ethiopia

Hart et al. (1989) was among the first to recognize a component in East African magmatism that could not be explained through the interaction of the depleted upper mantle and African Lithosphere. The discovery of an OIB PREMA component within lavas from Afar on the basis of converging isotopic arrays had an inferred composition that was remarkably similar to what we now acknowledge as the Afar plume component in terms of $^{87}Sr/^{86}Sr$ and $^{143}Nd/^{144}Nd$ isotope space, though it was less radiogenic in terms of Pb isotopes. Subsequent work suggested that lavas erupted through the relatively thin crust of northern Afar were the result of the mixing of a HIMU-like plume component with a depleted mantle component that was either contained within the upwelling plume or located in the regional upper mantle (Schilling et al., 1992; Deniel et al., 1994; Barrat et al., 1998). However, the discovery of elevated $^{3}He/^{4}He$ values in the region was inconsistent with HIMU (low $^{3}He/^{4}He$) being the primary reservoir that caused radiogenic Pb

isotopes – a different mantle plume component was required (Marty et al., 1996). Studies of the northwest Ethiopian flood basalts brought further clarity with respect to the composition of the Afar Plume, where the plume signature was thought to be best developed in the HT2 (high titanium type 2) basalts (Pik et al., 1998; Meshesha and Shinjo, 2008). This conclusion was supported by subsequent studies indicating elevated $^{3}He/^{4}He$ and unradiogenic $^{187}Os/^{188}Os$ in these lavas (Pik et al., 2006; Rogers et al., 2010). The convergence of regional arrays in modern lavas in the region in terms of $^{206}Pb/^{204}Pb$ isotope space at ~19.6 (Fig. 16), combined with the primitive helium isotope signatures (Fig. 17) prompted the assignment of the Afar plume component to the "C" mantle reservoir (Rooney et al., 2012a). This "C" reservoir (Hanan and Graham, 1996) is the preferred composition of the radiogenic Pb and primitive helium endmember of the plume, though other less well-constrained components could be present earlier in the development of the Ethiopian Large Igneous Province (Pik et al., 1998, 1999; Kieffer et al., 2004; Meshesha and Shinjo, 2007). This composition of the Afar plume is consistent with subsequent studies that have shown the Afar plume component is consistently of "C"-like composition (Nelson et al., 2012, 2019; Rooney et al., 2013; Alene et al., 2017; Feyissa et al., 2017; Ayalew et al., 2018). It should be noted that the composition of the HT2 Flood Basalts are not identical to the "C" isotopic reservoir given they likely formed through metasomatic interaction between the Afar plume and existing lithospheric mantle. Thus, these lavas should **not** be used as a proxy for the Afar plume composition.

4.3 The Plume in Kenya, Tanzania, and the Western Branch

Significantly more controversy surrounded the determination of the composition of a possible plume component south of Ethiopia. The thicker lithosphere, metasomatic hybridization, and subsequent melting of the existing lithospheric domains by plume-derived magmas (e.g., MacDonald et al., 2001) created ambiguity with respect to the precise signature of the plume

component in this region. As with studies in Afar, a HIMU-like reservoir was initially invoked as a plume composition on the basis of carbonatite studies (Bell and Simonetti, 1996) (Fig. 15), and basalts in Turkana (Class et al., 1994) (Fig. 13). This model was subsequently refined to suggest that the mixing line of EM1 to HIMU that is evident in East African carbonatites (Fig. 15) actually reflected contributions from different deep mantle domains (Bell and Tilton, 2001), though the origin of the less radiogenic domain remained unclear (e.g., Class et al., 1994). Subsequent work has shown the helium isotope values at Oldoinyo Lengai are SCLM-like displaying a $^{3}He/^{4}He$ of 6.75 (Fischer et al., 2009). A source within the lithospheric mantle is supported by work by Kalt et al. (1997) that suggested a more complex series of distinct domains is required to address the isotopic variability in East African carbonatites. The origin of the HIMU-like endmember might thus reflect radiogenic ingrowth in the lithospheric mantle as noted in the prior section.

An alternative approach in constraining the composition of the plume component south of Ethiopia focused on the generally basaltic magmatism within the Kenya Rift. Rogers et al. (2000) noted that the basalts were profoundly impacted by the lithospheric mantle in terms of $^{87}Sr/^{86}Sr$ and $^{143}Nd/^{144}Nd$, and that this effect became more pronounced nearer to the craton (Fig. 8). Rogers et al. (2000) noted that away from the craton, the plume had a greater influence over the magma compositions, while closer the craton the lithospheric mantle dominated. This approach suggested that the Kenya plume component was different from that in Afar by having a less radiogenic $^{143}Nd/^{144}Nd$ value, and also lacking the primitive He isotope signature evident in Afar (Rogers et al., 2000; George and Rogers, 2002). Furman et al. (2006b) suggested that volcanism in Turkana reflected a transition from a HIMU-like plume component within a heterogeneous plume towards a more “C”-like plume composition. The model for a distinct plume composition south of Ethiopia has been complicated by the discovery of primitive helium isotopes in the Rungwe Volcanic Province (Halldórsson et al., 2014) (Fig. 17). This suggests

that the “C”-like signature for the Afar province may be pervasive in East Africa, though best developed in the thinner lithosphere in the northern portions of the rift. Part of the complexity may result in the method by which the plume component contributes to magmatism.

MacDonald et al. (2001) suggests that the lithospheric mantle is metasomatized by a plume, and is subsequently melted in a form of thermo-mechanical erosion (e.g., Fig. 2). Direct evidence of such a process is evident in xenoliths from Ataq (Yemen) where amphibole veins within peridotite mantle xenoliths have the isotopic composition of the Afar plume (Baker et al., 1997). Melting of these veins yielded the Quaternary radiogenic-Pb volcanism on the Arabian plate in Yemen (Baker et al., 1997) (Fig. 18). A possible solution to the less radiogenic $^{143}Nd/^{144}Nd$ isotopes evident in the radiogenic Pb endmember south of Ethiopia (Fig. 8) may be linked to this process (see discussion in next section). The overprint of plume metasomatism upon the Kenya lithospheric mantle may have only partially overprinted the existing unradiogenic CLM component that is noted to broadly exist throughout the region (and is absent further north in Ethiopia). Thus, melts of this metasomatized lithospheric mantle might preserve a less radiogenic $^{143}Nd/^{144}Nd$ value than rocks to the north where less lithospheric mantle control on magmatism is evident. In reality, significantly more work is required in the region to fully assess the potential range of compositions that may form endmembers to magmatism, though to a first order the reader is suggested to assume the “C” mantle reservoir as an appropriate composition for a large part of the plume component that comprises the African Superplume (LLSVP).

5. Towards a New Paradigm

The existing concepts exploring contributions from various reservoirs to rift magmatism are based upon studies within specific regions. When assessed as a unified dataset, the data from the EARS reveals important isotopic vectors that are not apparent when considering individual

regions. Critically, coherent arrays that may have been apparent when considering one rock group (e.g., carbonatites) instead may join newly apparent arrays with a different mixing geometry. Such insights provide new constraints as to the potential mechanisms of reservoir mixing and possible contributions from lithospheric and sub-lithospheric reservoirs.

5.1 Lithospheric Sources in the Craton

When explored in more detail, the geometry of the arrays formed by lavas in the cratonic regions differs fundamentally from those in the mobile belt. Lavas in the mobile belt exhibit mixing trajectories between isotopic reservoirs that result in coupled changes to the $^{206}Pb/^{204}Pb$ and other isotopic systems as shown (Fig. 18). Such lateral arrays are distinct from lavas erupted within the cratonic regions, where instead, almost vertical arrays are evident in $^{207}Pb/^{204}Pb$, $^{87}Sr/^{86}Sr$, and $^{143}Nd/^{144}Nd$ at any given value of $^{206}Pb/^{204}Pb$ (Fig. 13).

A clue as to the origin and location of the isotopic reservoirs within the cratonic regions lies in their radiogenic $^{207}Pb/^{204}Pb$ values. Given the near exhaustion of the ^{235}U system in terms of ^{207}Pb production from modern U, the timing of the elevation in μ, which would have been required to generate radiogenic $^{206}Pb/^{204}Pb$, must have occurred at a much earlier period in Earth's history in comparison to the source of the Afar plume (which contains much less radiogenic $^{207}Pb/^{204}Pb$). While an unusual component within the Afar mantle plume could theoretically have been the source of this old Pb (e.g., Chakrabarti et al., 2009), the occurrence of this component in conjunction with: (A) The cratonic lithosphere, and (B) melts derived from lithologies dominated by amphibole and phlogopite (e.g., Foley et al., 2012), are strong evidence for lithospheric origin for these component(s), and preclude a direct origin from a mantle plume (e.g., Rosenthal et al., 2009). While some of the extreme isotopic signatures may be the result of crustal assimilation, the continued presence of these components within primitive magmas argues for a source within the lithospheric mantle (Rogers et al., 1998).

The origin of the younger radiogenic Pb component (radiogenic $^{206}Pb/^{204}Pb$, unradiogenic $^{207}Pb/^{204}Pb$), which anchors the other side of the isotopic arrays within the craton, remains poorly constrained. As I have previously described, multiple models exist that may explain the data and are mentioned here for clarity:

A) *No plume source:* Several authors have suggested that a lithospheric component may have developed within the cratonic region that had less extreme isotopic characteristics (Rogers et al., 1998; Furman and Graham, 1999; Rosenthal et al., 2009). A layered lithospheric mantle has been postulated, whereby the lower portions of the lithospheric mantle are younger and associated with either the Kibarian or Pan-African orogeny. Fusion of these lithospheric components results in surface magmatism (Rogers et al., 1998). This is a viable reservoir and may contribute to the mixing arrays seen, though the composition of this reservoir is difficult to resolve from the Afar plume component in a regional sense. Resolving the potential contributions from this more recent lithospheric component and the Afar plume necessitates detailed study on a local scale. It should be noted, however, that the recent discovery of elevated $^{3}He/^{4}He$ at Rungwe suggests that at least in some regions a mass contribution from a deeply sourced plume is also required.

B) *Direct Plume Source:* In this model, magmas are a direct mix of a melt of a hypothesized plume component (termed “V”), and components located within the lithospheric mantle (Castillo et al., 2014). This model relies upon magmas at Nyiragongo being an almost pure plume component, which is unlikely given the metasomatic origin of lavas from the region (see discussion in prior section) (Rosenthal et al., 2009).

C) *Indirect Plume Source:* It is currently unclear if melts from the Afar plume mix with melts derived from lithospheric mantle metasomes or if plume-derived melts metasomatized

the lower lithospheric mantle, which subsequently melted and mixed with older lithospheric metasomes. Whatever the precise mechanism, the occurrence of elevated $^{3}He/^{4}He$ at Rungwe requires mass contribution from a deeply sourced mantle plume, and an indirect model whereby metasomatic minerals may grow within the lithospheric mantle may solve the dilemma noted above.

D) *Hybrid model:* A possible resolution (and my preferred solution) is a model whereby a deeply sourced plume metasomatized the lower lithospheric mantle, which itself has a composition more akin to the younger metasomatic component noted in the 'no plume source' models above. Mixing of melts derived from this hybrid metasome with melts derived from more ancient metasomes at shallower levels within the cratonic lithospheric mantle would result in melts that have a metasomatic major and trace element signature and isotopic mixing characteristics similar to that seen in the data (Fig. 13). The composition of the deeply sourced plume component appears identical to that identified for the Afar Plume.

It should be noted that a consequence for existence of two reservoirs with elevated $^{206}Pb/^{204}Pb$ within the craton is that any attempt at correlation between $^{206}Pb/^{204}Pb$ and other isotopic indicators should be undertaken with extreme caution. Such problems become particularly acute when $^{206}Pb/^{204}Pb$ is used as an unambiguous indicator of Afar plume contribution to a magma in the cratonic regions.

5.2 The Afar Plume and the Mobile Belt

The influence of the Afar plume, which manifests as a relatively radiogenic Pb endmember, is typically most clearly exhibited within samples from the mobile belt. Here, there is clear correlation between various radiogenic isotopes and $^{206}Pb/^{204}Pb$. In all isotopic plots, the Afar

plume endmember, which has been previously defined as having relatively radiogenic $^{206}Pb/^{204}Pb$ equivalent to the “C” mantle reservoir (e.g., Furman et al., 2006; Rooney et al., 2012; Nelson et al., 2019), forms an endmember from which the data fan outwards (Fig. 18). Consequently, samples from within the mobile belt that contain more radiogenic $^{206}Pb/^{204}Pb$ likely have greater proportions derived from the Afar plume in their source as the Afar plume is the dominant reservoir with radiogenic $^{206}Pb/^{204}Pb$ in this region. Such an observation is consistent with the tendency for high $^{3}He/^{4}He$ to be correlated with more radiogenic $^{206}Pb/^{204}Pb$ (Fig. 18). The anchoring of the Pb isotope arrays by the Afar Plume for mobile belt lavas is particularly evident in terms of ternary Pb isotope space (Fig. 19). Within this ternary geometry, lavas broadly follow a trend from the Afar Plume member towards less radiogenic Pb compositions. This geometry has been previously interpreted as mixing between melts derived from the Afar plume, and a hybrid ambient upper mantle that is comprised of variable proportions of the depleted mantle reservoir and material associated with the Pan-African lithosphere (Rooney et al., 2012a) (Fig. 19).

Constraining the composition of the hybrid upper mantle, which anchors the unradiogenic side of the broad mixing array evident in ternary Pb isotopic space (Fig. 19), is complicated by crustal assimilation and potential contributions from the sub-continental lithospheric mantle. Few locales in the rift have a sufficient data density where mixing calculations can constrain the relative contributions from lithospheric and sub-lithospheric reservoirs. Despite such limitations insights as to the identity of the less radiogenic Pb component, evident in ternary Pb isotopic mixing space within the mobile belt, can be revealed by the broad compositional differences between the different regions. In areas where rifting is mature, such as Afar and the margins of the Gulf of Aden in Yemen, lavas typically form arrays emanating from the Afar plume outward towards relatively unradiogenic $^{207}Pb/^{204}Pb$ and $^{87}Sr/^{86}Sr$, and radiogenic $^{143}Nd/^{144}Nd$ (Fig. 18). Such isotopic characteristics are consistent with a greater influence from the depleted mantle

endmember in the formation of the hybrid upper mantle component. Conversely, where rifting is less mature (i.e., within the MER), the unradiogenic Pb component displays mixing trajectories in terms of $^{207}Pb/^{204}Pb$, $^{87}Sr/^{86}Sr$, and $^{143}Nd/^{144}Nd$ consistent with a greater contribution from the Pan-African lithosphere. Curiously, in Turkana and portions of the northern Kenya Rift, mixing trajectories suggest even less Pan-African lithosphere component than Yemen and Afar (Fig. 18). Such an observation can be interpreted in conjunction with existing structural data that shows that this region was impacted by an earlier rifting event during the Mesozoic. When considered together, the isotopic data from lavas erupted within the mobile belt highlights two processes: (A) the influence of the Afar plume in melt production, and (B) the variable contamination of the upper mantle by the Pan-African lithosphere. In regions where rifting is mature or has previously occurred, the influence of the Pan-African lithosphere is less than in regions where rifting is less mature.

The three-component model noted above provides an effective explanation for the observed isotopic variation, though when examined in detail, complexity is evident. The location of each of these three endmembers is less well-constrained – for example, potential metasomatism of the subcontinental lithospheric mantle by the Afar plume may yield magmas that isotopically resemble the Afar plume but have a metasomatic signature in terms of trace element patterns (Beccaluva et al., 2009). A melt from such a metasome would have the same isotopic signature as the Afar plume (e.g. primitive helium isotopes), but have trace element concentrations that are controlled by the modal mineralogy of the melting metasome, potentially explaining some of the scatter in terms of helium isotopes vs Zr/Nb (Fig. 17). Similarly, ancient metasomatic events impacting the sub-continental lithospheric mantle have resulted in the ingrowth of radiogenic $^{206}Pb/^{204}Pb$ unrelated to the Afar plume (e.g., Rooney et al., 2014b; Nelson et al., 2019). Indeed, some of the scatter at radiogenic values of $^{206}Pb/^{204}Pb$ (Fig. 18) may relate to samples that contain this fourth ancient metasomatic radiogenic Pb endmember. This ancient metasomatic

lithospheric endmember (or, family of endmembers) becomes particularly important when considering lavas that erupted through the cratonic lithosphere as has been discussed in the previous section. In ternary Pb space, the cratonic samples extend to values significantly more radiogenic in $^{206}Pb/^{204}Pb$, and form arrays that are typically displaced towards more thorogenic Pb (^{208}Pb derived from the decay of ^{232}Th) (Fig. 20).

The constraints available within the mobile belt on both endmembers to the isotopic arrays provide an opportunity to explore the variation of these isotopic systems with helium isotopes. Due to the hybridization of one of the endmembers (depleted mantle and Pan-African lithosphere) and the similarity of this hybrid endmember to the Afar Plume in terms of $^{87}Sr/^{86}Sr$ and $^{143}Nd/^{144}Nd$, little variation is evident in mobile belt lavas in terms of correlation between these systems and helium isotopes (Fig. 17). However, significant leverage on the mixing process between the plume and hybrid upper mantle can be gained when examining the Pb isotopic system. Here, clear correlations between the three Pb isotope systems and the Afar plume, translate to correlation with helium isotopes (Fig. 17). Less clear is any correlation between the degree of incompatible trace element enrichment (e.g., Zr/Nb) and helium isotopes, suggesting that the specific source reservoir contribution (i.e., the ratio of plume to hybrid upper mantle), may not be the dominant control on incompatible element concentrations in erupted lavas (Fig. 17). I have not discussed the data from Rungwe (in the cratonic region) in the context of variation of helium isotopes. The reason becomes apparent when considering the geometry of mixing in the cratonic region and complexities associated with enriched metasomes within the lithospheric mantle that may also exhibit radiogenic Pb values.

These data show that Sr-Nd-Pb isotopic arrays, both within the mobile belt and cratonic regions, roughly converge on the Afar plume composition (Fig. 16), suggesting that this component may exist throughout the EARS. Given the Afar Plume is the only recognized high

$^{3}He/^{4}He$ source in the region, this interpretation is consistent with observations of elevated $^{3}He/^{4}He$ extending discontinuously from Rungwe to Afar (Hilton et al., 2011; Halldórsson et al., 2014). These interpretations are further supported by evidence of a widespread thermal anomaly in the upper mantle beneath the EARS (Rooney et al., 2012c). When combined with the existing geophysical results (Ritsema et al., 1999, 2011; Bastow et al., 2010; Mulibo and Nyblade, 2013), the implication of these observations is that material derived from African LLSVP is present within the upper mantle throughout East Africa. A tentative conclusion may thus be drawn that the Afar Plume may represent the prevalent composition of material rising from the African LLSVP into the East African upper mantle.

6. Conclusions

The original observation of spatial and temporal variation in the degree of silica-saturation in rift lavas now appears resolved. Melt generated from amphibole- or phlogopite-bearing metasomes within the lithospheric mantle yields alkaline, silica-undersaturated lavas, while more silica-saturated lavas are primarily a function of melting from the sub-lithospheric domains in the upper mantle. Smaller degrees of melting from deeper regions of the sub-lithospheric mantle are not precluded, and may add additional complexity to this model, but this process is not necessary for explaining the existing key observations. The sourcing of silica-undersaturated melts within the lithospheric mantle is consistent with the observed tendency in the rift for initial melts within any given region to exhibit this composition, likely reflecting the initial destabilization and thinning of the lithospheric mantle. With continued lithospheric thinning, the trend towards silica-saturated compositions reflects melting of the sub-lithospheric (i.e. convecting) mantle. Given these lavas are derived from distinct domains, this model allows for the simultaneous eruption of both compositions. Where there is an observation of a temporal shift in magma

compositions from more silica-saturated to silica-undersaturated, there is typically a commensurate decrease in the degree of extension. A decrease in the rate of mantle upwelling and associated decompression reduces more silica-saturated melt-creation within the sub-lithosphere (convecting) upper mantle. During this reduced extension phase, metasomes within the lithospheric mantle (pre-existing, or those formed during the prior high-flux phase) may still yield melt upon minor thermobaric perturbation. Critical to this model is the abandonment of the concept that HREE fractionation is an unambiguous indicator of depth of melting where metasome-derived magmas are identified; melt generated from mantle metasomes may exhibit HREE fractionation that is unrelated to depth of melt generation, and instead may reflect the composition of the melt which initially formed the metasome, or the modal mineralogy of the metasome. Thus, the current interpretations where changes in HREE fractionation are the result of unusual shallowing and deepening of melt generation zones during rift evolution, may instead reflect changes in source.

The presence of mantle metasomes in the East African lithospheric mantle may also provide insights into the formation of carbonatite lavas. There is growing evidence that such lavas are not derived directly from the mantle and are instead a product of immiscibility from an alkaline silicate magma. These silicate magmas are derived from a source that is not particularly enriched in carbonate, thus the key to the immiscibility process is alkalinity, which facilitates retention of CO_2 in the silicate magma at sufficient concentrations to allow for subsequent carbonate immiscibility. Small degree melts of amphibole- or phlogopite-bearing metasomes in the East African lithospheric mantle are thought to create an ideal starting magma wherefrom carbonatite lavas may eventually form.

Other differentiation processes within the East African lithosphere yield evolved compositions through assimilation, fractional crystallization, and magma mixing within stacked

magma mush zones (Fig. 11). These magma mush zones are continuously (or episodically) fluxed by primitive rift magmas. Resorption of the cumulate crystals, and mingling/mixing of a diverse array of melts help explain the complex compositional range possible within any rift volcano (Fig. 11). Melt extraction is likely related to the crystal mush reaching discrete rigid locking points, helping to explaining the frequent observation of Daly Gaps in rift lavas.

Exploring the range of compositions evident in mafic rift lavas, six magma series have become apparent on the basis of variations in the primitive mantle normalized incompatible element diagrams. Type I lavas are associated with the Eocene and Oligocene flood basalt events. Type II lavas have an OIB signature and are most frequently associated with melts derived from lithospheric metasomes, though some compositions are posited by some as being derived from sub-lithospheric (convecting) domains. Type III lavas are the most common in the rift and are considered to represent melts of the ambient sub-lithosphere (convecting) mantle and comprised of a mixture of Afar Plume, depleted upper mantle, and African lithosphere. Type IV lavas are a mix of Type II and III lavas, and are found in regions that are transitioning between the two magma types during progressive lithospheric thinning. Type V lavas are associated with melt derived from phlogopite-bearing metasomes and are typically limited to the western branch of the EAR. Type VI lavas reflect the influence of an unusual depleted component of uncertain origin, though currently thought to be a minor component within the plume. These lava families do not have consistent isotopic fingerprints, revealing complexity in how these lava families form, and the magnitude of contributions from different isotopically-defined reservoirs to East African magmatism.

At its most elemental, the origin of lavas in East Africa is largely the result of either: (A) melting of easily fusible compositions located within the lithospheric mantle due to thermobaric perturbations of the lithosphere, or (B) melting of the sub-lithospheric (convecting) upper mantle

due to decompression caused by thinning of the plate during extension. The isotopic systematics of East African magmatism reveals significant complexity as to the specific reservoirs that may participate in the melting processes noted above. The most obvious heterogeneity in the composition of East African Rift lavas is the relationship between isotopically extreme values and proximity to the Tanzania craton. Here, the lithospheric mantle has undergone enrichment through the percolation of sub-lithospheric derived melts and fluids over an extended interval, which has resulted in a layered lithospheric mantle exhibiting extreme isotopic ratios. Elsewhere, the lithospheric mantle has also undergone enrichment but given the more juvenile age of this lithosphere, less extreme isotopic values have developed. These observations might lead the reader to conclude that lavas exhibiting trace element evidence of a derivation from a metasome (e.g. Type II) would thus display isotopic characteristics of ancient reservoirs within the lithospheric mantle. This is, however, not the case as material rising from the African LLSVP has also metasomatized the lithospheric mantle and thus lavas exhibiting a Type II signature (or any hybrid signature where this component may have contributed) may exist as any number of reservoirs or mixtures of these reservoirs. When the isotopic characteristics of magma suites from throughout the region are examined, the influence of the plume component is evident – arrays converge on composition of the Afar plume (some complexity is evident where the plume material has formed a hybrid plume-lithosphere component). The convergence of these arrays is remarkable and is strong support for a model wherein the prevalent composition of material rising from the African LLSVP in East Africa is broadly equivalent to the Afar plume. Material derived from the sub-lithospheric (convecting) upper mantle is typified by lavas with the trace element pattern Type III. These lavas exhibit an isotopic composition that incorporates the Afar Plume endmember, a depleted mantle endmember, and some form of lithospheric endmember. While in some Type III lavas, there is evidence of lithospheric overprint during magma differentiation, in others the linear arrays in

primitive lavas require an upper mantle where depleted mantle and lithosphere have mixed and then mix with Afar Plume melts. When one considers the potential of mixing between melts derived from these diverse range of potential reservoirs, it becomes clear that resolving the origin of a rift lava may be challenging.

References Cited

Alene, M., Hart, W.K., Saylor, B.Z., Deino, A., Mertzman, S., Haile-Selassie, Y., and Gibert, L.B., 2017, Geochemistry of Woranso–Mille Pliocene basalts from west-central Afar, Ethiopia: Implications for mantle source characteristics and rift evolution: Lithos, v. 282, p. 187–200.

Andres, M., Blichert-Toft, J., and Schilling, J.G., 2004, Nature of the depleted upper mantle beneath the Atlantic: evidence from Hf isotopes in normal mid-ocean ridge basalts from 79 degrees N to 55 degrees S: Earth and Planetary Science Letters, v. 225, p. 89–103.

Armitage, J.J., Ferguson, D.J., Goes, S., Hammond, J.O., Calais, E., Rychert, C.A., and Harmon, N., 2015, Upper mantle temperature and the onset of extension and break-up in Afar, Africa: Earth and Planetary Science Letters, v. 418, p. 78–90.

Ayalew, D., Jung, S., Romer, R.L., and Garbe-Schönberg, D., 2018, Trace element systematics and Nd, Sr and Pb isotopes of Pliocene flood basalt magmas (Ethiopian rift): A case for Afar plume-lithosphere interaction: Chemical Geology, v. 493, p. 172–188, doi:https://doi.org/10.1016/j.chemgeo.2018.05.037.

Baker, B.H., 1987, Outline of the petrology of the Kenya rift alkaline province: Geological Society, London, Special Publications, v. 30, p. 293–311.

Baker, J.A., Menzies, M.A., Thirlwall, M.F., and Macpherson, C.G., 1997, Petrogenesis of quaternary intraplate volcanism, Sana'a, Yemen: Implications for plume-lithosphere interaction and polybaric melt hybridization: Journal of Petrology, v. 38, p. 1359–1390.

Barrat, J.A., Fourcade, S., Jahn, B.M., Cheminee, J.L., and Capdevila, R., 1998, Isotope (Sr, Nd, Pb, O) and trace-element geochemistry of volcanics from the Erta'Ale range (Ethiopia): Journal of Volcanology and Geothermal Research, v. 80, p. 85–100.

Barrat, J.A., Joron, J.L., Taylor, R.N., Fourcade, S., Nesbitt, R.W., and Jahn, B.M., 2003, Geochemistry of basalts from Manda Hararo, Ethiopia: LREE-depleted basalts in Central Afar: Lithos, v. 69, p. 1–13.

Bastow, I.D., Pilidou, S., Kendall, J.M., and Stuart, G.W., 2010, Melt-Induced seismic anisotropy and magma assisted rifting in Ethiopia: evidence from surface waves: Geochemistry Geophysics Geosystems, p. Q0AB05, doi:10.1029/2010GC003036, doi:10.1029/2010GC003036.

Baudouin, C., Parat, F., Denis, C.M., and Mangasini, F., 2016, Nephelinite lavas at early stage of rift initiation (Hanang volcano, North Tanzanian Divergence): Contributions to Mineralogy and Petrology, v. 171, p. 64.

Beccaluva, L., Bianchini, G., Natali, C., and Siena, F., 2009, Continental flood basalts and mantle plumes: a case study of the Northern Ethiopian Plateau: Journal of Petrology, v. 50, p. 1377–1403.

Bell, K., and Blenkinsop, J., 1987, Nd and Sr Isotopic Compositions of East-African Carbonatites - Implications for Mantle Heterogeneity: Geology, v. 15, p. 99–102.

Bell, K., and Simonetti, A., 1996, Carbonatite magmatism and plume activity: Implications from the Nd, Pb and Sr isotope systematics of Oldoinyo Lengai: Journal of Petrology, v. 37, p. 1321–1339.

Bell, K., and Simonetti, A., 2010, Source of parental melts to carbonatites–critical isotopic constraints: Mineralogy and Petrology, v. 98, p. 77–89.

Bell, K., and Tilton, G.R., 2001, Nd, Pb and Sr isotopic compositions of east African carbonatites: Evidence for mantle mixing and plume inhomogeneity: Journal of Petrology, v. 42, p. 1927–1945.

Betton, P.J., and Civetta, L., 1984, Strontium and neodymium isotopic evidence for the heterogeneous nature and development of the mantle beneath Afar (Ethiopia): Earth and planetary science letters, v. 71, p. 59–70.

Biggs, J., Bastow, I.D., Keir, D., and Lewi, E., 2011, Pulses of deformation reveal frequently recurring shallow magmatic activity beneath the Main Ethiopian Rift: Geochemistry, Geophysics, Geosystems, v. 12, p. doi:10.1029/2011GC003662, doi:doi:10.1029/2011GC003662.

Bizimis, M., Salters, V.M., and Dawson, J.B., 2003, The brevity of carbonatite sources in the mantle: evidence from Hf isotopes: Contributions to Mineralogy and Petrology, v. 145, p. 281–300, doi:10.1007/s00410-003-0452-3.

Blichert-Toft, J., Agranier, A., Andres, M., Kingsley, R., Schilling, J.G., and Albarede, F., 2005, Geochemical segmentation of the Mid-Atlantic Ridge north of Iceland and ridge-hot spot interaction in the North Atlantic: Geochemistry Geophysics Geosystems, v. 6, p. Q01E19, doi:10.1029/2004GC000788.

Boynton, W.V., 1984, Cosmochemistry of the rare earth elements: meteorite studies, *in* Henderson, P. ed., Rare earth element geochemistry, Amsterdam, Elsevier, p. 63–114.

Brooker, R.A., and Kjarsgaard, B.A., 2011, Silicate–Carbonate Liquid Immiscibility and Phase Relations in the System SiO2–Na2O–Al2O3–CaO–CO2 at 0·1–2·5 GPa with Applications to Carbonatite Genesis: Journal of Petrology, v. 52, p. 1281–1305, doi:10.1093/petrology/egq081.

Carlson, R.W., Esperanca, S., and Svisero, D.P., 1996, Chemical and Os isotopic study of Cretaceous potassic rocks from southern Brazil: Contributions to Mineralogy and Petrology, v. 125, p. 393–405.

Castillo, P.R., Hilton, D.R., and Halldórsson, S.A., 2014, Trace element and Sr-Nd-Pb isotope geochemistry of Rungwe Volcanic Province, Tanzania: implications for a Superplume source for East Africa Rift magmatism: Frontiers in Earth Science, v. 2, p. 21.

Chakrabarti, R., Basu, A.R., Santo, A.P., Tedesco, D., and Vaselli, O., 2009, Isotopic and geochemical evidence for a heterogeneous mantle plume origin of the Virunga volcanics, Western rift, East African Rift system: Chemical Geology, v. 259, p. 273–289.

Chiasera, B., Rooney, T.O., Girard, G., Yirgu, G., Grosfils, E.B., Ayalew, D., Mohr, P., and Zimbelman, M.R.R., 2018, Magmatically assisted off-rift extension—The case for broadly distributed strain accommodation: Geosphere, v. 14, p. 1544–1563, doi:10.1130/ges01615.1.

Church, A.A., and Jones, A.P., 1995, Silicate—Carbonate Immiscibility at Oldoinyo Lengai: Journal of Petrology, v. 36, p. 869–889.

Class, C., Altherr, R., Volker, F., Eberz, G., and Mcculloch, M.T., 1994, Geochemistry of Pliocene to Quaternary alkali basalts from the Huri Hills, Northern Kenya: Chemical Geology, v. 113, p. 1–22.

Class, C., and Goldstein, S.L., 1997, Plume-lithosphere interactions in the ocean basins; constraints from the source mineralogy: Earth and Planetary Science Letters, v. 150, p. 245–260.

Clément, J.-P., Caroff, M., Hémond, C., Tiercelin, J.-J., Bollinger, C., Guillou, H., and Cotton, J., 2003, Pleistocene magmatism in a lithospheric transition area: petrogenesis of alkaline and peralkaline lavas from the Baringo-Bogoria Basin, central Kenya Rift: Canadian Journal of Earth Sciences, v. 40, p. 1239–1257.

Daoud, M.A., Maury, R.C., Barrat, J.A., Taylor, R.N., Le Gall, B., Guillou, H., Cotten, J., and Rolet, J., 2010, A LREE-depleted component in the Afar plume: Further evidence from Quaternary Djibouti basalts: Lithos, v. 114, p. 327–336, doi:DOI 10.1016/j.lithos.2009.09.008.

Davies, G.R., and Lloyd, F.E., 1989, Pb–Sr–Nd isotope and trace element data bearing on the origin of the potassic subcontinental lithosphere beneath south west Uganda, *in* Kimberlites and Related Rocks, Blackwell Scientific, Geologial Society of Australia Special Publication, v. 14, p. 784–794.

Davies, G.R., and Macdonald, R., 1987, Crustal influences in the petrogenesis of the Naivasha Basalt—Comendite Complex: combined trace element and Sr-Nd-Pb isotope constraints: Journal of Petrology, v. 28, p. 1009–1031.

Dawson, J.B., 2008, The Gregory rift valley and Neogene-recent volcanoes of northern Tanzania, *in* Geological Society of London.

Dawson, J.B., Pinkerton, H., Pyle, D.M., and Nyamweru, C., 1994, June 1993 eruption of Oldoinyo Lengai, Tanzania: exceptionally viscous and large carbonatite lava flows and evidence for coexisting silicate and carbonate magmas: Geology, v. 22, p. 799–802.

Dawson, J.B., Pyle, D.M., and Pinkerton, H., 1996, Evolution of natrocarbonatite from a wollastonite nephelinite parent: evidence from the June, 1993 eruption of Oldoinyo Lengai, Tanzania: The Journal of Geology, v. 104, p. 41–54.

Deniel, C., Vidal, P., Coulon, C., and Vellutini, P.J., 1994, Temporal evolution of mantle sources during continental rifting - the volcanism of Djibouti (Afar): Journal of Geophysical Research-Solid Earth, v. 99, p. 2853–2869.

Dickin, A.P., 2018, Radiogenic isotope geology: Cambridge university press.

Eggler, D.H., and Bell, K., 1989, Carbonatites, primary melts, and mantle dynamics: Carbonatites: Genesis and Evolution, p. 561–579.

Ferguson, D.J., Maclennan, J., Bastow, I.D., Pyle, D.M., Jones, S.M., Keir, D., Blundy, J.D., Plank, T., and Yirgu, G., 2013, Melting during late-stage rifting in Afar is hot and deep: Nature, v. 499, p. 70–73, doi:10.1038/nature12292 http://www.nature.com/nature/journal/v499/n7456/abs/nature12292.html#supplementary-information.

Feyissa, D.H., Shinjo, R., Kitagawa, H., Meshesha, D., and Nakamura, E., 2017, Petrologic and geochemical characterization of rift-related magmatism at the northernmost Main Ethiopian Rift: Implications for plume-lithosphere interaction and the evolution of rift mantle sources: Lithos, v. 282, p. 240–261.

Field, L., Blundy, J., Calvert, A., and Yirgu, G., 2013, Magmatic history of Dabbahu, a composite volcano in the Afar Rift, Ethiopia: Geological Society of America Bulletin, v. 125, p. 128–147, doi:10.1130/b30560.1.

Fischer, T.P., Burnard, P., Marty, B., Hilton, D.R., Füri, E., Palhol, F., Sharp, Z.D., and Mangasini, F., 2009, Upper-mantle volatile chemistry at Oldoinyo Lengai volcano and the origin of carbonatites: Nature, v. 459, p. 77–80.

Foley, S.F., Link, K., Tiberindwa, J.V., and Barifaijo, E., 2012, Patterns and origin of igneous activity around the Tanzanian craton: Journal of African Earth Sciences, v. 62, p. 1–18.

Foley, S., Musselwhite, D., and Van der Laan, S.R., 1999, Melt compositions from ultramafic vein assemblages in the lithospheric mantle: a comparison of cratonic and non-cratonic settings, *in* International Kimberlite Conference (7th: 1998), Red Roof Design, p. 238–246.

Furman, T., Bryce, J.G., Karson, J., and Iotti, A., 2004, East African Rift System (EARS) plume structure: Insights from quaternary mafic lavas of Turkana, Kenya: Journal of Petrology, v. 45, p. 1069–1088.

Furman, T., Bryce, J.G., Rooney, T., Hanan, B.B., Yirgu, G., and Ayalew, D., 2006a, Heads and tails: 30 million years of the Afar plume, *in* Yirgu, G., Ebinger, C., and Maguire, P. eds., The Afar Volcanic Province within the East African Rift System, Special Publication of the Geological Society, London, v. 259, p. 95–120.

Furman, T., and Graham, D., 1999, Erosion of lithospheric mantle beneath the East African Rift system; geochemical evidence from the Kivu volcanic province: Lithos, v. 48, p. 237–262.

Furman, T., Kaleta, K.M., Bryce, J.G., and Hanan, B.B., 2006b, Tertiary mafic lavas of Turkana, Kenya: Constraints on East African plume structure and the occurrence of high-mu volcanism in Africa: Journal of Petrology, v. 47, p. 1221–1244.

Furman, T., Nelson, W.R., and Elkins-Tanton, L.T., 2016, Evolution of the East African rift: Drip magmatism, lithospheric thinning and mafic volcanism: Geochimica Et Cosmochimica Acta, v. 185, p. 418–434.

Gautheron, C., and Moreira, M., 2002, Helium signature of the subcontinental lithospheric mantle: Earth and Planetary Science Letters, v. 199, p. 39–47, doi:http://dx.doi.org/10.1016/S0012-821X(02)00563-0.

George, R.M., and Rogers, N.W., 2002, Plume dynamics beneath the African Plate inferred from the geochemistry of the Tertiary basalts of southern Ethiopia: Contributions to Mineralogy and Petrology, v. 144, p. 286–304.

Ghiorso, M.S., and Sack, R.O., 1995, Chemical mass-transfer in magmatic processes .4. A revised and internally consistent thermodynamic model for the interpolation and extrapolation of liquid-solid equilibria in magmatic systems at elevated-temperatures and pressures: Contributions to Mineralogy and Petrology, v. 119, p. 197–212.

Goles, G.G., 1976, Some constraints on the origin of phonolites from the Gregory Rift, Kenya, and inferences concerning basaltic magmas in the Rift System: Lithos, v. 9, p. 1–8, doi:https://doi.org/10.1016/0024-4937(76)90051-7.

Graham, D.W., Blichert-Toft, J., Russo, C.J., Rubin, K.H., and Albarede, F., 2006, Cryptic striations in the upper mantle revealed by hafnium isotopes in southeast Indian ridge basalts: Nature, v. 440, p. 199–202.

Graham, D.W., Humphris, S.E., Jenkins, W.J., and Kurz, M.D., 1992, Helium Isotope Geochemistry of Some Volcanic-Rocks from Saint-Helena: Earth and Planetary Science Letters, v. 110, p. 121–131.

Green, D.H., 1973, Experimental melting studies on a model upper mantle composition at high pressure under water-saturated and water-undersaturated conditions: Earth and Planetary Science Letters, v. 19, p. 37–53.

Green, D.H., Hibberson, W.O., Kovács, I., and Rosenthal, A., 2010, Water and its influence on the lithosphere–asthenosphere boundary: Nature, v. 467, p. 448, doi:10.1038/nature09369 https://www.nature.com/articles/nature09369#supplementary-information.

Griffiths, P.S., and Gibson, I.L., 1980, The geology and petrology of the Hannington Trachyphonolite formation, Kenya Rift Valley: Lithos, v. 13, p. 43–53, doi:https://doi.org/10.1016/0024-4937(80)90060-2.

Guzmics, T., Berkesi, M., Bodnar, R.J., Fall, A., Bali, E., Milke, R., Vetlényi, E., and Szabó, C., 2019, Natrocarbonatites: A hidden product of three-phase immiscibility: Geology, v. 47, p. 527–530, doi:10.1130/G46125.1.

Guzmics, T., Mitchell, R.H., Szabó, C., Berkesi, M., Milke, R., and Abart, R., 2011, Carbonatite melt inclusions in coexisting magnetite, apatite and monticellite in Kerimasi calciocarbonatite, Tanzania: melt evolution and petrogenesis: Contributions to Mineralogy and Petrology, v. 161, p. 177–196.

Guzmics, T., Mitchell, R.H., Szabó, C., Berkesi, M., Milke, R., and Ratter, K., 2012, Liquid immiscibility between silicate, carbonate and sulfide melts in melt inclusions hosted in co-precipitated minerals from Kerimasi volcano (Tanzania): evolution of carbonated nephelinitic magma: Contributions to Mineralogy and Petrology, v. 164, p. 101–122.

Guzmics, T., Zajacz, Z., Mitchell, R.H., Szabó, C., and Wälle, M., 2015, The role of liquid–liquid immiscibility and crystal fractionation in the genesis of carbonatite magmas: insights from Kerimasi melt inclusions: Contributions to Mineralogy and Petrology, v. 169, p. 1–18.

Halldórsson, S.A., Hilton, D.R., Scarsi, P., Abebe, T., and Hopp, J., 2014, A common mantle plume source beneath the entire East African Rift System revealed by coupled helium-neon systematics: Geophysical Research Letters, v. 41, p. 2304–2311.

Hanan, B.B., Blichert-Toft, J., Pyle, D.G., and Christie, D.M., 2004, Contrasting origins of the upper mantle revealed by hafnium and lead isotopes from the Southeast Indian Ridge: Nature, v. 432, p. 91–94.

Hanan, B.B., and Graham, D.W., 1996, Lead and helium isotope evidence from oceanic basalts for a common deep source of mantle plumes: Science, v. 272, p. 991–995.

Harmer, R.E., and Gittins, J., 1998, The case for primary, mantle-derived carbonatite magma: Journal of Petrology, v. 39, p. 1895–1903.

Hart, W.K., Woldegabriel, G., Walter, R.C., and Mertzman, S.A., 1989, Basaltic volcanism in Ethiopia - Constraints on continental rifting and mantle interactions: Journal of Geophysical Research-Solid Earth and Planets, v. 94, p. 7731–7748.

Hay, D.E., and Wendlandt, R.F., 1995, The origin of Kenya rift plateau-type flood phonolites: Results of high-pressure/high-temperature experiments in the systems phonolite-H2O and phonolite-H2O-CO2: Journal of Geophysical Research: Solid Earth, v. 100, p. 401–410.

Hay, D.E., Wendlandt, R.F., and Keller, G.R., 1995a, Origin of Kenya Rift Plateau-type flood phonolites: Integrated petrologic and geophysical constraints on the evolution of the crust and upper mantle beneath the Kenya Rift: Journal of Geophysical Research: Solid Earth, v. 100, p. 10549–10557.

Hay, D.E., Wendlandt, R.F., and Wendlandt, E.D., 1995b, The origin of Kenya rift plateau-type flood phonolites: Evidence from geochemical studies for fusion of lower crust modified by alkali basaltic magmatism: Journal of Geophysical Research: Solid Earth, v. 100, p. 411–422.

Heumann, A., and Davies, G.R., 2002, U–Th Disequilibrium and Rb–Sr Age Constraints on the Magmatic Evolution of Peralkaline Rhyolites from Kenya: Journal of Petrology, v. 43, p. 557–577, doi:10.1093/petrology/43.3.557.

Hilton, D.R., Halldórsson, S.A., Barry, P.H., Fischer, T.P., de Moor, J.M., Ramirez, C.J., Mangasini, F., and Scarsi, P., 2011, Helium isotopes at Rungwe Volcanic Province, Tanzania, and the origin of East African Plateaux: Geophysical Research Letters, v. 38, p. doi:10.1029/2011GL049589.

Holmes, A., 1937, The Petrology of Katungite: Geological Magazine, v. 74, p. 200–219, doi:10.1017/s0016756800089718.

Hutchison, W. et al., 2016, A pulse of mid-Pleistocene rift volcanism in Ethiopia at the dawn of modern humans: Nature Communications, v. 7, p. 13192, doi:10.1038/ncomms13192 https://www.nature.com/articles/ncomms13192#supplementary-information.

Hutchison, W., Mather, T.A., Pyle, D.M., Boyce, A.J., Gleeson, M.L., Yirgu, G., Blundy, J.D., Ferguson, D.J., Vye-Brown, C., and Millar, I.L., 2018, The evolution of magma during continental rifting: New constraints from the isotopic and trace element signatures of silicic magmas from Ethiopian volcanoes: Earth and Planetary Science Letters, v. 489, p. 203–218.

Kabeto, K., Sawada, Y., Iizumi, S., and Wakatsuki, T., 2001a, Mantle sources and magma–crust interactions in volcanic rocks from the northern Kenya rift: geochemical evidence: Lithos, v. 56, p. 111–139, doi:https://doi.org/10.1016/S0024-4937(00)00063-3.

Kabeto, K., Sawada, Y., and Wakatsuki, T., 2001b, Different evolution trends in alkaline evolved lavas from the northern Kenya Rift: Journal of African Earth Sciences, v. 32, p. 419–433, doi:https://doi.org/10.1016/S0899-5362(01)90106-X.

Kalt, A., Hegner, E., and Satir, M., 1997, Nd, Sr, and Pb isotopic evidence for diverse lithospheric mantle sources of East African Rift carbonatites: Tectonophysics, v. 278, p. 31–45.

Kaszuba, J.P., and Wendlandt, R.F., 2000, Effect of carbon dioxide on dehydration melting reactions and melt compositions in the lower crust and the origin of alkaline rocks: Journal of Petrology, v. 41, p. 363–386.

Kepezhinskas, P., Defant, M.J., and Drummond, M.S., 1996, Progressive enrichment of island arc mantle by melt-peridotite interaction inferred from Kamchatka xenoliths: Geochimica Et Cosmochimica Acta, v. 60, p. 1217–1229.

Kieffer, B. et al., 2004, Flood and shield basalts from Ethiopia: Magmas from the African superswell: Journal of Petrology, v. 45, p. 793–834.

Krans, S.R., Rooney, T.O., Kappelman, J., Yirgu, G., and Ayalew, D., 2018, From initiation to termination: a petrostratigraphic tour of the Ethiopian Low-Ti Flood Basalt Province: Contributions to Mineralogy and Petrology, v. doi:10.1007/s00410-018-1460-7.

Latin, D., Norry, M.J., and Tarzey, R.J., 1993, Magmatism in the Gregory Rift, East Africa: evidence for melt generation by a plume: Journal of Petrology, v. 34, p. 1007–1027.

Latourrette, T., Hervig, R.L., and Holloway, J.R., 1995, Trace-element partitioning between amphibole, phlogopite, and basanite Melt: Earth and Planetary Science Letters, v. 135, p. 13–30.

Le Maitre, R.W., 2002, Igneous Rocks - A classification and glossary of terms: Cambridge, U.K., Cambridge University Press, 236 p.

Le Roex, A.P., Späth, A., and Zartman, R.E., 2001, Lithospheric thickness beneath the southern Kenya Rift: implications from basalt geochemistry: Contributions to Mineralogy and Petrology, v. 142, p. 89–106.

Lippard, S.J., 1973, The petrology of phonolites from the Kenya Rift: Lithos, v. 6, p. 217–234.

MacDonald, R., 1994, Petrological evidence regarding the evolution of the Kenya Rift valley: Tectonophysics, v. 236, p. 373–390.

MacDonald, R., Belkin, H.E., Fitton, J.G., Rogers, N.W., Nejbert, K., Tindle, A.G., and Marshall, A.S., 2008, The roles of fractional crystallization, magma mixing, crystal mush remobilization and volatile-melt interactions in the genesis of a young basalt-peralkaline rhyolite suite, the Greater Olkaria Volcanic Complex, Kenya rift valley: Journal of Petrology, v. 49, p. 1515–1547.

MacDonald, R., Davies, G.R., Bliss, C.M., Leat, P.T., Bailey, D.K., and Smith, R.L., 1987, Geochemistry of High-silica Peralkaline Rhyolites, Naivasha, Kenya Rift Valley: Journal of Petrology, v. 28, p. 979–1008, doi:10.1093/petrology/28.6.979.

Macdonald, R., Kjarsgaard, B.A., Skilling, I.P., Davies, G.R., Hamilton, D.L., and Black, S., 1993, Liquid immiscibility between trachyte and carbonate in ash flow tuffs from Kenya: Contributions to Mineralogy and Petrology, v. 114, p. 276–287.

MacDonald, R., Rogers, N.W., Fitton, J.G., Black, S., and Smith, M., 2001, Plume-lithosphere interactions in the generation of the basalts of the Kenya Rift, East Africa: Journal of Petrology, v. 42, p. 877–900.

MacDonald, R., and Scaillet, B., 2006, The central Kenya peralkaline province: Insights into the evolution of peralkaline salic magmas: Lithos, v. 91, p. 59–73.

Macdougall, J.D., 1995, Using short-lived U and Th series isotopes to investigate volcanic processes: Annual Review of Earth and Planetary Sciences, v. 23, p. 143–167.

Mana, S., Furman, T., Carr, M.J., Mollel, G.F., Mortlock, R.A., Feigenson, M.D., Turrin, B.D., and Swisher Iii, C.C., 2012, Geochronology and geochemistry of the Essimingor volcano: melting of metasomatized lithospheric mantle beneath the North Tanzanian Divergence zone (East African Rift): Lithos, v. 155, p. 310–325.

Mana, S., Furman, T., Turrin, B.D., Feigenson, M.D., and Swisher III, C.C., 2015, Magmatic activity across the East African North Tanzanian Divergence Zone: Journal of the Geological Society, v. 172, p. 368–389.

Marshall, A.S., MacDonald, R., Rogers, N.W., Fitton, J.G., Tindle, A.G., Nejbert, K., and Hinton, R.W., 2009, Fractionation of Peralkaline Silicic Magmas: the Greater Olkaria Volcanic Complex, Kenya Rift Valley: Journal of Petrology, v. 50, p. 323–359.

Marty, B., Pik, R., and Gezahegn, Y., 1996, Helium isotopic variations in Ethiopian plume lavas; nature of magmatic sources and limit on lower mantle contribution: Earth and Planetary Science Letters, v. 144, p. 223–237.

Mattsson, H.B., Nandedkar, R.H., and Ulmer, P., 2013, Petrogenesis of the melilititic and nephelinitic rock suites in the Lake Natron–Engaruka monogenetic volcanic field, northern Tanzania: Lithos, v. 179, p. 175–192.

Mazzarini, F., Rooney, T.O., and Isola, I., 2013, The intimate relationship between strain and magmatism: A numerical treatment of clustered monogenetic fields in the Main Ethiopian Rift: Tectonics, v. 32, p. 49–64, doi:10.1029/2012tc003146.

Menzies, M., and Murthy, V.R., 1980, Nd and Sr Isotope Geochemistry of Hydrous Mantle Nodules and Their Host Alkali Basalts - Implications for Local Heterogeneities in Metasomatically Veined Mantle: Earth and Planetary Science Letters, v. 46, p. 323–334.

Meshesha, D., and Shinjo, R., 2007, Crustal contamination and diversity of magma sources in the northwestern Ethiopian volcanic province: Journal of Mineralogical and Petrological Sciences, v. 102, p. 272–290, doi:10.2465/jmps.061129.

Meshesha, D., and Shinjo, R., 2008, Rethinking geochemical feature of the Afar and Kenya mantle plumes and geodynamic implications: Journal of Geophysical Research-Solid Earth, v. 113, p. doi: 10.1029/2007JB005549.

Mitchell, R.H., 2009, Peralkaline nephelinite–natrocarbonatite immiscibility and carbonatite assimilation at Oldoinyo Lengai, Tanzania: Contributions to Mineralogy and Petrology, v. 158, p. 589.

Mollel, G.F., Swisher III, C.C., McHenry, L.J., Feigenson, M.D., and Carr, M.J., 2009, Petrogenesis of basalt–trachyte lavas from Olmoti Crater, Tanzania: Journal of African Earth Sciences, v. 54, p. 127–143.

Möller, A., Mezger, K., and Schenk, V., 1998, Crustal age domains and the evolution of the continental crust in the Mozambique Belt of Tanzania: combined Sm–Nd, Rb–Sr, and Pb–Pb isotopic evidence: Journal of Petrology, v. 39, p. 749–783.

de Moor, J.M., Fischer, T.P., King, P.L., Botcharnikov, R.E., Hervig, R.L., Hilton, D.R., Barry, P.H., Mangasini, F., and Ramirez, C., 2013, Volatile-rich silicate melts from Oldoinyo Lengai volcano (Tanzania): Implications for carbonatite genesis and eruptive behavior: Earth and Planetary Science Letters, v. 361, p. 379–390.

Mulibo, G.D., and Nyblade, A.A., 2013, The P and S wave velocity structure of the mantle beneath eastern Africa and the African superplume anomaly: Geochemistry, Geophysics, Geosystems, v. 14, p. 2696–2715.

Muravyeva, N.S., Belyatsky, B.V., Senin, V.G., and Ivanov, A.V., 2014, Sr–Nd–Pb isotope systematics and clinopyroxene-host disequilibrium in ultra-potassic magmas from Toro-Ankole and Virunga, East-African Rift: Implications for magma mixing and source heterogeneity: Lithos, v. 210, p. 260–277.

Nash, W.P., Carmichael, I.S.E., and Johnson, R.W., 1969, The mineralogy and petrology of Mount Suswa, Kenya: Journal of Petrology, v. 10, p. 409–439.

Natali, C., Beccaluva, L., Bianchini, G., Ellam, R.M., Savo, A., Siena, F., and Stuart, F.M., 2016, High-MgO lavas associated to CFB as indicators of plume-related thermochemical effects: The case of ultra-titaniferous picrite–basalt from the Northern Ethiopian–Yemeni Plateau: Gondwana Research, v. 34, p. 29–48.

Nelson, W.R., Furman, T., van Keken, P.E., Shirey, S.B., and Hanan, B.B., 2012, Os-Hf isotopic insight into mantle plume dynamics beneath the East African Rift System: Chemical Geology, v. 320–321, p. 66–79.

Nelson, W.R., Hanan, B.B., Graham, D.W., Shirey, S.B., Yirgu, G., Ayalew, D., and Furman, T., 2019, Distinguishing Plume and Metasomatized Lithospheric Mantle Contributions to Post-Flood Basalt Volcanism on the Southeastern Ethiopian Plateau: Journal of Petrology, v. 60, p. 1063–1094, doi:10.1093/petrology/egz024.

Neukirchen, F., Finkenbein, T., and Keller, J., 2010, The Lava sequence of the East African Rift escarpment in the Oldoinyo Lengai–Lake Natron sector, Tanzania: Journal of African Earth Sciences, v. 58, p. 734–751.

Nonnotte, P., Benoit, M., Le Gall, B., Hémond, C., Rolet, J., Cotten, J., Brunet, P., and Makoba, E., 2011, Petrology and geochemistry of alkaline lava series, Kilimanjaro, Tanzania: new constraints on petrogenetic processes: Geol. Soc. Am. Spec. Pap, v. 478, p. 127–158.

Paslick, C., Halliday, A., James, D., and Dawson, J.B., 1995, Enrichment of the continental lithosphere by OIB melts; isotopic evidence from the volcanic province of northern Tanzania: Earth and Planetary Science Letters, v. 130, p. 109–126.

Paslick, C.R., Halliday, A.N., Lange, R.A., James, D., and Dawson, J.B., 1996, Indirect crustal contamination: evidence from isotopic and chemical disequilibria in minerals from alkali

basalts and nephelinites from northern Tanzania: Contributions to Mineralogy and Petrology, v. 125, p. 277–292.

Peccerillo, A., Barberio, M.R., Yirgu, G., Ayalew, D., Barbieri, M., and Wu, T.W., 2003, Relationships between mafic and peralkaline silicic magmatism in continental rift settings: A petrological, geochemical and isotopic study of the Gedemsa volcano, central Ethiopian rift: Journal of Petrology, v. 44, p. 2003–2032.

Pik, R., Deniel, C., Coulon, C., Yirgu, G., Hofmann, C., and Ayalew, D., 1998, The northwestern Ethiopian Plateau flood basalts. Classification and spatial distribution of magma types: Journal of Volcanology and Geothermal Research, v. 81, p. 91–111.

Pik, R., Deniel, C., Coulon, C., Yirgu, G., and Marty, B., 1999, Isotopic and trace element signatures of Ethiopian flood basalts; evidence for plume-lithosphere interactions: Geochimica Et Cosmochimica Acta, v. 63, p. 2263–2279.

Pik, R., Marty, B., and Hilton, D.R., 2006, How many mantle plumes in Africa? The geochemical point of view: Chemical Geology, v. 226, p. 100–114.

Pilet, S., Baker, M.B., and Stolper, E.M., 2008, Metasomatized Lithosphere and the Origin of Alkaline Lavas: Science, v. 320, p. 916–919, doi:10.1126/science.1156563.

Pilet, S., Ulmer, P., and Villiger, S., 2010, Liquid line of descent of a basanitic liquid at 1.5 Gpa: constraints on the formation of metasomatic veins: Contributions to Mineralogy and Petrology, v. 159, p. 621–643, doi:10.1007/s00410-009-0445-y.

Pinzuti, P., Humler, E., Manighetti, I., and Gaudemer, Y., 2013, Petrological Constraints on Melt Generation Beneath the Asal Rift (Djibouti) using Quaternary basalts: Geochemistry, Geophysics, Geosystems, p. 10.1002/ggge.20187, doi:10.1002/ggge.20187.

Price, R.C., Johnson, R.W., Gray, C.M., and Frey, F.A., 1985, Geochemistry of phonolites and trachytes from the summit region of Mt. Kenya: Contributions to Mineralogy and Petrology, v. 89, p. 394–409, doi:10.1007/bf00381560.

Purcell, P.G., 2018, Re-imagining and re-imaging the development of the East African Rift: Petroleum Geoscience, v. 24, p. 21–40.

Reagan, M.K., and Gill, J.B., 1989, Coexisting calcalkaline and high-niobium basalts from Turrialba Volcano, Costa Rica: Implications for residual titanates in arc magma sources: Journal of Geophysical Research: Solid Earth, v. 94, p. 4619–4633.

Ritsema, J., Deuss, A., van Heijst, H.J., and Woodhouse, J.H., 2011, S40RTS: a degree-40 shear-velocity model for the mantle from new Rayleigh wave dispersion, teleseismic traveltime and normal-mode splitting function measurements: Geophysical Journal International, v. 184, p. 1223–1236, doi:DOI 10.1111/j.1365-246X.2010.04884.x.

Ritsema, J., van Heijst, H.J., and Woodhouse, J.H., 1999, Complex shear wave velocity structure imaged beneath Africa and Iceland: Science, v. 286, p. 1925–1928.

Rogers, N.W., Davies, M.K., Parkinson, I.J., and Yirgu, G., 2010, Osmium isotopes and Fe/Mn ratios in Ti-rich picritic basalts from the Ethiopian flood basalt province: No evidence for core contribution to the Afar plume: Earth and Planetary Science Letters, v. 296, p. 413–422.

Rogers, N.W., Demulder, M., and Hawkesworth, C.J., 1992, An enriched mantle source for potassic basanites - Evidence from Karisimbi Volcano, Virunga volcanic province, Rwanda: Contributions to Mineralogy and Petrology, v. 111, p. 543–556.

Rogers, N.W., Evans, P.J., Blake, S., Scott, S.C., and Hawkesworth, C.J., 2004, Rates and timescales of fractional crystallization from 238U–230Th–226Ra disequilibria in trachyte lavas from Longonot volcano, Kenya: Journal of Petrology, v. 45, p. 1747–1776.

Rogers, N.W., James, D., Kelley, S.P., and de Mulder, M., 1998, The generation of potassic lavas from the eastern Virunga Province, Rwanda: Journal of Petrology, v. 39, p. 1223–1247.

Rogers, N., Macdonald, R., Fitton, J.G., George, R., Smith, M., and Barreiro, B., 2000, Two mantle plumes beneath the East African Rift system; Sr, Nd and Pb isotope evidence from Kenya Rift basalts: Earth and Planetary Science Letters, v. 176, p. 387–400.

Rogers, N.W., Thomas, L.E., Macdonald, R., Hawkesworth, C.J., and Mokadem, F., 2006, U-238-Th-230 disequilibrium in recent basalts and dynamic melting beneath the Kenya rift: Chemical Geology, v. 234, p. 148–168, doi:DOI 10.1016/j.chemgeo.2006.05.002.

Rooney, T.O., 2010, Geochemical evidence of lithospheric thinning in the southern Main Ethiopian Rift: Lithos, v. 117, p. 33–48.

Rooney, T.O., 2017, The Cenozoic magmatism of East-Africa: Part I — Flood basalts and pulsed magmatism: Lithos, v. 286, p. 264–301, doi:https://doi.org/10.1016/j.lithos.2017.05.014.

Rooney, T.O., Bastow, I.D., and Keir, D., 2011, Insights into extensional processes during magma assisted rifting: evidence from aligned scoria cones and maars: Journal of Volcanology and Geothermal Research, v. 201, p. 83–96, doi:doi: 10.1016/j.jvolgeores.2010.07.019.

Rooney, T.O., Bastow, I.D., Keir, D., Mazzarini, F., Movsesian, E., Grosfils, E.B., Zimbelman, J.R., Ramsey, M.S., Ayalew, D., and Yirgu, G., 2014a, The protracted development of focused magmatic intrusion during continental rifting: Tectonics, v. 33, p. 875–897, doi:DOI: 10.1002/2013TC003514.

Rooney, T., Furman, T., Bastow, I.D., Ayalew, D., and Gezahegn, Y., 2007, Lithospheric modification during crustal extension in the Main Ethiopian Rift: Journal of Geophysical Research, B, Solid Earth and Planets, v. 112, p. B10201, doi:10.1029/2006JB004916.

Rooney, T., Furman, T., Yirgu, G., and Ayalew, D., 2005, Structure of the Ethiopian lithosphere: Xenolith evidence in the Main Ethiopian Rift: Geochimica Et Cosmochimica Acta, v. 69, p. 3889–3910.

Rooney, T.O., Hanan, B.B., Graham, D.W., Furman, T., Blichert-Toft, J., and Schilling, J.-G., 2012a, Upper Mantle Pollution during Afar Plume–Continental Rift Interaction: Journal of Petrology, v. 53, p. 365–389, doi:10.1093/petrology/egr065.

Rooney, T.O., Hart, W.K., Hall, C.M., Ayalew, D., Ghiorso, M.S., Hidalgo, P., and Yirgu, G., 2012b, Peralkaline magma evolution and the tephra record in the Ethiopian Rift: Contributions to Mineralogy and Petrology, v. 164, p. 407–426, doi:DOI: 10.1007/s00410-012-0744-6.

Rooney, T.O., Herzberg, C., and Bastow, I.D., 2012c, Elevated mantle temperature beneath East Africa: Geology, v. 40, p. 27–30, doi:10.1130/g32382.1.

Rooney, T.O., Mohr, P., Dosso, L., and Hall, C., 2013, Geochemical evidence of mantle reservoir evolution during progressive rifting along the western Afar margin: Geochimica Et Cosmochimica Acta, v. 102, p. 65–88, doi:10.1016/j.gca.2012.08.019.

Rooney, T.O., Nelson, W.R., Ayalew, D., Hanan, B., Yirgu, G., and Kappelman, J., 2017, Melting the lithosphere: Metasomes as a source for mantle-derived magmas: Earth and Planetary Science Letters, v. 461, p. 105–118, doi:http://dx.doi.org/10.1016/j.epsl.2016.12.010.

Rooney, T.O., Nelson, W.R., Dosso, L., Furman, T., and Hanan, B., 2014b, The role of continental lithosphere metasomes in the production of HIMU-like magmatism on the northeast African and Arabian plates: Geology, v. 42, p. 419–422, doi:10.1130/g35216.1.

Rosenthal, A., Foley, S.F., Pearson, D.G., Nowell, G.M., and Tappe, S., 2009, Petrogenesis of strongly alkaline primitive volcanic rocks at the propagating tip of the western branch of the East African Rift: Earth and Planetary Science Letters, v. 284, p. 236–248, doi:10.1016/j.epsl.2009.04.036.

Rudnick, R., and Gao, S., 2003, Composition of the continental crust, *in* Rudnick, R. ed., The Crust, Oxford, Elsevier-Pergamon, Treatise on Geochemistry, v. 3, p. 1–64.

Rudnick, R.L., McDonough, W.F., and Chappell, B.W., 1993, Carbonatite metasomatism in the Northern Tanzanian mantle - Petrographic and geochemical characteristics: Earth and Planetary Science Letters, v. 114, p. 463–475.

Sack, R.O., Walker, D., and Carmichael, I.S.E., 1987, Experimental petrology of alkalic lavas - Constraints on cotectics of multiple saturation in natural basic liquids: Contributions to Mineralogy and Petrology, v. 96, p. 1–23.

Sato, K., Katsura, T., and Ito, E., 1997, Phase relations of natural phlogopite with and without enstatite up to 8 GPa: implication for mantle metasomatism: Earth and Planetary Science Letters, v. 146, p. 511–526, doi:https://doi.org/10.1016/S0012-821X(96)00246-4.

Scaillet, B., and MacDonald, R., 2003, Experimental constraints on the relationships between peralkaline rhyolites of the Kenya rift valley: Journal of Petrology, v. 44, p. 1867–1894.

Scaillet, B., and MacDonald, R., 2001, Phase relations of peralkaline silicic magmas and petrogenetic implications: Journal of Petrology, v. 42, p. 825–845.

Schilling, J.G., Kingsley, R.H., Hanan, B.B., and McCully, B.L., 1992, Nd-Sr-Pb isotopic variations along the Gulf of Aden - Evidence for Afar mantle plume continental lithosphere interaction: Journal of Geophysical Research-Solid Earth, v. 97, p. 10927–10966.

Sharygin, V.V., Kamenetsky, V.S., Zaitsev, A.N., and Kamenetsky, M.B., 2012, Silicate–natrocarbonatite liquid immiscibility in 1917 eruption combeite–wollastonite nephelinite, Oldoinyo Lengai Volcano, Tanzania: Melt inclusion study: Lithos, v. 152, p. 23–39.

Siegburg, M., Gernon, T.M., Bull, J.M., Keir, D., Barfod, D.N., Taylor, R.N., Abebe, B., and Ayele, A., 2018, Geological evolution of the Boset-Bericha Volcanic Complex, Main Ethiopian Rift: 40Ar/39Ar evidence for episodic Pleistocene to Holocene volcanism: Journal of Volcanology and Geothermal Research, v. 351, p. 115–133, doi:https://doi.org/10.1016/j.jvolgeores.2017.12.014.

Simonetti, A., and Bell, K., 1993, Isotopic disequilibrium in clinopyroxenes from nephelinitic lavas, Napak volcano, eastern Uganda: Geology, v. 21, p. 243–246.

Simonetti, A., and Bell, K., 1995, Nd, Pb and Sr isotopic data from the Mount Elgon volcano, eastern Uganda-western Kenya: implications for the origin and evolution of nephelinite lavas: Lithos, v. 36, p. 141–153.

Simonetti, A., and Bell, K., 1994, Nd, Pb and Sr isotopic data from the Napak carbonatite-nephelinite centre, eastern Uganda: an example of open-system crystal fractionation: Contributions to Mineralogy and Petrology, v. 115, p. 356–366.

Späth, A., Le Roex, A.P., and Opiyo-Akech, N., 2001, Plume-lithosphere interaction and the origin of continental rift-related alkaline volcanism; the Chyulu Hills volcanic province, southern Kenya: Journal of Petrology, v. 42, p. 765–787.

Stein, M., Navon, O., and Kessel, R., 1997, Chromatographic metasomatism of the Arabian-Nubian lithosphere: Earth and Planetary Science Letters, v. 152, p. 75–91.

Sun, S. s-, and McDonough, W.F., 1989, Chemical and isotopic systematics of oceanic basalts: Implications for mantle composition and processes., *in* Saunders, A.D. ed., Magmatism in the ocean basins, Geological Society of London Special Publication 42, p. 313–345.

Tappe, S., Foley, S.F., Kjarsgaard, B.A., Romer, R.L., Heaman, L.M., Stracke, A., and Jenner, G.A., 2008, Between carbonatite and lamproite—Diamondiferous Torngat ultramafic lamprophyres formed by carbonate-fluxed melting of cratonic MARID-type metasomes: Geochimica Et Cosmochimica Acta, v. 72, p. 3258–3286.

Van Straaten, P., 1989, Nature and structural relationships of carbonatites from Southwest and West Tanzania: Carbonatites: Genesis and Evolution. Unwin Hyman, London, p. 177–199.

Vollmer, R., Nixon, P.H., and Condliffe, E., 1985, Petrology and geochemistry of a U and Th enriched nephelinite from Mt. Nyiragongo, Zaire: its bearing on ancient mantle metasomatism: Bull. Geol. Soc. Finland, v. 57, p. 37–46.

Vollmer, R., and Norry, M.J., 1983, Possible origin of K-rich volcanic rocks from Virunga, East Africa, by metasomatism of continental crustal material: Pb, Nd and Sr isotopic evidence: Earth and Planetary Science Letters, v. 64, p. 374–386.

Weaver, S.D., 1977, The Quaternary caldera volcano Emuruangogolak, Kenya Rift, and the petrology of a bimodal ferrobasalt-pantelleritic trachyte association: Bulletin Volcanologique, v. 40, p. 209–230.

Weaver, S.D., Sceal, J.S.C., and Gibson, I.L., 1972, Trace-Element Data Relevant to Origin of Trachytic and Pantelleritic Lavas in East African Rift System: Contributions to Mineralogy and Petrology, v. 36, p. 181–194.

Weidendorfer, D., Schmidt, M.W., and Mattsson, H.B., 2017, A common origin of carbonatite magmas: Geology, v. 45, p. 507–510.

White, J.C., Espejel-García, V.V., Anthony, E.Y., and Omenda, P., 2012, Open System evolution of peralkaline trachyte and phonolite from the Suswa volcano, Kenya rift: Lithos, v. 152, p. 84–104, doi:https://doi.org/10.1016/j.lithos.2012.01.023.

Woodhead, J.D.;, 2001, Hafnium isotope evidence for “conservative” element mobility during subduction zone processes (J. M. ; Hergt, J. P. ; Davidson, & S. M. ; Eggins, Eds.): Earth and Planetary Science Letters, v. 192, p. 331–346.

Yaxley, G.M., Green, D.H., and Kamenetsky, V., 1998, Carbonatite metasomatism in the southeastern Australian lithosphere: Journal of Petrology, v. 39, p. 1917–1930.

Acknowledgements

I would like to thank all the authors I contacted who provided more details and answers to my queries on their work – there were many and I am not able to mention them all here. This work is a synthesis of all the hard work put in by the persons cited herein and the contributions from these persons should be acknowledged. Peter Purcell is thanked for providing the digital files for the rift maps used in the accompanying maps. Alex Steiner is given thanks for his assistance in collating the Turkana materials, discussions on the GIS aspects of the project, and insights into Turkana volcanism. Thanks is provided to the MSU Library and in particular Kathleen Weessies at the Map Library and the interlibrary loans group – they tried to obtain the requests I placed,

and most always succeeded. I am indebted to the persons who read and provided feedback on this work prior to publication: Val Finlayson, Ian Bastow. Andrew Kerr is thanked for his tireless efforts in editing this synthesis series. I am grateful for the formal peer reviews by Tobias P. Fischer and an anonymous reviewer, which significantly improved the manuscript. This work was supported by US National Science Foundation Grants: EAR 1551872 and EAR 1850606. Lastly, I acknowledge the NSF GeoPRISMS program which was part of the motivation for undertaking this synthesis.

Figure Captions

Figure 1: Cartoon illustrating the formation of a metasome within the lithospheric mantle. A metasomatic agent (fluid/melt) enters the lithosphere and crystallizes pyroxene-rich lithologies near the base of the lithosphere. This metasomatic agent may evolve by crystal fractionation and chromatographic interaction with the lithospheric mantle. When the amphibole stability field is reached, significant volumes of amphibole-rich lithologies may form. Destabilization of these easily fusible lithologies will yield melt with a metasomatic signature which may represent the origin of some Type II lavas. Mixing of these melts with sub-lithospheric magmas will yield Type IV magmas. Type V magmas may be produced where destabilization of phlogopite-rich metasomes occurs, typically at greater lithospheric depths adjacent to the Tanzania craton.

Figure 2: Cartoon depiction of melt generation processes within the Eastern Branch of the East African Rift System. The processes described in this caption are more fully explored in the text –

citations to the relevant papers linked to these ideas are presented there. The lithosphere in this region is a Pan-African aged mobile belt. The lithospheric mantle has been enriched with pyroxenite-bearing metasomes (deeper) and amphibole-bearing metasomes (shallower) generated by chromatographic metasomatism as fluids/melts passed through the lithospheric mantle. These metasomes have different potential origins: some are the same age as the lithosphere, other have formed more recently as plume-derived melts interacted with the lithosphere. The asthenosphere in this area has been hybridized and homogenized by mixing initially with lithospheric materials (depicted as down going arrows); the timing and precise mechanism of this hybridization is uncertain. Melts from this hybridized asthenosphere interact with plume material and melt by decompression to form Type III magmas (a mix of depleted mantle, plume, and lithosphere). These Type III magmas are the primary magma type found in the Eastern Branch of the East African Rift. Type II magmas result from the thermo-baric destabilization of amphibole-bearing metasomes within the lithospheric mantle. The isotopic characteristics of Type II magmas depend on the antiquity of the metasome: older metasomes may exhibit HIMU-like signatures, younger metasomes generate melt that isotopically resembles modern asthenospheric magmatism defined by Type III lavas. Note that some Type II magmas during the Oligocene-Miocene may result from delamination of the lithosphere. Type IV magmas are a hybrid of melts derived from the source of Type II and Type III magmas and may be formed when asthenosphere-derived Type III magmas interact with and destabilize existing lithospheric mantle metasomes. In a general sense, lavas erupted in regions least impacted by lithospheric thinning are more likely to exhibit Type II magma characteristics. Regions that have recently begun to thin or are in the process of lithospheric destabilization may exhibit Type IV magmas. Type III magmas are prevalent where rifting is more mature. Type I magmas are not shown here and are limited to the Eocene-Oligocene flood basalt events – their origin is linked to the plume but the precise process remains unclear. Type V magmas are found

within the Western Branch of the East African Rift system and are derived in a similar way to Type II lavas – destabilization of a metasome. However, Type V magmas require phlogopite and may be derived from the deeper zoned lithosphere of the Tanzania craton. Type VI magmas are found in Afar (mature rift) and their origin remains uncertain.

Figure 3: Primitive mantle normalized diagram (Sun and McDonough, 1989) showing the different magma types identified in East Africa. Type Ia lavas typified by sample 107 from the Oligocene LT flood basalts (Kieffer et al., 2004), Type Ib lavas typified by sample RG-93-73 from the Eocene flood basalts (George and Rogers, 2002), Type IIa lavas are typified by sample 3235 from the Miocene Gerba Geracha shield (Rooney et al., 2017); Type IIb lavas are typified by sample LAL3 from the HT2 Oligocene flood basalts (Beccaluva et al., 2009); Type III lavas are typified by sample N-21 from the Quaternary Kone caldera in the Main Ethiopian Rift (Furman et al., 2006a); Type IV lavas are typified by sample CI-37A from the Quaternary Central Island in Lake Turkana (Furman et al., 2004); Type V lavas are typified by sample NY34-02 from Nyamuragira volcano within the Virunga Volcanic Province (Chakrabarti et al., 2009); Type VI lavas are typified by sample GT61 from Manda Hararo in Afar (Barrat et al., 2003).

Figure 4: Map showing the generalized distribution of Precambrian rocks in East Africa, the distribution of Cenozoic volcanism, and the footprints of Cretaceous and Cenozoic rifting. In a general sense rifting occurs along the boundary of the between Neoproterozoic rocks and Mesoproterozoic and older rocks, however the Western Branch of the East African Rift does transit these rocks and generally follows the boundary of the craton (white shaded overlay). Outcrop shapes are derived from the USGS Surficial Geology of Africa (geo7_2ag), rifts are from Purcell (2018), the extent of the craton is taken from Foley et al. (2012).

Figure 5: Map showing the generalized distribution of Quaternary volcanics rocks from East Africa. Data sources are outlined in volume II through IV of the synthesis series. NTD = Northern Tanzania Divergence

Figure 6: Map showing the generalized distribution of Quaternary volcanics rocks from the northern portion of the Eastern Branch of the East African Rift System. Data sources are outlined in volume II through IV of the synthesis series.

Figure 7: Degree of enrichment of lavas from Quaternary East Africa lavas as determined by Zr-Nb and chondrite normalized (Boynton, 1984) La-Sm variations. Carbonatite samples continue in the vector shown and have been clipped for the purposes of avoiding data compression. Note the warm colors (Yemen, Afar, MER, Turkana, and the North Kenya Rift) are from regions where lavas erupted through mobile-belt lithosphere. In contrast, the cooler colors (South Kenya Rift / Tanzania, Rungwe, Kivu-Virunga, and carbonatites) are for suites emplaced upon the cratonic lithosphere. Note the separation in the suites with more enrichment in the incompatible trace elements in the lavas erupted in the cratonic regions. These data come from modern events only (0.5 Ma to present – classified as Axial in the prior synthesis papers). Small symbols represent samples that are either <5 wt. % MgO or where this information is unavailable. Large symbols reflect samples that have >5 wt. % MgO. MORB, OIB, and upper continental crust (Sun and McDonough, 1989; Rudnick and Gao, 2003) are shown for reference.

Figure 8: $^{87}Sr/^{86}Sr$-$^{143}Nd/^{144}Nd$ isotopic data for Quaternary rocks throughout East Africa. Note the warm colors (Yemen, Afar, MER, Turkana, and the North Kenya Rift) are from regions where lavas erupted through mobile-belt lithosphere. In contrast, the cooler colors (South Kenya

Rift / Tanzania, Rungwe, Kivu-Virunga, and carbonatites) are for suites emplaced upon the cratonic lithosphere. Note the separation in the suites with more radiogenic $^{87}Sr/^{86}Sr$ and less radiogenic $^{143}Nd/^{144}Nd$ in the lavas erupted in cratonic regions. These data come from modern events only (0.5 Ma to present – classified as Axial in the prior synthesis papers). The Pan African Lithosphere (PA), Depleted Mantle (DM) and Afar Plume endmembers of Rooney et al. (2012a), CLM component is that of Furman & Graham (1999), Enriched Mantle 2 (EM2), and HIMU are shown for comparison. Small symbols represent evolved samples that are either <5 wt. % MgO or where this information is unavailable. Large symbols reflect more mafic samples that have >5 wt. % MgO.

Figure 9: $^{87}Sr/^{86}Sr$-$^{143}Nd/^{144}Nd$ isotopic data for Quaternary rocks from the mobile belt region. These data come from modern events only (0.5 Ma to present – classified as Axial in the prior synthesis papers). The Pan African Lithosphere (PA), Depleted Mantle (DM) and Afar Plume endmembers of Rooney et al. (2012a), CLM component is that of Furman & Graham (1999), Enriched Mantle 2 (EM2), and HIMU are shown for comparison. Small symbols represent samples that are either <5 wt. % MgO or where this information is unavailable. Large symbols reflect samples that have >5 wt. % MgO.

Figure 10: Map showing the generalized distribution of Quaternary volcanics rocks from the southern portion of the Eastern Branch of the East African Rift System. Data sources are outlined in volume II through IV of the synthesis series. NTD = Northern Tanzania Divergence

Figure 11: Cartoon illustrating a conceptual model of the magma plumbing system of modern magmatism in the East African Rift modified after Mazzarini et al. (2013). In this model, primitive basaltic magma from the mantle may stall and evolve within dike complexes in the crust. On the basis of self-similar clustering models, these lavas are thought to leave these complexes at ~7-10 km and transit to the surface. The depth extent of the dike complexes may differ. Some dikes

become captured within magma mush zones in the shallow crust (0.2 – 0.4 km) and contribute to the development of silicic magmatism within the rift. Other dikes may directly erupt as monogenetic cindercones. This model was developed for the Central Main Ethiopian Rift but is broadly applicable throughout the East African Rift.

Figure 12: Multi isotopic variation of samples erupted at Olkaria (S. Kenya Rift) plotted as a function of $^{206}Pb/^{204}Pb$. The Pan African Lithosphere (PA), Depleted Mantle (DM) and Afar Plume endmembers of Rooney et al. (2012a), CLM component is that of Furman & Graham (1999), HIMU, and Enriched Mantle 2 (EM2) are shown for comparison. These endmembers are shown as discrete points but in reality these are regions of isotopic space and are shown as the center points for clarity. The crustal contamination vector is an indication of the impact of assimilation on the composition of lavas in this edifice.

Figure 13: Multi isotopic variation of samples erupted within the Cratonic region plotted as a function of $^{206}Pb/^{204}Pb$. Within the Mobile Belt, radiogenic values of $^{206}Pb/^{204}Pb$ tend to be associated with increased contributions from the Afar Plume. The Pan African Lithosphere (PA), Depleted Mantle (DM) and Afar Plume endmembers of Rooney et al. (2012a), CLM component is that of Furman & Graham (1999), HIMU, and Enriched Mantle 2 (EM2) are shown for comparison. These endmembers are shown as discrete points but in reality these are regions of isotopic space and are shown as the center points for clarity. These data come from modern events only (0.5 Ma to present – classified as Axial in the prior synthesis papers). Small symbols represent samples that are either <5 wt. % MgO or where this information is unavailable. Large symbols reflect samples that have >5 wt. % MgO.

Figure 14: Map showing the generalized distribution of Quaternary volcanics rocks from the Western Branch of the East African Rift System. Data sources are outlined in volume II through IV of the synthesis series. Note that Rungwe is not shown on this map due to scaling issues.

Figure 15: Sr-Nd and Pb isotopic plots of carbonatites from East Africa. Data are: Eastern Uganda (Tinderet, Napak, Bukusu, Kisingiri, Sukulu Hill, Tororo Hill); Homa Bay (Homa Mountain and Ruri); Shombole/Kerimasi; Oldoinyo Lengai; Toro Ankole (Fort Portal, Katwe-Kikorongo, Bunyaruguru). The EACL is the East Africa Carbonatite Line (Bell and Blenkinsop, 1987). The Pan African Lithosphere (PA), Depleted Mantle (DM) and Afar Plume endmembers of Rooney et al. (2012a), CLM component is that of Furman & Graham (1999), HIMU, and Enriched Mantle 2 (EM2) are shown for comparison. These endmembers are shown as discrete points but in reality these are regions of isotopic space and are shown as the center points for clarity.

Figure 16: Multi isotopic variation of samples erupted within the Craton and Mobile belt vs $^{206}Pb/^{204}Pb$. Mixing arrays (drawn by hand) are also shown as grey and orange arrows. The Pan African Lithosphere (PA) and Afar Plume endmembers of Rooney et al. (2012a), CLM component is that of Furman & Graham (1999), HIMU, and Enriched Mantle 2 (EM2) are shown for comparison. The Depleted Mantle (DM) endmember is not shown in these plots due to the compressive impact on the plotting of the dataset. These endmembers are shown as discrete points but in reality these are regions of isotopic space and are shown as the center points for clarity. These data come from modern events only (0.5 Ma to present – classified as Axial in the prior synthesis papers). Small symbols represent samples that are either <5 wt. % MgO or where this information is unavailable. Large symbols reflect samples that have >5 wt. % MgO.

Figure 17: Isotopic variation versus helium isotope ratios for Quaternary rocks in the region. The Pan African Lithosphere (PA), Depleted Mantle (DM), and Afar Plume endmembers of Rooney

et al. (2012a), HIMU, and Enriched Mantle 2 (EM2) are shown for comparison. These endmembers are shown as discrete points but in reality these are regions of isotopic space and are shown as the center points for clarity. A value of $^{3}He/^{4}He$ (R/R_A) of 5 was assumed for HIMU (e.g., Graham et al., 1992), a value of 19.6 was assigned for the Afar plume on the basis of previous work (Marty et al., 1996), the Pan-African Lithosphere component was assigned a value of 6, and the depleted mantle component a values of 8.1 (Gautheron and Moreira, 2002). It should be noted that a crustal reservoir is not shown but would be close to 0 in terms of R/R_A (Marty et al., 1996). Given the potential concentration differences between the various reservoirs, hyperbolic mixing is likely a factor in the geometry of this figure. These data come from modern events only (0.5 Ma to present – classified as Axial in the prior synthesis papers). Small symbols represent samples that are either <5 wt. % MgO or where this information is unavailable. Large symbols reflect samples that have >5 wt. % MgO.

Figure 18: Multi isotopic variation of samples erupted within the Mobile Belt plotted as a function of $^{206}Pb/^{204}Pb$. Within the Mobile Belt, radiogenic values of $^{206}Pb/^{204}Pb$ tend to be associated with increased contributions from the Afar Plume. The Pan African Lithosphere (PA), Depleted Mantle (DM) and Afar Plume endmembers of Rooney et al. (2012a), CLM component is that of Furman & Graham (1999), and Enriched Mantle 2 (EM2) are shown for comparison. The HIMU endmember is not shown in these plots due to the compressive impact on the plotting of the dataset. These endmembers are shown as discrete points but in reality these are regions of isotopic space and are shown as the center points for clarity. These data come from modern events only (0.5 Ma to present – classified as Axial in the prior synthesis papers). Small symbols represent samples that are either <5 wt. % MgO or where this information is unavailable. Large symbols reflect samples that have >5 wt. % MgO.

Figure 19: Ternary Pb isotope plot displaying ^{206}Pb-^{207}Pb-^{208}Pb for samples erupted within the mobile belt. Topography of this plot is outlined by Hanan and Graham (1996). Each line represents 0.25 % of each isotope. Mixing in this space is linear. The Pan African Lithosphere (PA), Depleted Mantle (DM) and Afar Plume endmembers of Rooney et al. (2012a), and Enriched Mantle 2 (EM2) are shown for comparison. The HIMU endmember is not shown in these plots due to the compressive impact on the plotting of the dataset. These endmembers are shown as discrete points but in reality these are regions of isotopic space and are shown as the center points for clarity. These data come from modern events only (0.5 Ma to present – classified as Axial in the prior synthesis papers). Small symbols represent samples that are either <5 wt. % MgO or where this information is unavailable. Large symbols reflect samples that have >5 wt. % MgO.

Figure 20: Ternary Pb isotope plot displaying ^{206}Pb-^{207}Pb-^{208}Pb for samples erupted within the mobile belt and craton together. Topography of this plot is outlined by Hanan and Graham (1996). Each line represents 0.25 % of each isotope. Mixing in this space is linear. The Pan African Lithosphere (PA), Depleted Mantle (DM) and Afar Plume endmembers of Rooney et al. (2012a), and Enriched Mantle 2 (EM2) are shown for comparison. The HIMU endmember is not shown in these plots due to the compressive impact on the plotting of the dataset. These endmembers are shown as discrete points but in reality these are regions of isotopic space and are shown as the center points for clarity. These data come from modern events only (0.5 Ma to present – classified as Axial in the prior synthesis papers). Small symbols represent samples that are either <5 wt. % MgO or where this information is unavailable. Large symbols reflect samples that have >5 wt. % MgO.